Department of Pharmacology
University College London
Gower Street
London WC1E 6BT

Agonist-induced inhibition of the M-current: involvement of the phosphoinositide cycle

by

Joanna Shaw Winks

A thesis submitted for the degree of

Doctor of Philosophy

University of London

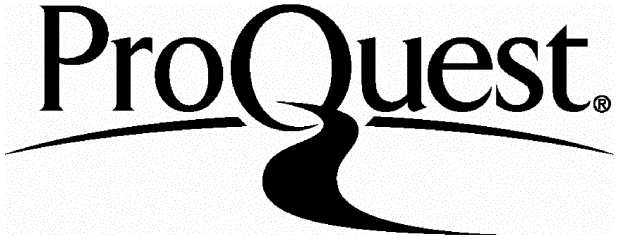

For Mum and Dad

Abstract

M-type potassium channels are closed by activation of G protein-coupled receptors which couple to phospholipase C activation. I have investigated the proposed role of the hydrolysis and depletion of phosphatidylinositol-4,5-bisphosphate (PIP_2) in the closure of these channels produced by two different agonists (the muscarinic agonist, oxotremorine-M, and the peptide, bradykinin) in primary mammalian sympathetic neurons. Simultaneous electrophysiological recording of the M-current and imaging of the localization of a fluorescent PIP_2-binding construct, GFP-PLC-δ PH, has provided a valuable tool for investigation of the involvement of PIP_2 levels in M-channel closure.

I found that over-expression of the neuronal calcium-sensor protein NCS-1, which enhances PIP_2 synthesis by increasing the activity of the enzyme PI4-kinase, reduced the net decrease in membrane PIP_2 following application of bradykinin and, in parallel, reduced the sensitivity of M channels to closure by bradykinin. This reduction in sensitivity was partly reversed by the PI4-kinase inhibitor wortmannin. I also found that over-expression of the next enzyme in the synthetic pathway, PI5-kinase, reduced both the net decrease in membrane PIP_2 and the sensitivity of the M channels to both agonists. This (plus other evidence) suggests that membrane PIP_2 depletion is a key factor in the regulation of M channels by both of these agonists.

Acknowledgements

I would like to thank all the members of Professor David Brown's group, past and present, for their help, support and patience during my PhD.

I thank Jon Robbins for his infectious enthusiasm and for getting me interested in electrophysiology in the first place, and then for delivering me to UCL on the back of his motorbike !. I thank David Brown and Alexander Selyanko for agreeing to take me on, and then, after the untimely and very sad loss of Alex at the end of 2001, Steve Marsh for taking over. Steve is due my special thanks for his help and support over the past two years, for turning me into a scientist and also for "toughening me up" !.

Thanks also to the girls, especially Gayle Passmore and Lucine Tatulian, who have given their friendship and support and listened over many cups of coffee !.

Thanks to Bevster, for company on countless Sunday evenings in the lab injecting cells, for all the hours spent on the M4, for buying the BP2 and for sharing my highs and lows over the past 2 years with me – I hope we have many years, with a higher proportion of highs than lows, ahead !.

Finally, thanks to my family; to my mum, dad and brother Paul for always being there, and for giving me their love and support every step of the way.

Communications

J.S.Winks; F.C.Abogadie; P.Delmas; J.L.Weiss; R.D.Burgoyne and D.A.Brown, Possible role for calcium sensor NCS-1 in M-current modulation. Society for Neuroscience Abstracts 2002.

J.S.Winks and S.J.Marsh, Agonist-induced phosphatidylinositol-4,5-bisphosphate (PIP_2) hydrolysis and M-current inhibition in sympathetic neurons: effects of the neuronal calcium sensor protein NCS-1, Abstracts of the Physiological Society Meeting, UCL, December 2002.

J.Winks, L.Tatulian, A.K.Filippov, F.Abogadie, S.J.Marsh and D.A.Brown, Effects of PI4P5-kinase (PI5-k) over-expression on transmitter-induced inhibition of M- and GIRK currents, Society for Neuroscience Abstracts, in press.

Table of Contents

RESULTS

List of Figures

List of Abbreviations

ACh - acetylcholine

BK - bradykinin

G_M – conductance of M-current

GFP – green fluorescent protein

GFP-PLC-δ PH – GFP-tagged pleckstrin homology domain of phospholipase C-δ_1

G-protein – GTP-binding protein

GTP – guanosine 5'-triphosphate

IC_{50} – half-maximal inhibitory concentration

I_M – M-current

IP_3 – inositol 1,4,5 trisphosphate

M_1***-mAChR*** – M_1 muscarinic acetylcholine receptor

oxo M – oxotremorine M

PI 4-K – phosphatidylinositol 4 kinase

PI 5-K – phosphatidylinositol 4 phosphate 5 kinase

PI – phosphatidylinositol

PIP – phosphatidylinositol 4 phosphate

PIP_2 – phosphatidylinositol 4,5 bisphosphate

PLC – phospholipase C

SCG – superior cervical ganglion

$V_{1/2}$ – half-maximal activation voltage (at which half of the available channels are active

K – calcium binding ratio

CHAPTER ONE

INTRODUCTION

1.1 The neuronal M-current

1.1.1 Discovery of the M-current

The 'M-current' (I_M) was first identified more than twenty years ago after an inquiry into the mechanism whereby activation of muscarinic receptors depolarises sympathetic ganglion cells. Brown and Adams (1980) used sympathetic neurones from the bullfrog to investigate this effect of muscarinic agonists, and they discovered that these agonists couple to, and inhibit, a voltage-dependent, non-inactivating potassium current. Thus, the M-current was 'born', and so christened due to its coupling to muscarinic receptors. The unique properties of the M-current, and the implications of its manipulation for the control of neural excitability have made it a popular area of study. Comparable currents have now been identified in a number of different neuronal cell types and neural cell lines, and even in some non-neuronal cells, and the molecular correlates of the channel have been proposed, with considerable evidence in their favour. This has allowed the study of M-like currents in cell lines transfected with these molecular correlates and with the appropriate receptors.

1.1.2 Where is the M-current found ?

After first being discovered in bullfrog sympathetic ganglion neurons (Brown and Adams, 1980), the M-current has since been identified in rat sympathetic superior cervical ganglion neurons (Constanti and Brown, 1981), amphibian dorsal

root ganglion neurons (Tokimasa et al., 1993), mammalian central neurons (e.g. Halliwell and Adams, 1982; Constanti and Sim, 1987; Moore et al., 1988), neuron-like NG108-15 neuroblastoma x glioma cells (Brown and Higashida, 1988) and rat pheochromocytoma PC12 cells (Villarroel et al., 1989).

1.1.3 Kinetics and Physiological relevance of I_M

I_M is the only persistent, voltage-sensitive potassium current that is activated at sub-threshold potentials in rat superior cervical ganglion cells (SCGs) (Constanti and Brown, 1981). It is fully deactivated at potentials more negative than –70 mV, and appears to be fully activated by –10 mV, although contamination by activation of other large, outward currents at potentials positive to –30 mV complicates the measurement. Thus, M-currents are usually recorded within the range of –20mV to –60mV.

The conductance of I_M, (G_M), follows a sigmoidal activation curve between –60 mV and –10 mV. As the threshold for action-potential activation in these cells is around –40 mV (resting potential is around –60 mV), it follows that I_M activation would have a braking effect on action-potential firing.

Injection of depolarising current into a cell at rest (-60 mV) will bring the membrane potential into the activation range for I_M. As the cell depolarises further, G_M increases inducing a secondary (outward) current. This outward current will 'dampen' the effect of the depolarising current and hence, may prevent action-potential firing. It is therefore believed that the function of the M-current in vivo is to

stabilize the membrane potential and to prevent fluctuations from eliciting unwanted action potentials.

The voltage-sensitivity of G_M produces pronounced outward rectification in the steady-state current-voltage curve, as demonstrated by Adams et al (1982), who found that simulating the replacement of G_M with an equivalent fixed K^+ conductance led to a linear steady-state current-voltage curve. Removal of the voltage-sensitivity of G_M also meant that the voltage deflections produced by relatively small current injections (~ 0.4 nA) were approximately twice as large, which further demonstrates the stabilizing role of I_M.

The above paragraphs outline the physiological role of the M-current at the cellular level. The identification of its probable molecular correlates in 1998 (Wang et al., 1998) provides a clinical perspective to the work.

1.1.4 Molecular Correlates of the M-channel and its clinical relevance.

Several candidates have been suggested as the genes responsible for M-current expression, all encoding members of the six transmembrane domain K^+ channel family, but the evidence for the involvement of the KCNQ gene family is the most compelling.

Evidence for KCNQ subunits as molecular correlates of the M-current

The first KCNQ gene, KCNQ1, was identified in cardiac myocytes as the gene which, when mutated, is responsible for more than 50% of inherited cardiac long QT syndrome (Wang et al, 1996), hence the original name given to the gene family, "KvLQT". This KCNQ subtype combines with a β accessory subunit, KCNE1, which removes the rectification of the channel and modifies its kinetics, to form the cardiac slow delayed rectifier channel, IK_S (Sanguinetti et al., 1996).

A mutation in the gene now known to be KCNQ2, was present in a family where the condition "Benign Familial Neonatal Convulsions" (BFNC), a dominantly inherited epileptic disorder of newborns, was evident (Biervert et al, 1998; Charlier et al, 1998; Singh et al, 1998). This provided evidence that KCNQ2 is involved in the regulation of cell excitability (as expected from the M-current). Also, Charlier et al (1998) found a mis-sense mutation in the critical pore region of KCNQ3 in perfect co-segregation with the BFNC phenotype (the same conserved amino acid is mutated in KCNQ1 in an LQT patient; Wang et al, 1996). The fact that mutations in either KCNQ2 or 3 cause the same inherited epilepsy suggests that they do form heteromeric channels which regulate cell excitability.

The neuronal location of the mRNAs for both KCNQ2 and 3 suggested them as promising candidates for the neuronal M-channel. The expression of KCNQ2 message in superior cervical ganglia, coeliac ganglia and superior mesenteric ganglia was almost identical to the percentage of these neurons that displayed the M-current (Yang et al, 1998). A discrepancy was noticed however, as KCNQ2

message was highly evident in cerebellum, an area of the brain which is reported not to express M-current (Watkins and Mathie, 1996). The discovery that co-expression of KCNQ2 and 3 produces a substantial, synergistic increase in current amplitude compared to the currents through the individually expressed channels (an increase in current density of around 11-fold compared to KCNQ2 homomers) and that expression patterns of the mRNAs for both subunits were found to overlap in areas where the M-current is found, but did not overlap in the cerebellum helped to explain this discrepancy (Wang et al., 1998).

KCNQ2- and 3-associated channels were expressed, both individually and together, in Xenopus oocytes, and the currents measured and compared to I_M. The current produced is very similar to I_M, both biophysically and pharmacologically, with a half-activation potential of approximately -40mV and a strong sensitivity to block by muscarinic agonists in M_1 receptor-expressing cells (Wang et al., 1998). The relatively specific M-channel blockers linopirdine and its analogue XE991 were also found to block the KCNQ2/3-associated current.

It was proposed by Wang et al (1998) that the KCNQ3 subunit somehow facilitated the expression of the KCNQ2 subunits, perhaps via the formation of a heteromeric complex of both, rather than the whole cell M-current being made up of homomeric KCNQ2 channels and homomeric KCNQ3 channels. They investigated this possibility by observing the sensitivities of the individual channels to blockade by tetraethylammonium (TEA), and then comparing these to the sensitivity of the channels after co-injection of both mRNAs.

The homomultimeric KCNQ 2 channel is very sensitive to TEA (K_d ~0.16 mM). This is due to the presence of a tyrosine residue at position 323 within the pore region that determines sensitivity to blockade by TEA (tyrosine here confers high sensitivity). Due to the presence of a threonine residue at this same critical position within its pore, the KCNQ 3 channel exhibits a low sensitivity to TEA (Mackinnon and Yellen, 1990). When the subunits were co-expressed, the resulting channels showed an intermediate level of sensitivity to blockade by TEA (K_d ~3.5 mM), which indicates that they do indeed co-assemble into a heteromeric complex (Wang et al, 1998). The same results were obtained when subunits were expresses in Chinese Hamster Ovary (CHO) cells (Hadley et al., 2000). The native M-channels in rat sympathetic neurons, hippocampal and olfactory cortex neurons all exhibit a similar, intermediate level of sensitivity to TEA blockade (see Wang et al, 1998), supporting the theory that they are KCNQ 2 + 3 heteromers.

Analysis of the single channel properties of heteromeric KCNQ 2/3 channels expressed in Chinese Hamster Ovary (CHO) cells has shown them to resemble previously characterised neuronal M-type channels (Selyanko et al., 2001).

Further work on the TEA sensitivity of native M-currents in SCG neurons revealed that these native channels, in adult rats (6 weeks old) adopt the same configuration as channels formed in CHO cells by expression of a KCNQ2/3 tandem construct, i.e. a 1:1 stoichiometry (Hadley et al., 2003). Hadley et al. also reported an additional small proportion of current carried by KCNQ2 homomers in 17 day old rats (this is the age of rat used throughout this thesis).

Shah et al. used RT-PCR, staining and TEA-sensitivity studies to determine the molecular correlates of the M-current in rat hippocampal neurons, and reported that KCNQs 2, 3 and 5 contributed to the M-current in these neurons (Shah et al., 2002).

Evidence for other subunits as the molecular correlates of the neuronal M-channel

The M-like current in the mouse neuroblastoma x rat glioma cell line (NG 108-15 cells) is a compound current, which has been shown to be made up of a slow component and a fast component. The slow component is inhibited by a compound named WAY-123.398, and is believed to be conducted through erg channels, and the fast component is inhibited by linopirdine and is believed to be conducted through KCNQ 2/3 heteromers (Selyanko et al., 1999; Meves et al., 1999).

Stansfeld et al (1997) proposed the involvement of ether-a-go-go channels in the conductance of the native M-current. Both the drosophila (D-eag) and rat (r-eag) homologues of this channel produce non-inactivating currents, and the single channel conductance through these channels is around 8 pS – similar to that of rat M-channels which express two low conductance levels, 7pS and 11pS. However, Stansfeld et al. compared activation kinetics of the *Drosophila* eag current, rather than the rat eag current, with the rat M-current. In a discussion on the subject, Mathie and Watkins (1997) point out that the r-eag channel currents have been shown to have rather different, faster deactivation kinetics than the drosophila homologue. This fact is reiterated by Marrion (1997b) who states that "the

activation and deactivation kinetics of r-eag are so different (to D-eag) that a comparison with M-current would not be convincing". Marrion also discusses differences between the permeability properties of the r-eag pore and the mammalian M-channel pore; the M-channels are permeable to Cs^+ ions, a property which is not shared by r-eag. Conversely, r-eag channels are permeable to Na^+ ions and M-channels are not (Marrion et al., 1997b). These differences appear to suggest that r-eag, at least expressed homomerically, is not responsible for the M-current.

It is possible however, that r-eag may co assemble with other subunits, or that the M-current may be conducted, in part, through r-eag homomers.

1.2 Receptor modulation of the M-current

The subject at the core of much of the work done on the M-current since its discovery is the mechanism of its inhibition via receptor activation. Elucidation of the coupling mechanism between receptor and channel would provide us with novel, possibly more rapid and also more precise means of controlling the current. This could provide the basis in the future for several novel therapeutics for epilepsy and other diseases involving abnormalities in neuronal excitability.

The M-current is inhibited via activation of a number of different receptor types. As well as the muscarinic receptor, these include the bradykinin B2 receptor and UTP-sensitive P2Y purinoceptors. All these receptors couple to a G-protein, which has been proven to be an essential part of the transduction pathway.

1.2.1 G-protein-coupled receptors, G-protein cycle and its involvement in the inhibition of the M-current

Structure of G-protein-coupled receptors

At rest, G-protein-coupled receptors are bound to G-protein heterotrimers consisting of the α subunit and the βγ dimer. These inactive G-proteins are bound to guanosine diphosphate, as shown in Figure 1.1.

The G-protein cycle

At rest, the G-protein trimer, comprising the α and βγ subunits, is bound to guanosine diphosphate (GDP). Once the G-protein is activated by receptor activation, GDP is exchanged for guanosine triphosphate (GTP). The G-protein trimer splits into two parts, the α subunit and the βγ dimer, GTP remaining bound to the α subunit. When this GTP is hydrolysed by the innate GTPase properties of the α subunit, to form GDP once again, the "active" period of the α subunit is over and it rebinds to a βγ dimer, ready to be activated again. GDP gains a phosphate from adenosine triphosphate to form GTP, ready to bind once again to an activated G-protein. This cycle is shown in Figure 1.1.

Constitutively active α subunits can be created by adding the non-hydrolysable analogue of GTP, GTPγS to the cell. By the same token, if a stably inactive analogue, GDPβS, which binds to the α subunit and then cannot be phosphorylated, is added to the cell, this reduces the amount of G-proteins which are available for activation.

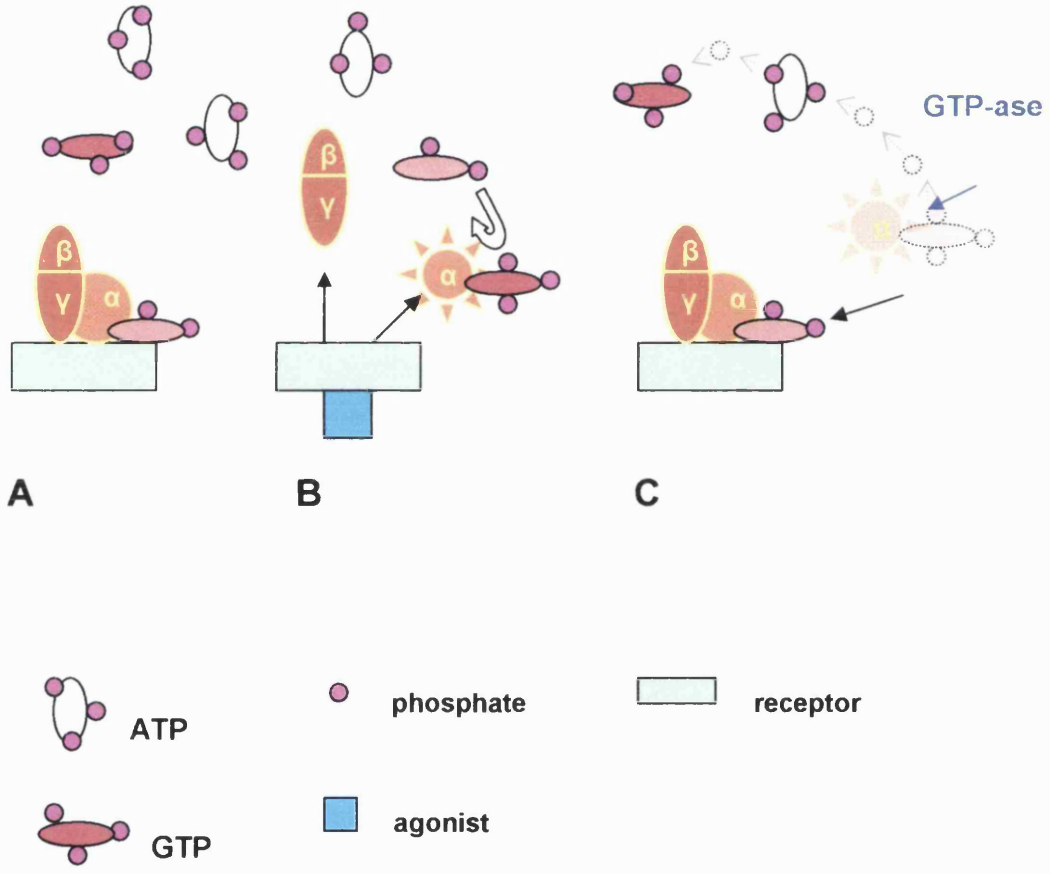

Figure 1.1. The G-protein cycle. A. At rest, the G-protein trimer is bound to GDP. B. On receptor activation, GDP is exchanged for GTP, and the trimer splits into the βγ dimer and the α subunit, which are free to bind to effectors. C. Innate GTPase properties of the α subunit cause hydrolysis of GTP; βγ dimer and α subunit rejoin in the resting configuration , bound to GDP.

Experimental evidence that a G-protein is involved

Pfaffinger (1988) and Robbins et al (1993) conducted experiments involving the addition of different G-protein activators/ inhibitors to the pipette solution.

When GTPγs (non-hydrolysable activator of G-protein) was added to the pipette solution, recovery of I_M inhibition following washout of ACh was prevented. This was the case both in M_1 and M_3 receptor- transfected NG108-15 cells (Robbins et al, 1993) and sympathetic ganglion cells (Pfaffinger, 1988).

It was expected that, in concurrence with the above results, the addition of the stable analogue of GDP, GDPβs, to the pipette solution would prevent receptor-mediated inhibition of I_M; however, it produced no suppression of the ACh-mediated inhibition in NG108-15 cells, and only a partial block of the same in sympathetic ganglion cells. Although this result was not expected, it does not disprove the involvement of a G-protein. A likely explanation for this anomalous result is that the rate of GTP production in these cell types is high.

Once the presence of a G-protein had been confirmed, its identity was investigated.

Identity of the G-protein

Pre-treatment for 24 hours with 500 ng ml^{-1} of pertussis toxin, which inhibits the activation of G-proteins of the G_o/G_i variety, did not significantly reduce the inhibitory effect of ACh on I_M in sympathetic neurons (Pfaffinger, 1988).

Robbins et al (1992) also tested the effects of adding 2.5 mM of the C-terminal decapeptide of GAP-43 to the pipette solution – this would modify the activity of the G-protein, G_o. It had no effect on responses to ACh in M_1-mACh receptor-transfected NG-108-15 cells, meaning that the G-protein involved is not of the G_o variety.

These results indicate that the G-protein involved is of the pertussis toxin-insensitive G_q /G_{11} variety. In agreement with this are the observations of Jones et al (1995). They investigated the involvement of a G-protein in the transduction pathway between activation of the bradykinin B2 receptor and inhibition of the M-current, as well as the muscarinic M_1 receptor pathway (Jones et al, 1995). They carried out studies on rat sympathetic neurons, in which bradykinin would appear to be a very potent inhibitor of I_M. This inhibition was unaffected by pertussis toxin or microinjection of antibodies to $G\alpha_o$. It was however, selectively inhibited by microinjection of antibodies to $G\alpha_{q/11}$. Caulfield et al (1994) had concluded the same using the muscarinic agonist, oxotremorine-M on SCG cells. Haley et al (1998) transfected SCG neurones with DNA plasmids encoding antisense sequences against the 3' untranslated regions of Gα subunits, to further investigate the specific G-protein subunits involved in the inhibition of the M-current. In cells with reduced $G\alpha_q$, the muscarinic inhibition of I_M was attenuated, compared with that in uninjected cells, or those injected with $G\alpha_o$ antisense. In contrast, reduction of $G\alpha_{11}$ levels did not attenuate muscarinic inhibition of I_M. To investigate the possible involvement of the G-protein βγ dimers, Haley et al overexpressed the C terminus of β adrenergic receptor kinase (BARK 1), which binds free βγ subunits.

This did not attenuate muscarinic inhibition of the M-current at a concentration which can reduce βγ mediated inhibition of calcium current via muscarinic M_2 and M_4 receptors (Delmas et al., 1998). They also found that overexpression of $\beta_1\gamma_2$ dimers did not reduce the M-current density in SCG neurons. This work suggests that the α subunit of G_q as the subunit involved in muscarinic inhibition of I_M. From more recent work in $G\alpha_q$ knock-out mice, Haley et al. (2000) report that murine muscarinic M-current inhibition is mediated in part by G_q, more substantially by G_{11}, and partly by a PTX-sensitive G-protein, whereas the bradykinin-induced I_M inhibition in mice is mediated wholly by G_{11}. The transduction pathways in rat and mouse neurons appear to be different, and most of my work has been carried out in rat SCGs, but information on other cell types could provide useful clues nonetheless.

Pertussis toxin (100 ng ml^{-1}) did not alter the UTP-induced inhibition of I_M in SCG neurons (Bofill-Cardona et al, 2000). This inhibition was also unaffected by pre-treatment with Cholera toxin. Bofill-Cardona et al also found that the inhibitory actions of bradykinin (1 μM) and the muscarinic agonist oxotremorine M (10μM) on I_M were unaffected by pre-treatment with either toxin.

Thus, the above results indicate that a G-protein of the G_q/G_{11} variety is involved in the transduction pathway between receptor activation and I_M inhibition. They also suggest that it is the α subunit of this G-protein, rather than the βγ dimer, which is involved.

1.2.2 The involvement of a diffusible Second Messenger, and its identity

Experiments were carried out to determine whether this G-protein interacts directly with M-channels, or whether a diffusible second messenger is necessary (Selyanko et al, 1992).

It was originally proposed by Adams et al (1982b) that a cytoplasmic messenger generated by a cascade reaction subsequent to G-protein activation is involved. This proposal was tested using the patch-clamp method on rat sympathetic neurons. Single M-channel currents within the cell-attached patch were recorded and the effects of applying muscarine via the patch pipette and then to the cell membrane outside the patch were investigated.

If the inhibition results from a membrane-delimited interaction between the receptor and adjacent channels, only the former method of agonist application would have produced inhibition of I_M. Alternatively, if a diffusible messenger were necessary, the latter method would have produced results.

In fact, Selyanko et al (1992) found that M-channel activity persists when muscarine is applied via the pipette and is inhibited when it is applied to the cell membrane outside the patch. This probably indicates the existence of a diffusible second messenger, which transmits the message from receptors outside the patch to M-channels within it. Also, suppression of the M-current occurs with an obvious delay and is slow to develop, which further suggests the participation of a diffusible second messenger.

Marrion suggests however, that action on a cell-attached patch does not necessarily exclude the direct action of a G-protein (Marrion, 1997a). He questions previous assumptions that the interface between the membrane and the patch pipette glass prevents access of the activated G-protein to its substrate. He suggests that it is the lifetime of the activated G-protein (i.e. before the GTP bound to it is hydrolysed and the α subunit becomes deactivated) that determines whether it could travel far enough to cross this interface.

The Identity of the Second Messenger

G-proteins of the G_q/G_{11} subtype couple to phospholipase C (to be described in detail later), which hydrolyses phosphatidylinositol 4,5, bisphosphate. Much interest has been shown recently in the possible role of phosphoinositides in the inhibition of the M-current i.e. the hydroysis of phosphatidylinositol 4,5 bisphosphate (PIP_2) and its subsequent removal from M-channels, causing channel closure. As much of my work also focuses on this possible pathway, I shall discuss the findings to date in detail. However, I shall precede this discussion with an outline of the literature on other possible second messengers. There are many who contest the theory of phosphoinositide involvement, or certainly in the coupling pathways of some receptors to M-current inhibition, and without conclusive proof to the contrary, other avenues must be considered.

In fact, the only part of this pathway that has been proven is the G-protein of the $G_{q/11}$ variety. This G-protein couples to phospholipase C (PLC), so PLC itself

and the products/ consequences of its activation are obvious candidates for investigation.

Involvement of phospholipase C

Phospholipase C hydrolyses the phospholipid phosphatidylinositol 4,5 bisphosphate, generating inositol 1,4,5 trisphosphate (IP_3) and diacylglycerol (DAG). Any receptor which couples to this pathway suppresses the M-current. Fukuda et al (1988) found that acetylcholine suppressed the M-like current in NG108-15 cells expressing the M_1 or M_3 subtypes of the muscarinic acetylcholine receptor (mAChR; which are coupled to the PLC hydrolysis of PIP_2) but that it did not suppress the M-like current in NG 108-15 cells expressing the M_2 or M_4 mAChR subtypes (not coupled to PLC hydrolysis of PIP_2). This suggests the involvement of the PLC cascade. (Many of the experiments to investigate the transduction mechanism were carried out on the mouse neuroblastoma x rat glioma cell line (NG108-15 cells). These cells are useful for M-current investigations because they are easy to culture and also because of the presence of another current, $I_{K(Ca)}$. $I_{K(Ca)}$ is a transient, outward potassium current which is activated when IP_3 causes a release of calcium from the endoplasmic reticulum. The presence of this current proves useful as an index of Ca^{2+} release via the PLC-IP_3-Ca^{2+} cascade.

Neomycin, which inhibits phospholipase C-induced IP_3 production, prevented the generation of $I_{K(Ca)}$ by acetylcholine in M_1-mACHR -transfected NG-

108 cells. This demonstrates that it was indeed having the expected effect on the cell. ACh-mediated inhibition of I_M was unaffected by the same concentration of neomycin, suggesting that phospholipase C is not involved in the muscarinic pathway for inhibition in NG-108 cells (Robbins et al, 1992).

Another compound for investigating the inhibition of PLC is the aminosteroid U73122 (and also its inactive analogue U73343; Jin et al., 1994). Cruzblanca et al reported, in 1998, that 1μM U73122 greatly suppressed the bradykinin-induced inhibition of I_M in rat SCG neurons, but had no effect on the muscarinic inhibition (Cruzblanca et al. 1998). In 2000, Bofill-Cardona et al. observed a similar result from their experiments with U73122 – treatment for 15 minutes with 1μM of the aminosteroid greatly reduced bradykinin- and UTP-induced M-current inhibition but had less of an effect on the oxotremorine M-induced inhibition (although it did reduce average inhibition from around 80% to around 52%). The inactive analogue U73343 had no effect on any of the agonists' ability to inhibit I_M. Later on, in 2002, Suh and Hille found that increasing the concentration of U73122 from 1μM to 3μM significantly suppressed the muscarinic pathway as well as the bradykinin pathway (while the same concentration of the inactive analogue, U73343, had no effect on either pathway), suggesting that the muscarinic pathway also involves phospholipase C (Suh and Hille, 2002).

If phospholipase C were shown not to be involved, this would provide strong evidence that it is not depletion of PIP_2 which is responsible for M-current inhibition (but not conclusive as there other ways to reduce PIP_2), but proving that PLC is

involved does not prove the involvement of PIP_2 depletion. Activation of phospholipase C is responsible for the generation of inositol 1,4,5 trisphosphate (IP_3) and diacylglycerol (DAG), via hydrolysis of phosphoinositide 4,5 bisphosphate. IP_3 and DAG also activate several other second messengers. Below is a discussion on the progress made in investigating some of the second messengers produced by activation of PLC.

Involvement of Protein Kinase C (PKC)

PKC is activated by DAG (one of the products of PIP_2 hydrolysis by PLC). Phorbol esters, which cause activation of PKC (Brown et al, 1988), have been shown to suppress M-currents in a number of cell types; namely sympathetic neurons (Brown et al, 1989), NG108-15 (Higashida and Brown, 1986) and PC12 cells (Villarroel et al, 1989). This phorbol ester-induced suppression of I_M is antagonised by inhibitors of protein kinase C, such as staurosporin, but agonist-evoked inhibition is not affected. This finding suggests that PKC is not involved in the transduction pathway.

Robbins et al (1993) found that neither phorbol dibutyrate (PDB) nor staurosporin (activator and inhibitor of PKC respectively) had a significant effect on ACh-mediated suppression of the M-current in NG108-15 cells – further evidence against PKC's role in agonist-induced suppression.

Marrion's opinion (expressed in his 1997 review 'Control of M-current'), is that protein kinase C may be responsible for part of the effect of agonist upon the M-current. He bases this idea around the fact that data gathered from investigations with phorbol esters suggests the existence of two interconvertible populations of M-channels. These two populations differ in that one is only responsive to suppression by an agonist and the other is sensitive to both phorbol esters and agonist. He argues that as the M-current in so many different cell types is sensitive to phorbol esters, it is too early to exclude the role of PKC in agonist-mediated suppression altogether.

In a recent publication, Hoshi et al. (2003) report that PKC bound to A-kinase anchoring protein 150 (AKAP 150) participates in serine phosphorylation of KCNQ2, which facilitates M_1-mAChR-induced inhibition of the M-current. A mutant form of AKAP 150 (AKAP ΔA), which cannot bind PKC, and also PKC inhibitors (which compete with DAG) reduced M_1-mAChR-induced KCNQ2 phosphorylation and hence, M-current inhibition.

Arachidonic Acid

Arachidonic acid can be formed by the metabolism of DAG by diglyceride lipase or via the action of phospholipase A_2 (activated by an IP_3-mediated rise in cytosolic Ca^{2+} concentration). Marrion (1997a) reports evidence for the

involvement of arachidonic acid (or one of its metabolites) in the modulation of M-current (although not necessarily its inhibition, see later).

Somatostatin enhances M-current in hippocampal neurons, an enhancement that is mimicked by application of arachidonic acid (Moore et al, 1988). Also, leukotriene C4 (LTC4) can augment M-current and the action of somatostatin in these cells. LTC4 is produced when arachidonic acid is metabolised by 5-lipoxygenase. The action of somatostatin can be blocked by a lipoxygenase inhibitor (Schweitzer et al, 1990), which suggests that activation of somatostatin receptors causes the release of arachidonic acid from hippocampal neurons (Kanterman et al, 1990).

In the above experiments, arachidonic acid, its activators and metabolites have been shown to enhance M-current, but muscarinic agonists (plus bradykinin, UTP etc) only induce suppression. Arachidonic acid has also been found to enhance the M-current in bullfrog sympathetic neurons (Yu et al, 1995), although in these cells a metabolite of arachidonic acid formed by 12-lipoxygenase appears to be responsible (i.e. 12-HETE).

Robbins et al (1993) reported inhibition of I_M by > 10μM arachidonic acid in NG108-15 cells. This inhibition appears not to be due to metabolism of arachidonic acid by the lipoxygenase or cyclo-oxygenase (COX) pathways because the same effect could be produced using ETYA, an analogue of arachidonic acid, which actually inhibits these two enzymes. Arachidonic acid has been found to activate certain isozymes of phospholipase C (PLC-γ) (Rhee, 2001) so it could in fact be inhibiting I_M here by stimulating hydrolysis of PIP_2.

Further evidence to discount the involvement of COX or lipoxygenase was provided by experiments that showed that the action of arachidonic acid was not prevented by indomethacin or nordihydroguaretic acid (NDGA), inhibitors of COX and lipoxygenase respectively.

In experiments involving agonist-induced suppression of I_M in NG108-15 cells, Robbins et al found that ACh-mediated suppression was not significantly reduced in the presence of 50μM ETYA, 50μM NDGA, 50μM indomethacin or the phospholipase inhibitor BPB. They conclude that it is unlikely that arachidonic acid and its metabolites contribute significantly to the inhibitory action of ACh.

Inositol Trisphosphate (IP_3) and/ or a rise in intracellular calcium

IP_3 can act to liberate calcium from intracellular stores, so if IP_3 is involved in the transduction pathway between receptors and M-current inhibition, it is most likely to be due to this property.

There is, in fact, conflicting data on the subject of whether or not different agonists produce a calcium rise when they stimulate IP_3, with some studies showing a rise in intracellular calcium only when the cell is stimulated with bradykinin and not the muscarinic agonist oxotremorine M, and others showing rises (albeit variable in magnitude) by both agonists :-

Pfaffinger et al (1988) reported that a rise in intracellular calcium is associated with agonists that cause suppression of the M-current in frog sympathetic neurons.

Marsh et al (1995) did not detect a rise on addition of the muscarinic agonist oxotremorine M to rat sympathetic neurons, but this may be because the methods of Ca^{2+} detection used (i.e. FURA 2/ INDO imaging of the entire cell, without taking confocal slices) would be unable to resolve a rise if it were highly localised to the submembrane area. Del Rio et al (1999) detected an oxotremorine M-induced rise in calcium with FURA 2 in rat sympathetic neurons voltage clamped at -25mV but not when clamped at -60mV. Delmas et al (2002) detected calcium rises in superior cervical ganglion neurons on agonist stimulation of the bradykinin receptor, but not the M_1-mACh receptor. They attribute this to coupling of bradykinin receptors to IP_3 receptors via spatially restricted complexes, a link not formed between M_1-mACh receptors and IP_3 receptors. However, this work was carried out in neurons voltage-clamped at -60mV, and Delmas refers to the aforementioned publication by del Rio et al when he states that, in fact, the resting level of cytosolic calcium can influence the coupling of M_1-mACh receptors to IP_3 receptors. Del Rio et al have shown this by recording rises in cells held at the depolarised voltage of -25mV, where calcium entry is stimulated, raising resting calcium levels. The modern hypothesis appears to be then, that both agonists are able to mobilise calcium at depolarised potentials, but bradykinin produces a stronger, larger calcium signal.

Several early studies on different cell types reported that IP_3 applied directly to the intracellular solution (in the absence of added calcium chelators) did not inhibit the M-current, either when applied via iontophoretic injection or a more sustained application via the patch pipette. This held true in bullfrog (Pfaffinger et

al, 1988), and rat (Brown et al, 1989) sympathetic neurons and in NG108-15 cells (Robbins et al, 1993). In the cell line, the transient Ca^{2+}-activated K^+ current was induced by both methods of IP_3 application, indicating that it was dialysing into the intracellular fluid properly.

Chen et al (1993), reported that intracellular application of heparin (which is an IP_3 receptor antagonist and therefore prevents the IP_3-induced release of Ca^{2+} from the intracellular store), does not block suppression of M-current by muscarine in bullfrog sympathetic neurons. Robbins et al (1993) found that 1mM heparin did suppress ACh-mediated inhibition of I_M in NG108-15 cells. They explained this result by citing the poor selectivity of heparin for the IP_3 receptor. In fact, heparin has been shown to inhibit receptor coupling to G-proteins (Willuwett and Aktories, 1988) so the effect of intracellular heparin on the ACh- and noradrenaline-mediated inhibition of $I_K(Ca)$ was investigated. Suppression of this transient current by the two agonists is unlikely to involve IP_3 as both inhibitions are mediated by a pertussis toxin sensitive G-protein (which does not couple to phospholipase C). The inhibitory effect of both agonists on $I_K(Ca)$ was reduced by 1mM heparin, which suggests that interference at the G-protein level was behind its effects on I_M inhibition.

Intracellular application of IP_3 in CA1 hippocampal pyramidal cells does appear to suppress the M-current (Dutar and Nicoll, 1988). Cruzblanca et al reported that dialysis of rat sympathetic neurons with 100μM IP_3 significantly reduces M-current density. M-current density in IP_3-dialysed cells had decreased by 51% more at 10 minutes after breakthrough than in cells dialysed with a control

intracellular solution (Cruzblanca et al, 1998). This dialysis also reportedly greatly attenuated the ability of bradykinin to inhibit the M-current, reducing the maximum inhibition of this agonist from 49.2 ± 6.0% (n=4) to 5.0 ± 3.2% (n=6). The publication also states that the inhibition by oxotremorine M was not attenuated by the dialysis with IP_3. This inhibition by IP_3 is suggested to be due to the liberation of intracellular calcium rather than a direct action of IP_3 itself, as both depletion of intracellular calcium stores with thapsigargin and antagonism of the IP_3 receptor with either heparin or PPS, a polyanionic synthetic polymer of β-D-xylopiranose, blocked the bradykinin-induced inhibition of the M-current (Cruzblanca et al., 1998). The above summary of information appears to rule out the direct action of IP_3 on M-channels as a possible second messenger, but suggests that IP_3 is involved in the inhibition of the M-current by some agonists by virtue of its ability to mobilize intracellular calcium.

Adams and Brown showed in 1982 that the M-current in bullfrog sympathetic ganglion neurons is unaffected either by removal of extracellular calcium or intracellular iontophoresis of calcium (Adams and Brown, 1982). Since then, contradictory results have been obtained, such as those reported by Tokimasa and Akasu (1990), who found that removal of extracellular Ca^{2+} did in fact reduce M-current. Kirkwood et al (1991) suggested that the agonist-induced rise in intracellular calcium concentration by may be involved in suppression of the M-current in frog sympathetic neurons when this agonist-induced inhibition of the M-current was blocked by high concentrations of BAPTA. In the same year, Beech et al found the same to be true in rat sympathetic neurons, but they proposed that this

effect of BAPTA may actually be a result of the intracellular calcium concentration being lowered to below resting levels by the chelator rather than prevention of the agonist-evoked rise (Beech et al, 1991). This tells us, unsurprisingly, that the transduction pathway requires a minimum cytosolic calcium concentration.

Pfaffinger et al (1988), among others, found that high concentrations of intracellular BAPTA had little/ no effect on agonist-evoked suppression of the M-current, however several other papers were published at the end of the 1990s which point out differences in the sensitivities of M-current inhibition, by different agonists, to intracellular calcium chelation and PLC inhibition. Cruzblanca et al (1998) state that M-current inhibition by bradykinin was suppressed by the phospholipase C inhibitor U73122, was also suppressed by buffering intracellular calcium with 20mM of the calcium chelator BAPTA, and was occluded by allowing IP_3 to diffuse into the cell via the patch pipette. They reported that the muscarinic inhibition was not suppressed by any of these treatments.

Another agonist which couples to inhibition of the M-current, the purinergic agonist UTP, appears to utilize the same, calcium dependent pathway as bradykinin. Bofill-Cardona et al (2000) demonstrated that UTP inhibits M-channels in SCG neurons in a PLC, IP3 and calcium-dependent manner. The UTP-induced inhibition of the M-current was blocked by the PLC inhibitor U73122, but not by the inactive analogue U73343 (Jin et al, 1994). Xestospongin C, a noncompetitive antagonist of IP_3 receptors (Gafni et al, 1997), greatly reduced the inhibitory effect of UTP on I_M. It had no effect on the inhibitory effect of oxotremorine M on the M-current, which proves that it was not interfering with the receptor-mediated

modulation of I_M by some unspecific effect. Thapsigargin, which depletes intracellular calcium stores in SCG neurons via inhibition of the endoplasmic Ca^{2+}-ATPase, significantly reduced the inhibitory action of UTP on the M-current and intracellular application of BAPTA prevented the inhibition of I_M by UTP. Removal of extracellular calcium however, had no effect on this inhibition, which suggests that it is release of calcium from intracellular stores, and not transmembrane entry of calcium, which is involved in the transduction pathway between UTP receptors and inhibition of I_M. ATP is an agonist at the same purinergic receptor subtype as UTP (the P_{2Y} receptor), but appears to inhibit the M-current via a different mechanism to that used by UTP. It is reported that the ATP-induced M-current inhibition in bullfrog sympathetic neurons is attenuated by U73122 (but not the inactive isomer), but it is not attenuated by inhibiting PKC or by preventing the IP_3-dependent calcium rise, either by depleting the intracellular stores with thapsigargin, or by antagonizing the IP_3 receptors with heparin or xestospongin C (Stemkowski et al., 2002).

Selyanko and Brown used single channel recordings in 1996 to investigate the effect of direct application of calcium to excised membrane patches from rat SCG neurons (Selyanko and Brown, 1996). They recorded rapidly and reversibly inhibited M-channel activity on application of calcium in 28 out of 44 patches. The fact that this effect was reversible on removal of calcium, and also persisted in the absence of ATP, implied that it was not due to phosphorylation or dephosphorylation. This suggests that calcium might act directly on the M-channel

and does not depend on the activity of an associated kinase or phosphatase (Selyanko and Brown, 1996; Marrion, 1997). However, the fact that only 28 out of 44 patches responded to calcium encouraged the idea that the effect of calcium is not direct, but results from an action on a secondary protein which does not always remain associated with the patch when it is excised (Marrion et al, 1997a). Saimi and Kung's 2002 review on calmodulin highlights its actions as the calcium sensor of several types of calcium-modulated ion channel which are modulated without the involvement of kinases or phosphatases (Saimi and Kung, 2002). Gamper and Shapiro (2002) investigated the role of calmodulin as the calcium sensor which translates the bradykinin-induced calcium rise into M-channel closure. They found that the bradykinin-induced inhibition of M-current was greatly reduced in rat SCG neurons transfected to overexpress either wild-type calmodulin or a dominant-negative form of calmodulin. They explain the reduction in inhibition in both transfected cell types (rather than just those expressing the dominant negative) by pointing out that overexpression of the wild-type increases tonic calcium modulation i.e. mimics the bradykinin-induced suppression of the M-current, so therefore the M-current density in these cells should be greatly reduced already. The current in the wild-type CaM was indeed much smaller than in control or DN CaM expressing cells, which held up their theory. Importantly, the muscarinic inhibition of the M-current was unaffected by the expression of CaM or its dominant negative.

According to this literature, bradykinin and M_1 muscarinic receptors couple to inhibition of the M-current via different transduction pathways. UTP is reported to

inhibit the M-current via the same, calcium-dependent pathway as bradykinin (Bofill-Cardona et al, 2000). This pathway is sensitive to block by the PLC inhibitor U73122, by inhibition of IP_3 receptors, by pre-emptying of the intracellular calcium stores or by chelation of the IP_3-induced calcium rise. The muscarinic pathway is reported to be either less sensitive or insensitive to these treatments, although it has now been shown to involve phospholipase C. ATP is reported to inhibit the M-current in frog neurons via a PLC-dependent, but calcium-independent pathway (Stemkowski et al., 2002). Gamper and Shapiro's theory is that the bradykinin pathway is dependent on calmodulin ie calmodulin is bound to the channels and commutes the IP_3-induced calcium rise into channel closure, while the muscarinic pathway does not involve calmodulin but possibly does involve a phosphoinositide (Gamper and Shapiro, 2002; Suh and Hille, 2002).

This chapter so far has introduced the subject of the pathway(s) involved in agonist-induced inhibition of the M-current. Apart from the Gamper and Shapiro paper (Gamper and Shapiro, 2002), it seems that most of the recent publications on the subject have focussed on the muscarinic pathway for inhibition of I_M, and have investigated the proposed involvement of the depletion of phosphatidylinositol 4,5 bisphosphate in the closure of M-channels. Many studies have looked at the products of phospholipase C activation as possible second messengers, but it is only recently that they have started to focus on what is depleted by PLC.

1.3 Phosphoinositide 4,5 bisphosphate (PIP_2) and regulation of the M-current

Almost twenty years ago, Higashida and Brown (1986) observed that bradykinin causes hydrolysis of PIP_2 AND inhibition of the M-current, but they did not link the two directly together, instead postulating on the activation of diacylglycerol (DAG – a metabolite of PIP_2) as the inhibitor. Stimulation of ALL receptors which mediate inhibition of the M-current leads to hydrolysis of PIP_2 via activation of G-proteins and phospholipase C. Recently, much attention has been given to this hydrolysis as the possible mechanism for M-current inhibition.

1.3.1 What is PIP_2 ?

PIP_2 belongs to a group of intracellular molecules known as phosphoinositides. These phosphoinositides are a group of phospholipids with the common feature of an inositol head group, but with different properties according to the number and position of phosphate groups attached to this inositol ring. PIP_2 is found predominantly in the inner leaflet of eukaryotic plasma membranes (Tolias and Carpenter, 2000)

Inositol exists as a molecule on its own and is found in the cytosol. Phosphatidylinositol (PI) is formed by the fusing of inositol and a phosphorylated form of DAG by PI synthase in the endoplasmic reticulum. PI is then transported to the plasma membrane, in exchange for phosphatidylcholine, by PI transfer protein (PI-TP). In the membrane, activation of phosphatidylinositol 4 kinase (PI 4-K) adds

a phosphate group at the "4" position on the inositol ring, producing phosphatidylinositol 4-phosphate (PIP). The polyphosphoinositide of interest in terms of M-current inhibition is the next in the sequence, phosphatidylinositol 4,5 bisphosphate (PIP_2). This is formed from PIP by the addition of a phosphate group at the "5" position on the inositol ring, catalysed by the enzyme phosphatidylinositol 4,5-kinase (PI 5-K). PIP_2 can also reportedly be formed via phosphorylation of PI 5 P at the "4" position, but this pathway produces only a very small percentage of PIP_2 (Tolias et al., 2000).

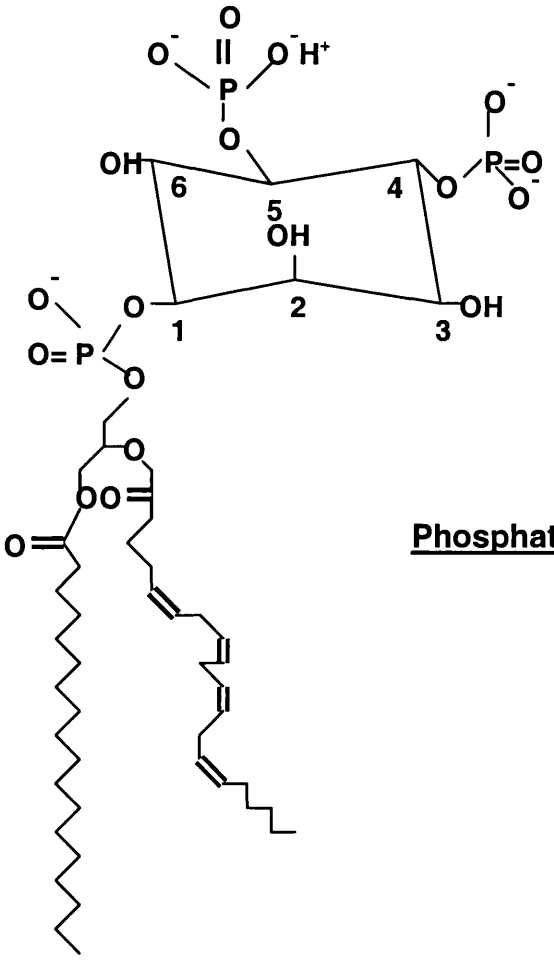

Figure 1.2. Chemical structure of PIP_2 (proportions not accurate). Figure adapted from McLaughlin et al., 2002).

PIP_2 can be further phosphorylated by phosphatidylinositol 3,4,5-kinase (PI 3-K) to produce phosphoinositide 3,4,5 trisphosphate (PIP_3). Phosphorylation at any stage in the cycle by different kinases can lead to the formation of polyphosphoinositides of different configuration i.e. differently placed phosphate groups such as in phosphoinositide 3,4 bisphosphate (PI 3,4 P_2). There are many different variations, their properties being determined by the phosphorylation state; however phosphatidylinositol 4,5 bisphosphate is the major polyphosphoinositide in mammalian cells (McLaughlin et al, 2002), comprising over 99% of the doubly phosphorylated phosphoinositides (Vanhaesebroeck et al., 2001) and its most abundant precursor is PI 4 P formed from PI (phosphate group at the "1" position).

When PIP_2 is hydrolysed by phospholipase C (as discussed in detail in a later section), it is cleaved into its two constituent parts, inositol 1,4,5 trisphosphate (IP_3) and diacylglycerol (DAG). IP_3 travels into the cytosol where it is eventually dephosphorylated sequentially by the inositol phosphatases, each removing one phosphate group, until inositol is left. Thus, the cycle begins again with the formation of phosphatidylinositol and so on. There is constant, basal activity in this cycle, so at rest there is always movement between the various states of phosphorylation, although comparable rates of phosphorylation and dephosphorylation keep the proportions of each phosphoinositide in the total phosphoinositide pool fairly stable. PIP_2 comprises about 1% of the phospholipid in the plasma membrane in human erythrocytes (McLaughlin et al, 2002) and about 2.2% in PC12 cells (Koizumi et al., 2002). Although I have stated earlier that PIP_2 is the most abundant phosphoinositide in mammalian cells, we must not forget that

there are many other types of phospholipid. McLaughlin et al (2002) state that if all the phospholipids in the plasma membrane of a typical mammalian cell (assumed spherical with a 10μM radius) were dissolved in the cytoplasm, then they would be present at an effective concentration of around 1mM. If PIP_2 makes up about 1% of these phospholipids then the effective concentration of PIP_2 in the cell is around 10μM (so, presumably they are at a much higher concentration in the plasma membrane as the volume is so much smaller). PIP_2 has many reported functions inside the cell, aside from production of the second messengers IP_3 and DAG when it is hydrolysed by PLC. These two products of PIP_2 hydrolysis themselves activate other second messenger pathways in the cell, such as Ca^{2+} release from intracellular stores and activation of protein kinase C (PKC). PIP_2 also acts as the substrate for the enzyme PI 3-kinase, which adds a phosphate group at the "3" position to form phosphatidylinositol 3,4,5 trisphosphate (PIP_3), itself a valuable cellular second messenger (Czech, 2000). PIP_2 also acts as a membrane anchor, functions in cytoskeletal attachment to the membrane (decreasing the level of PIP_2 produced a dramatic release of the cytoskeleton from the membrane (Raucher et al., 2000)), has been shown to be involved in exocytosis, endocytosis, membrane trafficking and, most importantly for the purposes of this thesis, PIP_2 has been shown to be involved in the regulation of ion channels (as discussed later).

Below is a simplified diagram of the phosphoinositide cycle

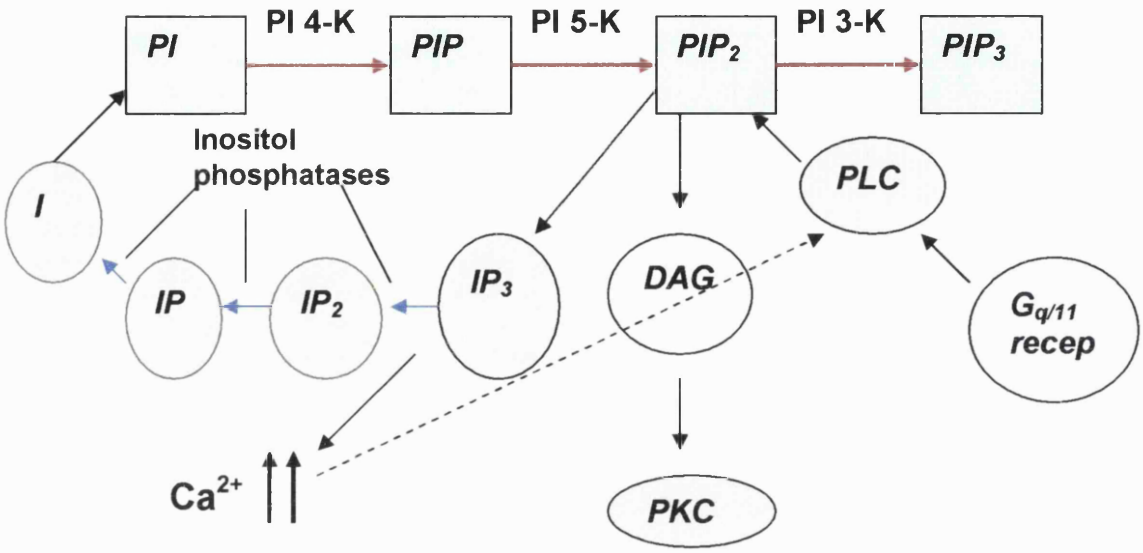

Figure1. 3. Simplified diagram illustrating the phosphoinositide cycle

1.3.2 Hydrolysis of PIP_2 by phospholipase C

PIP_2 is postulated to be bound to the channels in their open configuration, therefore keeping them open (Zhang et al., 2002; Suh and Hille, 2002; Ford et al., 2003). Phosphoinositide-specific phospholipase C isozymes are a related group of proteins that cleave the polar head group from inositol phospholipids, such as PIP_2, and are under the control of cell surface receptors. There are eleven different mammalian isoforms of phospholipase C, four of the β subtype, two of the γ, four of the δ and one of a recently discovered subtype, ε. It is believed to be a member of

the PLC-β subtype which couples receptors to M-current inhibition (Haley et al, 2000).

Activation of phospholipase C subtypes

The α subunits of all four members of the G_q subfamily (α_q, α_{11},α_{14} and α_{16}) can activate PLC-β isozymes but not PLC-γ, PLC-δ or PLC-ε (Lopez et al., 2001; Taylor et al., 1999; Smrcka et al., 1991). Not all of the PLC-β isozymes are expressed in all neurons, with β_2 expressed only in hematopoietic cells and β_4 limited only to certain neuronal cells. The receptor types which couple to the M-current in rat sympathetic neurons, eg bradykinin and muscarinic M_1, are proposed to activate the $G\alpha_q$-PLC-β signalling pathway, so this subtype of PLC is almost certainly involved in the agonist-induced I_M inhibition we observe in rat SCGs (although perhaps not exclusively – see Discussion). This activation of PLC-β isozymes by Gα subunits most likely happens in the cell membrane, as activated GTP-bound $G\alpha_q$ subunits remain attached to the cell membrane even after separation from their associated βγ dimer and PLC-β is also loosely associated with the cell membrane (Rhee, 2001).

PLC-β isozymes, with the exception of PLC-β_4, are also activated by Gβγ dimers, but these dimers exhibit a high affinity only for -β_2, the enzyme not present in neuronal cells (Rhee, 2001), so it is unlikely that this activation pathway is involved in agonist-induced inhibition of the M-current in SCG neurons. In support of this, activation of $G_{i/o}$ G-proteins does not cause inhibition of the M-current, even though these subtypes also liberate βγ subunits.

PLC-γ is activated by receptor protein tyrosine kinases, however this action is initiated by activation of growth factor receptors (Noh et al., 1995) and these receptors have not been shown to couple to inhibition of the M-current; neuronal growth factor (NGF) is used in the culture medium for SCG neurons, and increasing the concentration of NGF in the media does not reduce the current density of the M-current (Marsh and Winks, unpublished results). Antigen and immunoglobulin receptors also couple to activate PLC-γ, but again these receptors do not couple to inhibition of I_M. The only way in which the receptors we are concerned with could possibly activate this subtype of phospholipase C is via the production of PI 3,4,5 P_3 from PIP_2 by PI 3 kinase. PIP_3 interacts with the PH domain of Bruton's tyrosine kinase, which contributes to PLC-γ activation (Rhee, 2001). PI 3 kinase is activated by βγ dimers, which are liberated on activation of G-protein-coupled receptors. Arachidonic acid also stimulates PLC-γ (Hwang et al., 1996) as does phosphatidic acid (Jones and Carpenter, 1993; Zhou et al., 1999), an immediate product of phospholipase D. Arachidonic acid has been observed to modulate the M-current (see earlier section on second messengers), but its normal action is to enhance the current rather than to inhibit it, which suggests it must have actions in neurons other than to activate phospholipase C-γ.

The mechanism(s) of activation of phospholipase C-δ isozymes by membrane receptors is less well understood than for the other subtypes, although it is known that the sensitivity of the δ isozymes to calcium is much greater than that of the β, γ or ε isozymes (Rhee, 2001; Young et al., 2003). An interesting observation by Kim et al. (1999) was that PLC-δ1 overexpressed in PC12 cells was

activated by capacitative calcium entry in response to the PLC-β/ IP_3 Ca^{2+} rise generated by bradykinin. This observation is most interesting, as it suggests a possible role for PLC-δ1 in the bradykinin-induced inhibition of the M-current (see Results and Discussion section for further discussion). PLC-δ is also potentially activated by a newly discovered type of G-protein, G_h. This G-protein is activated by α_1-adrenergic, oxytocin and thromboxane receptors.

PLC-ε is activated by growth factor activation of Ras, so is unlikely to be of interest with regard to M-current inhibition.

Structure of phospholipase C

Different subtypes of PLC differ in structure and size, the largest being the PLC-ε isozymes at 230-260 kDa and the smallest being PLC-δ at around 85 kDa, with the β and γ isozymes somewhere in between at 120-155 kDa . The amino acid sequences of the enzymes differ markedly between subtypes, but there are two relatively conserved regions, the X and Y regions, which form the catalytic core (ref) and have a sequence homology of around 60% among all 11 mammalian PLC isozymes. Members of the β, γ and δ subtypes all contain an NH_2 terminal pleckstrin homology domain (PH domain). PH domains are protein modules of approximately 120 amino acids in length, which were first described in pleckstrin, the major substrate for protein kinase C in platelets (Harlan et al., 1994). The PH domain is present in many signalling proteins and binds to polyphosphoinositides, including PIP_2. The β, γ and δ subtypes also contain EF-hand domains and a C2

domain. The β and γ isozymes contain additional regulatory motifs that are not present in the δ subtype.

All four subtypes of PLC require some Ca^{2+} for catalytic function, although the sensitivity of the δ-type isozymes is greater than that of the other three subtypes.

Mechanism of hydrolysis of PIP_2 by PLC

The PLC enzymes bind to the inositol head group of their polyphosphoinositide substrates via the PH domain. Eukaryotic forms of PLC have an order of substrate preference which is generally PI 4,5 P_2 > PI 4 P > PI. When bound to the substrate and catalytically active, the PLC enzyme catalyses hydrolysis of the phosphodiester bond connecting the glycerol backbone of the lipid moiety and the inositol polyphosphate headgroup of PIP_2, thereby cleaving PIP_2 into IP_3 and DAG.

1.3.3 PIP_2 as the regulator of ion channels

PIP_2 is known to be a regulator of ion channel activity. Its presence is necessary to maintain the open state of certain inwardly rectifying potassium channels. K_{ATP} and GIRK channels are maintained in the open state by the presence of bound PIP_2, and the agonist-mediated inhibition of these channels, which is via activation of pertussis toxin-insensitive G-proteins, has been shown to be due to the hydrolysis, and therefore depletion, of local PIP_2 (Huang et al., 1998; Kobrinsky et al., 2000; Xie et al., 1999). An increase in PIP_2 levels at the

cytoplasmic face of the sarcolemma in guinea pig ventricular cells lowers the sensitivity of K_{ATP} channels to inhibition by ATP (Oketani et al., 2002), and overexpression of the kinase which phoshonylates PIP to produce PIP_2 (PI 4 P 5-kinase) also reduces the sensitivity of this channel to ATP in a heterologous expression system (Shyng et al., 2000). In 2002, Runnels et al. reported that PIP_2 also controlled the activity of the Ca^{2+}-conducting channel TrpM7 (Runnels et al., 2002), and in the same year it was reported that receptor-mediated hydrolysis of PIP_2 caused inhibition of P/Q- and N-type voltage-gated calcium channels in both oocytes and neurons (Wu et al., 2002). Wu et al. stated that PIP_2 also inhibits P/Q-type channels by altering the voltage dependence of the channels and therefore making them more difficult to open.

PIP_2 binds to K_{ir} channels electrostatically when the negative charges on the phospholipids interact with specific residues on the channel (Lopes et al.,2002). Positively charged poly-lysine has been shown to block all KCNQ channels (family to which molecular correlates of the M-channel, KCNQ 2 and KCNQ 3 belong), and it is suggested that this is due to competition of the positively charged molecule with the channels for binding to negatively charged PIP_2 (Lopes et al., 2002).

The above information, combined with the fact that many studies have shown the involvement of PLC in the agonist-induced inhibition of the M-current, have led to the suggestion that PIP_2 depletion is responsible for M-channel closure.

Evidence so far for PIP_2 as a regulator of the M-current

Some of the investigations into whether net PIP_2 reduction does actually inhibit the M-current have been carried out on KCNQ 2/3 heteromers expressed in cell lines, and other experiments have been conducted on native M-channels in neurons.

Hydrolysis of intracellular ATP is required for the recovery of the M-current on agonist washout (Suh and Hille, 2002). This is proposed to be because recovery requires transfer of a phosphate from ATP for the regeneration of a product broken down during agonist inhibition i.e. PIP_2. This follows on from the work in 1998 by Simmons and Schneider that showed that the presence of a hydrolysable form of ATP in the pipette solution, or extracellular metabolic substrates such as glucose or pyruvate, were necessary to slow the rundown of I_M under whole cell recording conditions (Simmons and Schneider, 1998).

Wortmannin, at micromolar concentrations, is an inhibitor of the enzyme PI 4 kinase which phosphorylates PI to form PI 4 P, the precursor of PIP_2. Treatment of cells with wortmannin slowed or prevented recovery of the M-current, or KCNQ 2/3 heteromeric channels; this was the case in bullfrog sympathetic ganglion neurons (Ford et al., 2003), in superior cervical ganglion neurons (Suh and Hille, 2002) and expressed KCNQ 2/3 channels in tsA-201 cells (Suh and Hille, 2002). Use of a fluorescent marker for PIP_2, the green fluorescent protein-tagged pleckstrin homology domain of phospholipase C-δ_1 (GFP-PLCδ PH; Varnai and Balla, 1998; and see next section) indicates that wortmannin does slow regeneration of PIP_2 at the plasma membrane, (or possibly reduces IP_3

metabolism) and that this slowing correlates with the wortmannin-induced slowing of the M-current recovery (Zhang et al., 2002).

Interruption of the lipid cycle after diacylglycerol, with the DAG kinase inhibitor R59022 (40μM), caused a slowing of the recovery of the M-current after successive inhibitions by ATP (Ford et al., 2003). The slowing of the recovery here was suggested to be due to the prevention of PI generation by R59022, and the fact that recovery from inhibition by ATP became progressively slower with successive responses indicates that there was originally a pool of PI which had to be depleted before the slowing of the recovery was seen.

The addition of PIP_2 antibodies to the patch pipette significantly reduced ATP-induced M-current inhibition in bullfrog sympathetic ganglion neurons, but did not reduce the amplitude of the M-current in these cells per se (Ford et al., 2003). The PIP_2 antibody is reported to reduce M-current amplitude more in some cell types than others and it is proposed that this difference in effect stems from the different affinities of different channels for PIP_2 (Zhang et al., 1999).

PIP_2 applied to excised inside-out patches activated channels showing typical M-channel kinetics in rat SCG neurons (Zhang et al., 2002), indicating that PIP_2 activates native M-currents.

The above summary of recent findings suggests strongly that the depletion of PIP_2 is involved in the agonist-induced inhibition of the M-current, but the theory is not yet proven conclusively.

1.4 Green fluorescent protein-tagged phospholipase C-δ pleckstrin homology domain – a marker for PIP_2 levels in the plasma membrane

A novel fluorescent marker for PIP_2 hydrolysis, the pleckstrin homology domain of phospholipase C δ_1, tagged with a molecule of green fluorescent protein (GFP-PLC-δ PH), has been used to observe PIP_2 hydrolysis.

The GFP-tagged PLC-δ PH domain marker was developed in order to be able to visualize changes in PIP_2 levels in the cell's plasma membrane in response to stimuli. As mentioned earlier, it is the PH domain of a phospholipase C enzyme which binds to the inositol head group of its substrate. The PH domain of PLC-δ_1 has a very high affinity for PI 4,5 P_2 (K_D = 1.7μM) and also for I 1,4,5 P_3 (K_D = 0.21 μM) (Lemmon and Ferguson, 2000). The strong selectivity of PLC-δ PH for I 1,4,5 P_3 is illustrated by Ferguson et al (1995) who explain the importance of the phosphate groups at the 1, 4 and 5 positions, and that further groups at the 3 or 6 positions impede this binding (hence the lower affinity of the PLC-δ PH domain for PI 3,4,5 P_3).

The theory behind the GFP-PLC-δ-PH construct is that it should bind to PIP_2 and enable the experimenter to visualise the localization of this phospholipid in the cell via fluorescence microscopy. In the quiescent cell, the fluorescence should be localised to the plasma membrane as this is where PIP_2 is located. This has been shown to be the case in several cell types, and it has been reported that this membrane localisation of the GFP-PLC-δ PH construct is not entirely due to its binding to PIP_2, but that motifs located within the C-terminal half of the PH domain

provide auxiliary contacts with additional membrane components (Varnai et al., 2002). Varnai and Balla (1998) showed that binding to PIP_2 was necessary for this membrane localisation however, as mutations in three critical base residues within the PH domain, which have been shown to contribute to the high affinity binding of PLC-δ to PIP_2 (Ferguson et al., 1995), prevented this localisation; mutation of a non-charged residue in the same region had no effect (Varnai and Balla, 1998). Expression of GFP alone does not show a specific localization within the cell and is evenly distributed throughout the cytosol (Varnai and Balla, 1998; and my own observations). Varnai and Balla developed a GFP-PLC-δ PH construct and investigated its properties and its reliability as an indicator of spatiotemporal changes in PIP_2 at the single cell level. Despite their findings, and their conclusion that it is indeed a reliable indicator of PIP_2 depletion and resynthesis, other groups dispute this and argue that, because of the construct's higher affinity for IP_3 than for PIP_2, it is an indicator of IP_3 generation and breakdown rather than of PIP_2 depletion and resynthesis (Hirose et al., 1999; Nash et al., 2001; Nahorski et al., 2003).

It is reported that, in cells transfected with the GFP-PLC-δ PH construct, activation of endogenous PLCs by either receptor stimulation or by ionophores, produced rapid and reversible redistribution of the fluorescence from the membrane to the cytosol. According to Varnai and Balla, these changes in localisation of the fluorescent construct correlate very closely with cellular PIP_2 mass, as measured by lipid extraction followed by alkaline hydrolysis to liberate IP_3, which was then quantified by a radioreceptor assay. When the ratio between

plasma membrane and cytosolic fluorescence, and the total PIP_2 mass in the cell were plotted against time, there was a noticeable delay in the relocalisation of the fluorescent signal to the membrane, as compared with the resynthesis of PIP_2. Varnai and Balla explained this anomaly by pointing out that membrane relocalisation of the fluorescence was preceded by the appearance of fluorescence at intracellular sites, and suggested that these are the initial sites of PIP_2 resynthesis (after all, the measurement of PIP_2 mass is measuring PIP_2 mass throughout the whole cell and not just in the plasma membrane). There is opposition to these results however, as it is reported by Nash et al. (2001) that changes in cytosolic GFP-PLC-δ PH fluorescence most closely paralled the pattern of rising IP_3 levels in the cell rather than that of falling PIP_2 levels, also measured by radioreceptor-based assays (Nash et al., 2001). It is also reported that co-transfection of the construct along with the catabolic enzyme $Ins(1,4,5)P_3$ 5-phosphatase (this enzyme dephosphorylates IP_3 rapidly and so acts as an "IP_3 sink", preventing IP_3 accumulation in the cytosol) prevented agonist-induced translocation (Hirose et al., 1999). In favour of the use of the construct for monitoring PIP_2 levels rather than IP_3, Varnai and Balla investigated whether the inhibition of PIP_2 resynthesis, after ionomycin treatment and subsequent Ca^{2+} chelation, would prevent the plasma membrane relocalisation of the fluorescent construct. They inhibited the enzymes which generate PIP_2 from PI (PI 4-kinase ad PI 5-kinase), and compared these inhibitors' abilities to prevent PIP_2 resynthesis with their abilities to prevent the relocalisation of the GFP-PLC-δ PH construct to the plasma membrane. Inhibition of these two enzymes would still

allow IP_3 to accumulate in the cytosol as in a normal response. Both inhibitors, quercetin (100μM) and phenylarsine oxide (PAO; 100μM) prevented both the resynthesis of PIP_2 and the relocalisation of the fluorescent construct to the plasma membrane on chelation of calcium.

Another publication in favour of the construct being reliable as an indicator of PIP_2 hydrolysis is that by Van der Wal (2001). Van der Wal et al. monitored PLC-δ PH translocation via fluorescence resonance energy transfer (FRET) in response to rapid UV flash-evoked release of caged IP_3 (van der Wal et al., 2001). Cells were transfected with both CFP- (cyan fluorescent protein) and YFP- (yellow fluorescent protein) tagged versions of the PLC-δ PH construct and fluorescence energy transfer between the two constructs was used to monitor the localisation of the constructs (CFP was excited at 425 ± 5nm and the emission of CFP at 475 ± 15nm and of YFP at 530 ± 20nm were simultaneously monitored. When the constructs are at the plasma membrane they are within resonance distance and FRET occurs; when the constructs translocate away from the plasma membrane due to PLC-induced hydrolysis of PIP_2, the distance between the fluorophores increases and FRET no longer takes place between them. Thus, the donor (CFP) emission intensity increases, while the acceptor (YFP) emission decreases. The ratio of CFP to YFP emission is taken as a measure of the translocation of the PLC-δ PH construct). The amount of IP_3 produced during agonist-stimulation of the G-protein-coupled receptor/ PLC pathway has been measured at between 0.1 and 10μM (Varnai et al., 2002), and when this IP_3 is produced via hydrolysis of PIP_2,

the GFP-PLC-δ PH construct translocates away from the membrane and into the cytosol.

When Van der Wal et al (2001) used the flash photolysis technique to accurately release amounts of IP_3, no translocation was seen on release of 1μM IP_3, a very small amount at 10μM, and a larger amount at 100μM IP_3, although even the amount of translocation elicited by 100μM IP_3 was less than that induced by 1μM bradykinin. Van der Wal et al concluded that translocation of the GFP-PLC-δ PH construct was in fact reporting changes in PIP_2 rather than in IP_3, but that high concentrations of IP_3 (i.e. 100μM) could distort the PIP_2-reporting ability of this construct.

Xu et al. recently did an extensive study on the PIP_2/ IP_3 reporting properties of GFP-PLCδ PH (Xu et al., 2003), where they constructed a model to simulate localisation of the probe according to different changes in PIP_2/ IP_3 concentrations. They included parameters such as basal and max/ min levels of PIP_2 and IP_3, rates of PIP_2/IP_3 synthesis and decay at rest and during PLC activity, surface to volume ratio of the cell, the affinities of the probe for PIP_2 and IP_3 and the amount of probe present in the cell. They concluded that translocation is sensitive to both IP_3 and PIP_2 and that the extent of its sensitivity to each varies according to the surface to volume ratio of the cell and also, importantly, the amount of the probe expressed in the cell.

1.5 Aims of my PhD study

The aim of my PhD project was to investigate the transduction pathway between receptor activation and inhibition of the M-current. Recent developments in the field have led to this work focussing mainly on the phosphoinositide cycle and its involvement in this agonist-induced inhibition of I_M. I have looked at the effects of altering the activity of various members of the phosphoinositide cycle on the inhibition of the M-current by both the muscarinic receptor agonist oxotremorine M and the peptide bradykinin. I have used electrophysiological and microfluorescence techniques, and also a novel indicator of PLC activity (GFP-PLC-δ PH described above) to investigate the similarities and differences between the inhibition of the M-current by these different agonists, and the involvement of the phosphoinositide cycle in either or both.

CHAPTER TWO

Materials and Methods

2.1 Tissue Culture and preparation of neurons for experimentation

Superior Cervical Ganglion neurons (SCG) were cultured from 17-day-old Sprague Dawley rats (either sex) after terminal anaesthesia using CO_2, followed by decapitation in accordance with Home Office regulational procedures.

2.1.1 Dissection of rat superior cervical ganglia and culture of SCG neurons

On removal, SCG were immediately placed in a 35mm Petri dish containing Hanks Balanced Salts Solution (HBSS) plus 10mM Hepes. The SCG were then cleaned and cut into with small scissors to increase the surface area and therefore aid digestion. The clean SCG were then placed into collagenase solution (800 iu Collagenase Class 2 (*Sigma*), 12mg bovine serum albumin (BSA; *Sigma*) and 2ml HBSS + Hepes) and incubated for 15 mins at 37˚C. They were then washed twice with HBSS + 10mM Hepes and placed in trypsin solution (2mg trypsin, bovine type XII S (*Sigma*), 12mg BSA, 2ml HBSS + 10mM Hepes) for 30 mins at 37˚C.

Digested fragments were then transferred into 2ml growth medium (42ml L-15 + GlutaMAX (*Sigma*), 8.5ml 1.26% $NaHCO_3$ (24mM) (*Gibco*), 5ml FCS (*Sigma*), 1.15ml 30% Glucose, 0.61ml 200mM L Glutamine (2mM) (*Gibco*), 50ng/ml NGF 7S (*Sigma*)). The tissue was triturated until the mixture became cloudy, at which point the mixture was pulsed in the centrifuge and the supernatant transferred to a sterile centrifuge tube. This procedure was

repeated using a total of 10ml growth media, following which the cell suspension was spun for 5 mins at 800rpm, the supernatant poured off and the cells resuspended in 5ml growth media.

Sterile culture/ recording chambers, consisting of glass rings (diameter 16mm, height 3mm, approx volume 500µl) attached to borosilicate glass coverslips (BDH, 22 x 22mm, thickness 0.13-0.17mm) with silicone elastomer (Sylgard®, *Dow Corning*; cured at 180˚C for 2 hours), were coated with a laminin substrate for 1 hour (10µg ml^{-1} in HBSS). Just before use these chambers were placed into 35mm petri dishes, washed and cell suspension plated onto the coverslips. Dishes were then incubated at 37˚C in 95% O_2/ 5% CO_2 for 4 hours to allow cells to adhere to the coverslip before 500µl fresh growth medium was added. Dishes are incubated until required for transfection/ recording and are usually used within 4 days.

2.1.2 Transfection of SCG neurons via intranuclear injection

Neurons were injected one to two days after culture. Sharp electrodes (> 50MΩ resistance) were pulled from 1.2mm outer diameter, 0.69mm internal diameter non-filamented borosilicate glass (*Clark Biomedical*) and filled with cDNA plasmid dissolved in injection solution (154mM NaCl, 5mM Hepes, 2.5mM KCl, 0.5mM $MgCl_2$ – pH adjusted to ~ 7.4 using NaOH; after mixing with plasmid (100ng/µl of each cDNA plasmid to be injected), injection solution is filtered by centrifuging at 13000rpm in a 0.2µm filter, and is then refrigerated for a maximum of two weeks awaiting use).

Injections were performed using the Eppendorf automated micro-injector (Transjector 5246). CO_2 was maintained at ~ 5%, in the enclosed area where

the cells were placed, throughout the injection period. Positive pressure is constant and neurons were impaled briefly in the nucleus with the sharp electrode – transient swelling of the nucleus was visible as the cDNA plasmid/ injection solution entered. Several cells were injected in each dish as the survival rate varies with the health of the culture. After injection, neurons were returned immediately to the incubator to allow protein to express.

2.1.3 cDNA plasmids

A number of different cDNA plasmids have been used throughout this thesis. They are listed below.

eGFP-PLC-δ PH – pleckstrin homology domain of phospholipase C-δ_1, in egfp-C1 vector (*Clontech*). Obtained from K. Young (University of Leicester) and originally from T. Meyer (Stanford University).

NCS-1 – rat neuronal calcium sensor protein 1, in pcDNA 3.1 vector. Obtained from J. Weiss (University of Liverpool).

GFPmPIP 5-K-1 beta – phosphatidylinositol 4 phosphate 5-kinase enzyme in pcDNA 3.1 vector, containing GFP sequence or. Obtained from N. Davis (LSU Med. Ctr)

GFPmPI5-K-1 beta (K179M) – mutant phosphatidylinositol 4 phosphate 5-kinase, lacking kinase activity, in pcDNA 3.1 vector, containing GFP sequence. Obtained from N. Davis (LSU Med. Ctr)

eGFP – enhanced green fluorescent protein, in pcDNA 3.1 vector.

pDSRed2-N1– red fluorescent cloning vector (*Clontech*)

All plasmids contained the cytomegalovirus (CMV) promoter.

2.2 Electrophysiological recording

2.2.1 Apparatus

Neurons in culture/ recording chambers were transferred to the stage of an inverted Nikon Diaphot microscope and cells were superfused with external solution (see Methods section 2.2.4.1) via a gravity-driven system at ~ 10-12 ml/min. Cells were observed using a X40 oil immersion lens (*Nikon*).

Electrophysiological experiments were conducted under voltage-clamp conditions, using an axopatch 200A patch-clamp amplifier (*Axon Instruments*). Data was acquired using pClamp software (Clampex version 8.1; *Axon Instruments*). Voltage protocols were created within the Clampex program run on a Dell personal computer, and an input signal sent from the computer via an analogue-to-digital converter interface (Digidata 1200; *Axon Instruments*) to the amplifier. Data was sampled at 1kHz and filtered at 10kHz.

Chloride-coated silver wire was used both for the recording electrode and the bath ground, and these were freshly coated with chloride ions regularly via electrolysis in NaCl solution. Recording pipettes of 1.5-3 MΩ were pulled on a vertical pipette puller (*Narishige* PC-10) from thin-walled (1.5mm outer diameter, 1.17mm inner diameter) filamented borosilicate glass (*Clark Biomedical*) and the tips were fire-polished using a microforge (*Narishige*, MF-830).

2.2.2 Perforated-patch recording configuration

Currents were recorded in the perforated-patch clamp configuration unless otherwise stated. Recording in this configuration reduces dialysis of the intracellular compartment with the pipette solution, so reducing the loss of soluble components. Loss of certain cellular components through dialysis in the whole-cell recording configuration leads to current "rundown" (Brown et al., 1995).

In the perforated-patch recording configuration, the antibiotic amphotericin B was used to form pores in the plasma membrane in the patch within the seal formed between pipette and membrane (Rae et al., 1991). These pores are of a size which allow the flow of monovalent ions, and therefore allow electrical continuity between the recording pipette and the intracellular environment, but not the dialysis of larger molecules, so preventing the loss of vital intracellular components. Amphotericin B is stored in the fridge in powder form and a fresh solution of 2-3mg dissolved and sonicated in 10µl mg^{-1} dimethyl sulfoxide (DMSO) was made daily; 2µl this solution were added to 1ml filtered intracellular solution to produce a final amphotericin B concentration of 200µg ml^{-1}. Recording pipettes were dipped in filtered amphotericin-free intracellular solution for a few seconds before back-filling with the amphotericin-containing solution, as amphotericin can interfere with gigaohm seal formation.

After the formation of a gigaohm seal (>1 GΩ) between the recording pipette and the cell membrane, the cell was held in the cell-attached configuration at a membrane potential of -60mV as the amphotericin began to perforate the cell membrane and thus reduce the access resistance. Access resistance was monitored via the increase in transient capacity current

amplitude in response to a 10mV hyperpolarising pulse. When the access resistance has stabilised at around 10MΩ current recording can begin. Cells which stabilise at an access resistance greater than 20MΩ were discarded.

2.2.3 Whole-cell recording configuration

This recording configuration was used when it was necessary to dialyse the cell with the intracellular recording solution. This technique has been used occasionally in this thesis.

After the formation of a gigaohm seal in the cell-attached mode, the whole-cell configuration was achieved by applying a short and strong suction, resulting in the rupture of the membrane patch and a low access resistance (< 5MΩ).

2.2.4 Recording solutions

2.2.4.1 Extracellular

For electrophysiological recordings in the perforated patch configuration and for microfluorescence recordings (including calcium imaging) the following extracellular solution was used.

NaCl	120 mM
Glucose	11.1 mM
HEPES	5 mM
$NaHCO_3$	22.6 mM
KCl	3 mM

$CaCl_2$ 2.5 mM

$MgCl_2$ 1.2 mM

NaOH to pH 7.4

For experiments involving the whole-cell recording configuration, 2mM pyruvic acid was added to the above solution to try to reduce rundown of the M-current (Simmons and Schneider, 1998).

2.2.4.2 Intracellular solutions

For perforated-patch recordings of the M-current, the following standard solution was used

KCl – 30mM

K Acetate – 100mM

HEPES – 20mM

EGTA – 10mM

$MgCl_2$ – 3mM

KOH to pH 7.4

For perforated-patch recordings of the N-type calcium current (Chapter 4, section 4.3.2.5) the following intracellular solution was used:

CsCl – 140mM

$MgCl_2$ – 1mM

BAPTA – 0.1mM

$CaCl_2$ – 0.1mM

HEPES – 10mM

CsOH to pH 7.4

2.2.5 Voltage protocols

The standard protocol used for recording the M-current throughout this thesis is a depolarised holding potential of -20mV, to preactivate the current and also to inactivate some other transient contaminating currents that may be present, with a hyperpolarising pulse to -50mV to deactivate the M-current, allowing measurement of the deactivation tail.

The current-voltage relationship of the M-current was recorded using a holding potential of -20mV, with a 2 second hyperpolarising pulse every 20 seconds. The first hyperpolarising pulse was to -30mV, with subsequent pulses 10mV more hyperpolarised than the last, with the final pulse to -110mV.

For measurement of the calcium buffering capacity of the cell (Chap 4, section 4.3.2.5) N-type calcium currents were recorded by holding the cell at -70mV and depolarising to +5mV for 200ms. Currents were leak-subtracted by blockade with $CoCl_2$ and subtracting the blocked trace from the unblocked. A full explanation of this method as a measure of the cells' calcium buffering capacity, can be found in Chapter 4, section 4.3.2.5.

Analysis of M-current recordings is dealt with in Chapter 3.

2.3 Fluorescence microscopy

2.3.1 General Apparatus

Fluorescence microscopy was carried out using the same Nikon Diaphot inverted microscope described in the experimental apparatus for electrophysiology. The excitation light source was a monochromator (Polychrome II, *T.I.L.L. Photonics GmbH.*) The excitation wavelength was controlled using an Apple Macintosh computer and Openlab software (version 3.0), linked to a monochromator (as illustrated in Figure 4), and was varied according to which dye was being imaged. Light leaving the monochromator was reflected up onto the cells by a dichroic mirror (varied according to the desired excitation wavelength of the dye). Light passed through optional neutral density filters and also an electronically controlled shutter before reaching the cells, so as to control light intensity and exposure duration respectively, limiting photobleaching of the dye. Emitted light was passed through a bandpass filter (again, different wavelength for different dye) before being captured on to a 12-bit grey-scale digital camera (controlled by the computer). Focus and exposure time of the camera, digital gain and camera binning were adjusted to optimise the quality of the images.

2.3.1.1 GFP-PLC-δ PH/ GFP/ FITC imaging

Cells were excited at a wavelength of 475 nm, reflected by a 510 nm dichroic mirror. Emitted light was passed through a 530 nm bandpass filter, and a FITC pseudo colour palette was applied to the acquired grey-scale images. For monitoring of GFP-PLC-δ PH translocation successive images were taken with minimum delay (according to the exposure time of the camera but usually > 1 image per second). For more on acquisition and analysis of GFP-PLC-δ PH data please see Chapter 3 (section 3.3).

2.3.1.2 Red Fluorescent Protein (RFP)/ rhodamine/ TRITC imaging

Cells were excited at a wavelength of 535 nm, reflected by a 580 nm dichroic mirror. Emitted light was passed through a 610 nm bandpass filter, and a TRITC pseudo colour palette was applied to the acquired grey-scale images.

2.3.1.3 Digital deconvolution of images

Images obtained with the above equipment are subject to a certain amount of blurring, caused by light "haze" emitted from above and below the plane of focus. To remove this blurring without the use of laser confocal microscopy, a technique called "digital deconvolution" is employed. This technique corrects and removes the noise and haze originating from images in other focal planes using mathematical algorithms, the simplest of which is the "nearest neighbour algorithm" (Agard et al., 1989; Casteleman, 1996). This algorithm calculates the contribution of light noise from the focal planes above and below the desired slice, and subtracts them. An automation was designed

"in house", using Openlab software, which automatically focused the microscope to the bottom of the cell, and then programmed it to acquire several optical slices (≈ 20) in 0.5μm steps up through the cell. An image from a particular focal plane was corrected using the nearest 5 neighbours algorithm (ie using 5 optical slices above and 5 below the chosen plane). The algorithm contains the point spread function (P.S.F) of the microscope, which can be estimated once the objective, immersion solution, camera resolution and binning are known. Digital deconvolution of images enables the experimenter to visualise the localisation of fluorescence in the cell without the "noise" associated with convention optical microscopy. Examples of a standard image and a deconvolved image from the same cell are given in Chapter 3 (Figure 15, section 3.3.1).

2.3.2 Calcium imaging using the dual-excitation dye FURA 2

The imaging equipment used for recording changes in intracellular calcium concentration is essentially the same as that used for other imaging experiments.

FURA 2 is a dual-excitation fluorescent Ca^{2+} indicator, the properties of which mean that it changes its configuration when it binds Ca^{2+}, and this change in configuration means that its excitation spectrum also changes. Unbound FURA 2 is maximally excited at 380 nm and Ca^{2+}-bound FURA 2 at 350 nm. Light is emitted at 510 nm by both bound and unbound dye.

FURA 2 loaded cells (see below for loading protocol) are excited alternately by light of wavelengths 350 nm and 380 nm, with fast switching

between wavelengths controlled by the computer and executed by the monochromator system. Excitatory light is reflected onto cells by a 430 nm dichroic mirror. Light is emitted from the cells at a wavelength of 510 nm and passes through a 510 nm bandpass filter. Intensity of emitted light is measured and recorded for consecutive excitations at 350 nm (I_{350}) and 380 nm (I_{380}), and hence the ratio of bound to unbound dye (I_{350}/I_{380}) is calculated by the computer. On a pre-calibrated rig, this ratio can be translated online into a value for $[Ca^{2+}]_i$.

2.3.2.1 Loading of cells with FURA 2

Cells to be used for whole-cell patch clamp experiments were loaded with FURA 2 via the patch pipette. Cells were left for at least 10 minutes after "break-through" into the whole-cell configuration to allow the dye to equilibrate throughout the cell.

Cells to be used for perforated-patch electrophysiological recording, or for experiments not involving voltage-clamp, were loaded with FURA 2 via incubation with the acetoxymethyl (AM) ester form of the dye, which is able to cross the plasma membrane. Once in the cytoplasm, the ester moiety is cleaved by endogenous esterases. The stock solution of FURA 2 AM was prepared in DMSO and pluronic acid at a concentration of 5mM, and 0.5µl of this stock solution was added to the culture chamber (which contained 500 µl growth media) resulting in a final concentration of 5µM FURA 2 AM. Cells were incubated for around 30 mins at 37˚C to allow the FURA 2 AM to enter the cell. Once loaded with the dye, dishes were transferred to the microscope stage and

superfused for at least 10 minutes with the standard extracellular solution to remove any excess FURA 2 AM before recording.

2.3.3 Simultaneous electrophysiological and fluorescence recording – special considerations

A fluorescent cell was located and the focus and exposure of the camera set. The cell was then patched under transmitted light. Transmitted light was then switched off while the membrane permeabilised, as amphotericin is sensitive to light. When the access resistance was suitably low (< 15MΩ) fluorescent light was switched on and the focus and camera exposure time checked and, if necessary, slightly altered. Most of the focus adjustments had to be completed before the cell was patched, as movement of the cell due to lens adjustments would displace the electrode. The membrane potential was then set to the holding potential, ready for electrophysiological recording to begin. M-current recording was initiated by a digital pulse which was triggered by commencement of the imaging recording, hence the two recordings were started at exactly the same time so that time-courses could be compared.

2.4 Immunocytochemistry

Immunocytochemistry was used to test the expression of NCS-1 in both uninjected and injected SCG neurons.

2.4.1 Procedure

Cells for immunocytochemistry were cultured on glass coverslips in 4 well plates (*Nunclon*). Cells were fixed with 0.2% gluteraldehyde/2% paraformaldehyde (in phosphate buffered saline, PBS; *Sigma*) for 20 mins at room temperature. Fixed cells were then permeabilised with 0.1% triton X100 (*Sigma*) in PBS for 15 mins. After washing the cells several times in PBS, they were incubated for 1 hour in a blocking buffer consisting of 10mg ml^{-1} bovine serum albumin (BSA; *Sigma*) in PBS, and then for 1 hour in the primary antibody, anti-NCS-1. A secondary antibody conjugated to a fluorescent marker was then used so that the localisation of the primary antibody could be visualised under fluorescence microscopy. The anti-NCS-1 antibody was raised in rabbit, so an anti-rabbit secondary antibody was used (swine anti-rabbit IgG), which was conjugated to tetramethylrhodamine B isothiocyanate (TRITC). After several washes with PBS, the coverslips were removed from the four-well plates and mounted onto slides using a mounting medium, where they were then sealed using clear nail varnish. Slides were refrigerated until examination under fluorescence microscopy, which was usually within a few days as staining can fade if left for too long. The level of auto-fluorescence was estimated by performing the immunocytochemistry procedure without antibodies and then checking these slides under fluorescence microscopy. Another control

experiment was to compare staining against a specimen whch had been stained with the secondary antibody alone to estimate the amount of unspecific binding of the primary antibody.

Specimens were photographed using the same equipment described for GFP-PLC-δ_1 PH, but anti-NCS-1 antibody staining was visualised at the wavelength and with the same dichroic mirror/ bandpass filter as used to visualise rhodamine, as the secondary antibody was conjugated with TRITC.

RESULTS

CHAPTER THREE

The M-current in rat superior cervical ganglion (SCG) neurons, features of its inhibition by oxotremorine M and bradykinin

3.1 Basic Features of the M-current in rat SCGs.

3.1.1 Recording M-currents

M-currents were recorded from dissociated rat superior cervical ganglion neurons using the equipment described in Methods. The voltage protocol used (as shown in Figure 3.1.) was one with a depolarised holding potential of –20 mV, to preactivate the M-current and to allow voltage-dependent inactivation of other, contaminating currents, such as the A-type potassium current. A one second hyperpolarising pulse to –50 mV every 15 seconds allows deactivation of the M-current and reactivation on repolarisation to the holding potential. On hyperpolarisation to -50mV the M-current switches off slowly with a characteristically shaped deactivation tail, which can be fitted with two exponentials.The amplitude of this deactivation tail is used to represent the true amplitude of the M-current, avoiding contamination by other currents which may be present at –20 mV. Figure 3.1 below shows the voltage protocol waveform and the accompanying M-current recording.

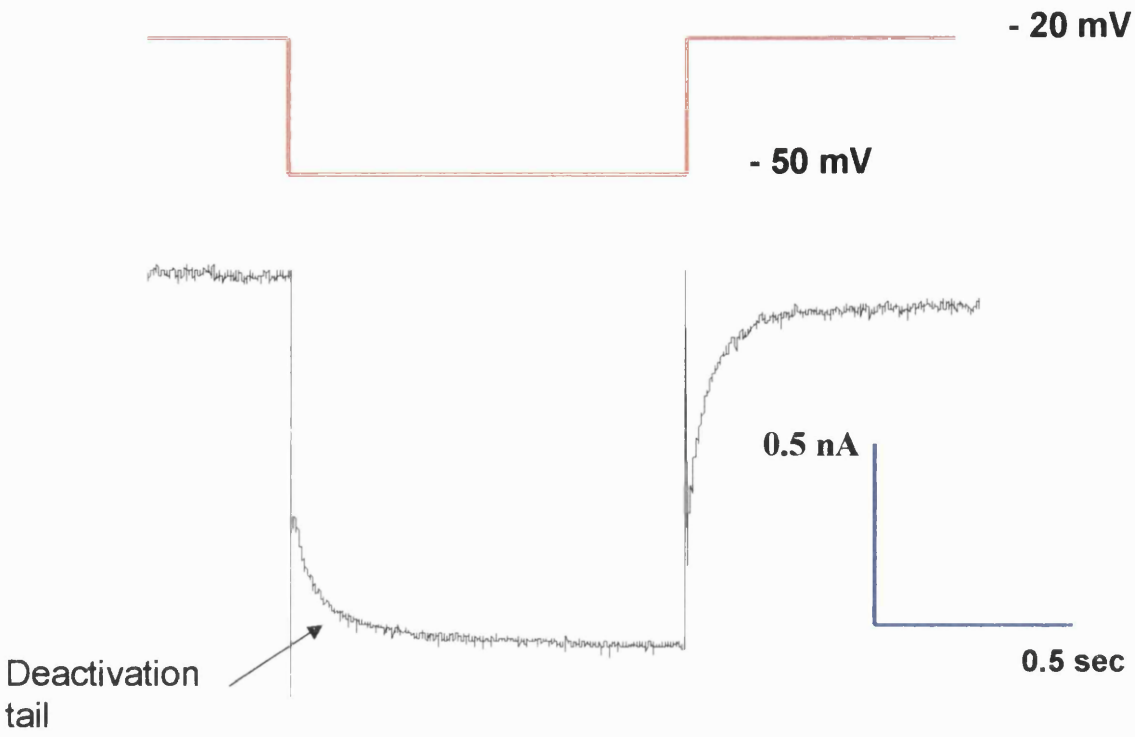

Figure 3.1. Voltage protocol for recording of M-currents, with M-current trace shown below – note slow deactivation of the current on hyperpolarisation to -50mV, and subsequent slow reactivation on repolarisation to the holding potential of -20mV.

3.1.2 Analysis of the M-current

M-currents were analysed using pClamp software (version 8.1; Axon instruments).

The deactivation tail was fitted with two exponentials between two points, one just after the end of the capacity transient generated by the hyperpolarising step, and the other at a point where the current had reached a steady state (see Figure 3.2). These exponentials were extrapolated back as far as the first and last samples of the hyperpolarising pulse. Figure 3.2 shows this double exponential fit and the fit broken down into the two individual exponential components.

The total amplitude of the deactivation tail is calculated as the sum of the amplitudes of both exponential components at zero time (the first sample of the hyperpolarising pulse).

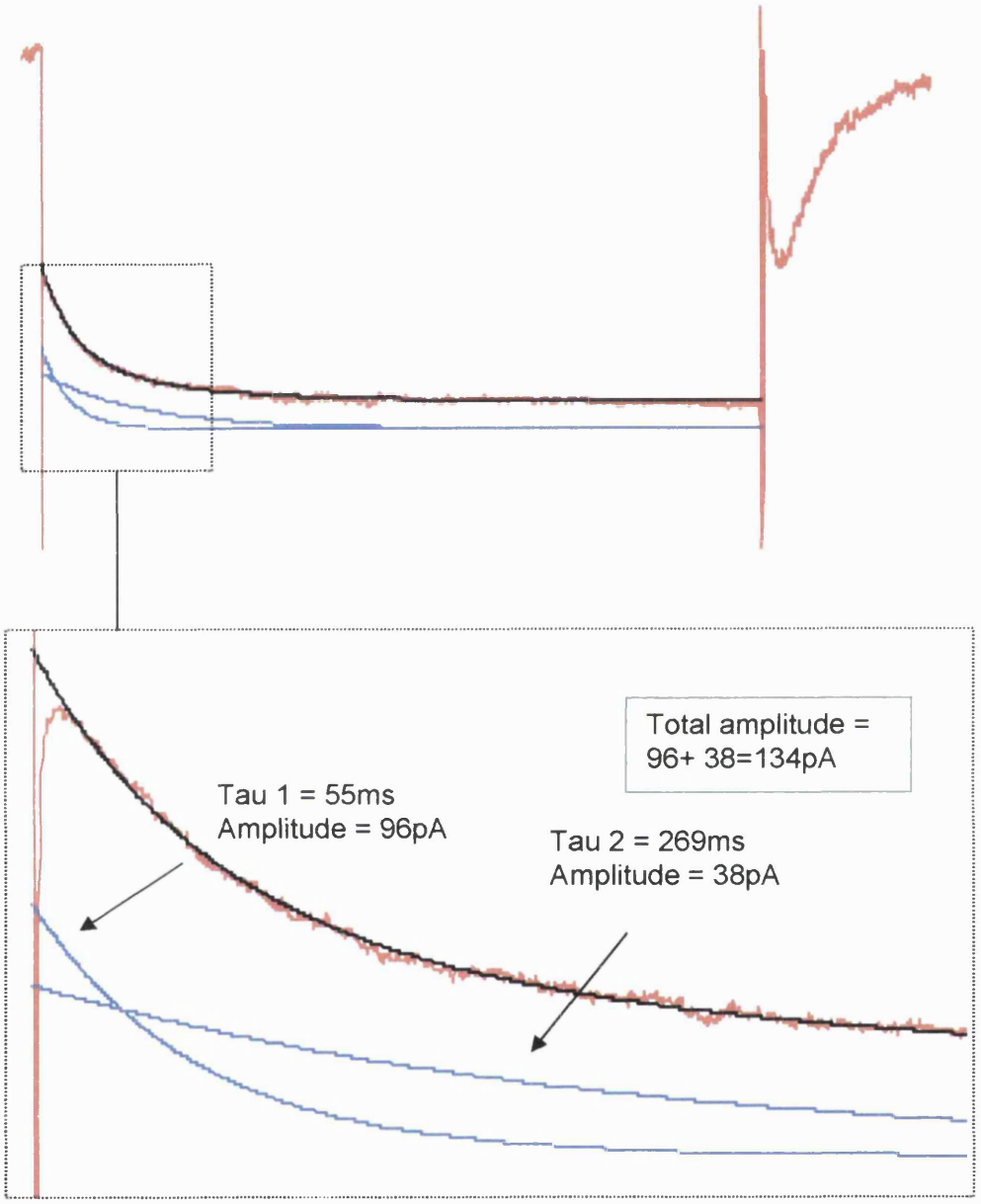

Figure 3.2. Double exponential fit of M-current deactivation relaxation, and the fit broken down into two single exponential components.

3.1.3 Timecourse of deactivation relaxation

The timecourses (tau) of both exponentials are given by the analysis programme, Clampfit 8. The average values from a sample of 10 SCG neurons are shown below :-

Average values from a sample of 10 SCG neurons							
Tau1(ms)	A1(pA)	Tau2(ms)	A2(pA)	A1+A2	% A1	% A2	Tau1/Tau2
50± 4.2	***115± 19.3***	***245± 20***	***44± 7.8***	***163± 23.3***	***69.3± 2.5***	***30.7± 2.5***	***0.2***

As seen in the table above, the fast tau (tau 1) was on average one fifth of the duration of the slow tau (tau 2), and is the predominant contributor to the amplitude of the current deactivation, contributing almost 70% of the total amplitude. These data are shown in Figure 3.3. in bar chart form.

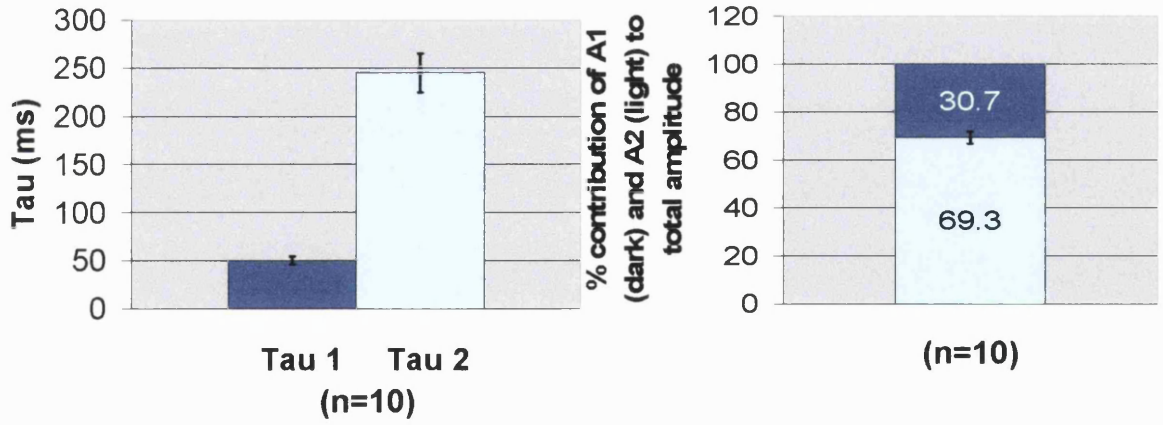

Figure 3.3. On average, the fast exponential component of the M-current deactivation relaxation fit is one fifth the length of the slow component, and makes up almost 70% of the total relaxation amplitude.

3.1.4 Current-voltage relationship of the M-current

The current-voltage relationship of the M-current was observed using a protocol with a depolarised holding potential of –20 mV, as in the standard recording protocol, to preactivate the M-current. Hyperpolarising pulses of 1 second duration were performed every 20 seconds, the first pulse to –30 mV and the voltage becoming more hyperpolarised with each pulse in 10 mV increments until the last pulse at –110 mV. Figure 3.4 shows the voltage protocol waveform and the corresponding M-current recording.

As figure 3.4 shows, the amplitude of the deactivation relaxation is fairly small on the first hyperpolarising pulse to -30mV, indicating that not many of the channels which are open at the holding potential of -20mV are closed by this 10mV hyperpolarisation. The deactivation tail amplitude increases progressively with successive pulses until it reaches a maximum with a hyperpolarisation to -50mV. As the pulses become more hyperpolarised, the amplitude of the relaxation decreases further, until there is no relaxation at the potassium reversal potential of around -80mV. After this point, subsequent pulses show an inward current switching off on hyperpolarisation as the direction of the potassium ions through the M-channels has been reversed. Figure 3.4C shows a plot of the average M-current conductance plotted against voltage from a sample of 5 SCG neurons.

Current relaxations amplitudes were measured as before by fitting the data with a double exponential function. These amplitudes were plotted to produce a simple graph of the current amplitude/ membrane potential (V_m), and the reversal

potential (V_{rev}) of the M-current was measured from this plot. The driving force at each hyperpolarising step was then calculated from this reversal potential (driving force =$|V_m|$ - $|V_{rev}|$). The amplitude of the current relaxation at each membrane potential is then divided by the driving force at that potential to obtain a measure of the M-current conductance at that potential. The largest value for conductance is noted (G_{-20} – as the holding potential is -20mV and the M-current conductance is not maximal at this potential) and all other values subtracted from it to obtain corrected values. All "corrected" conductances are then divided by the largest value for normalisation (obviously the largest value has now become "1"). The data is then plotted and fitted with a Boltzmann equation ($G/G_{-20} = 1/(1+ \exp(V_{1/2} – V)/k$ where $V_{1/2}$ is the membrane potential at which the conductance, G, is half of G_{-20} and k is the slope, measured in mV, and quantifies the voltage range over which there is an e-fold change in conductance. Each cell was analysed individually and fitted with a Boltzmann equation. The values for $V_{1/2}$ and k were then averaged and a Boltzmann fit was simulated using these average values as non-variable. The points plotted in Figure 3.4C are the average normalised conductances at each voltage (± SEM) and the Boltzmann curve plotted is the simulated curve using the averaged values for $V_{1/2}$ and k.

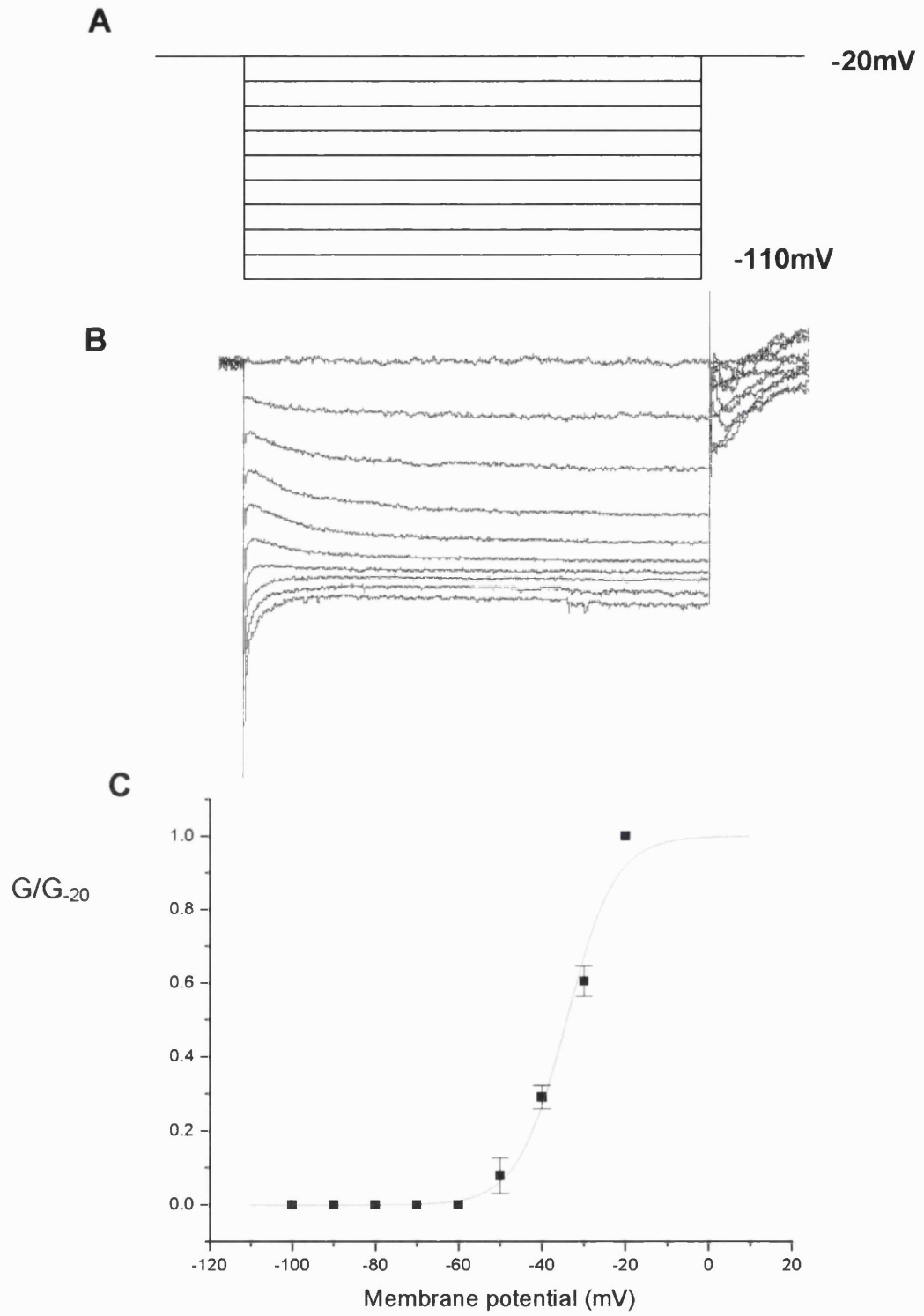

Figure 3.4. Current-voltage relationship of the M-current. A.voltage protocol; holding potential of -20mV with hyperpolarising pulses of one second every 20 seconds, starting with a potential of -30mV and hyperpolarisation increasing by 10mV with each subsequent pulse, to reach a potential of -110mV.B. Corresponding current trace. C. Averaged conductance of M-current in rat SCG (n=5) – data is fitted with a Boltzmann equation showing $V_{1/2}$=-34mV and slope =5.82.

3.2 Agonist-induced inhibition of the M-current

3.2.1 General features of M-current inhibition

As described in the introduction, stimulation of G-protein-coupled receptors can induce inhibition of the M-current. This inhibition appears as a reduction in outward holding current at -20mV as well as a reduction in the amplitude of the deactivation tail. The black trace in Figure 3.5 shows the M-current before inhibition, and the red trace shows an example of an M-current during inhibition. Inhibition is measured as the percentage decrease in total amplitude of the deactivation tail at -50mV.

As mentioned before, many agonists couple to inhibition of the M-current. The two agonists used most frequently in my work are the muscarinic acetylcholine receptor agonist, oxotremorine M, and the peptide bradykinin, which inhibits the M-current in SCG neurons via the bradykinin B_2 receptor. The features of the M-current inhibition by these two agonists differ somewhat and the similarities and differences are described in the next section.

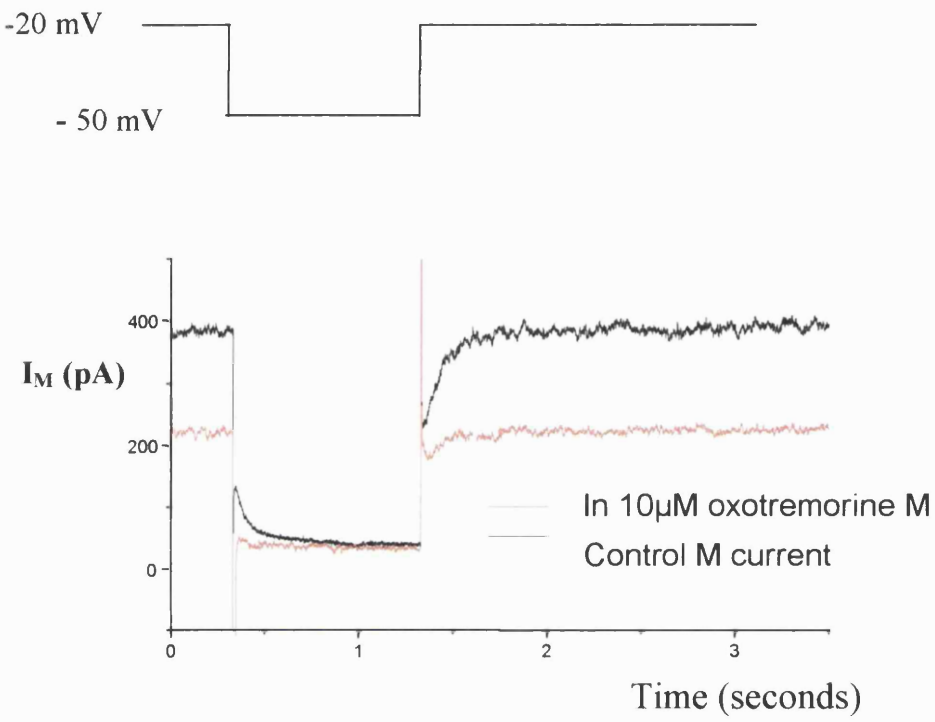

Figure 3.5. Example of inhibition of the M-current. The black trace shows the M-current before inhibition and the red trace shows the same current during inhibition – note the reduction in both outward holding current and amplitude of the deactivation tail.

3.2.2 M-current inhibition by the muscarinic agonist oxotremorine M

Oxotremorine M is an agonist at muscarinic acetylcholine receptors. It does not show specificity for any subtype of muscarinic receptor but activates them all. Only the odd numbered muscarinic receptor subtypes, 1 and 3, couple to inhibition of I_M i.e. the subtypes which couple to pertussis toxin insensitive G-proteins. It has been shown to be muscarinic receptors of the M_1 subtype which couple to inhibition of the M-current in rat SCG neurons, as the muscarine-induced I_M inhibition was blocked by the selective M_1 antagonist pirenzipine, and not by the selective M_2 and M_2/M_4 antagonists gallamine and himbacine respectively (Marrion et al., 1989; Bernheim et al., 1992).

Oxotremorine M was applied to neurons at room temperature, via bath perfusion. A maximal dose of oxotremorine M, 10μM, produced a reduction in the deactivation tail amplitude of around 75%. In my system, the average time from the onset of the response to the peak was approximately 30 seconds. For a 30 second drug application, the current had generally recovered to approximately its original amplitude after around 175 seconds after onset (see Fig 3.6 for plot of deactivation tail amplitude of a typical cell showing typical duration of response).

The response was repeatable, with maximum inhibition possible as soon as the current had recovered and stabilised from the previous inhibition (see Fig 3.7).

Average amplitude of response = 76.7 ± 4.27 % (n=12)

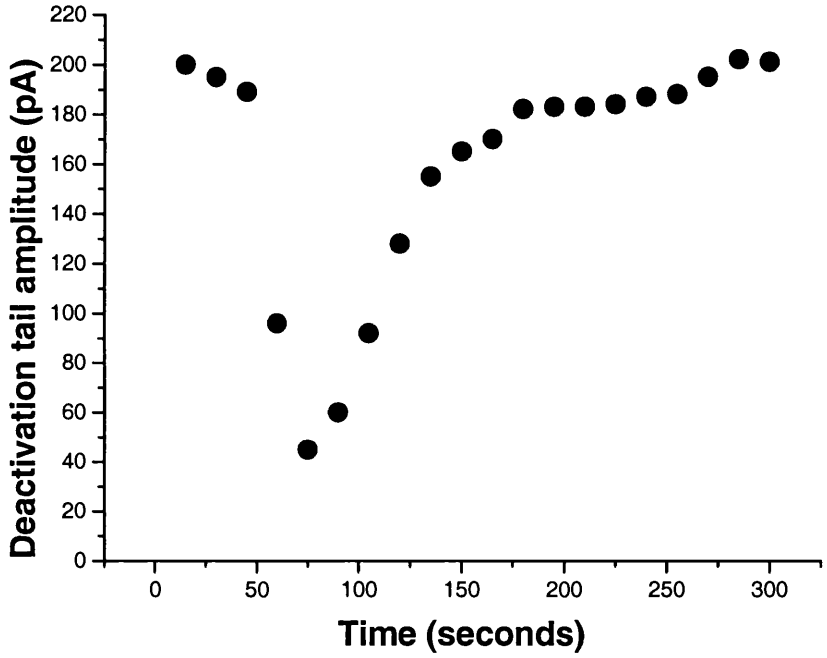

Figure 3.6. Plot of changes in deactivation tail amplitude with time during a response to 10μM oxotremorine M

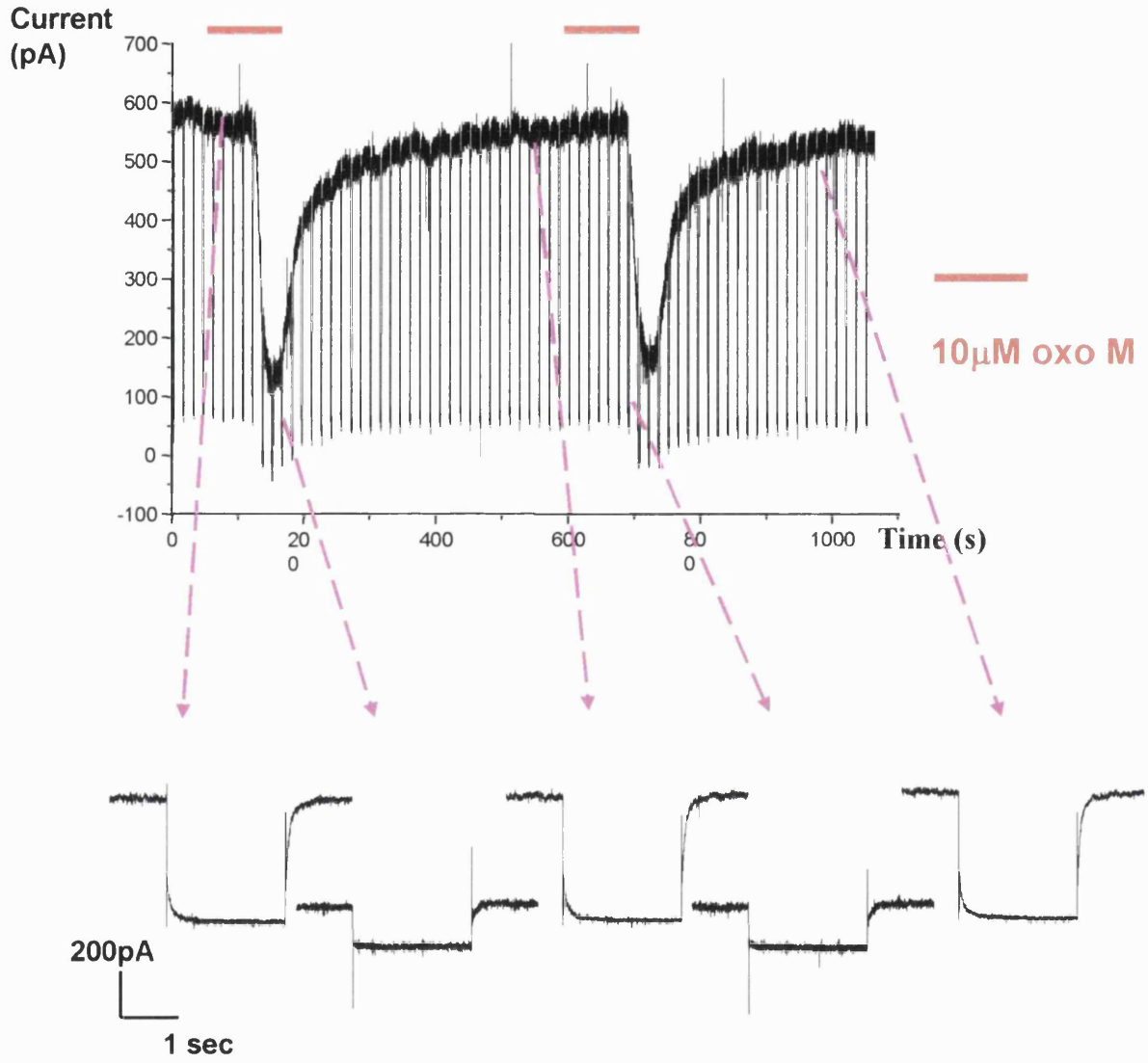

Figure 3.7. Concatenated trace showing changes in holding current amplitude with time on addition of 10μM oxotremorine M. Below the main picture are pictures of individual M-current traces at the points in the recording indicated with the arrows. These individual traces show the reduction in outward holding current, and also the reduction in the amplitude of the deactivation tail, during inhibition with oxo M. The figure shows that the inhibition is fully reversible and repeatable.

3.2.2.1 Inhibition of the M-current by oxotremorine M is dose-dependent

The inhibition of the M-current by oxotremorine M is not an "all or nothing" response, but rather the degree of inhibition is dependent on the dose of agonist. Doses were added cumulatively and the inhibition by each dose was allowed to plateau before addition of the next. Fig 3.8a is a continuous trace showing the stepwise reduction in outward holding current in response to the cumulative addition of increasing doses of oxotremorine M.

Figure 3.8b is an averaged dose-response curve for the inhibition of M-current in rat SCGs by oxotremorine M. It shows that the IC_{50} for oxotremorine M under my experimental conditions is around 0.9 μM.

3.2.2.2 Inhibition of the M-current by oxotremorine M is mediated via the M_1 muscarinic acetyicholine receptor.

It is believed to be the M_1 muscarinic acetylcholine receptor (M_1-mAChR) which couples to inhibition of the M-current in SCG neurons as stated above. This was confirmed using the M_1-mAChR-specific antagonist pirenzipine. Perfusion of the cells for 10 minutes with 5μM pirenzipine almost completely blocked inhibition of the M-current by a maximal dose of oxotremorine M (10μM) (n= 4).This strongly suggests that it is in fact the M_1 subtype of muscarinic acetylcholine receptor which

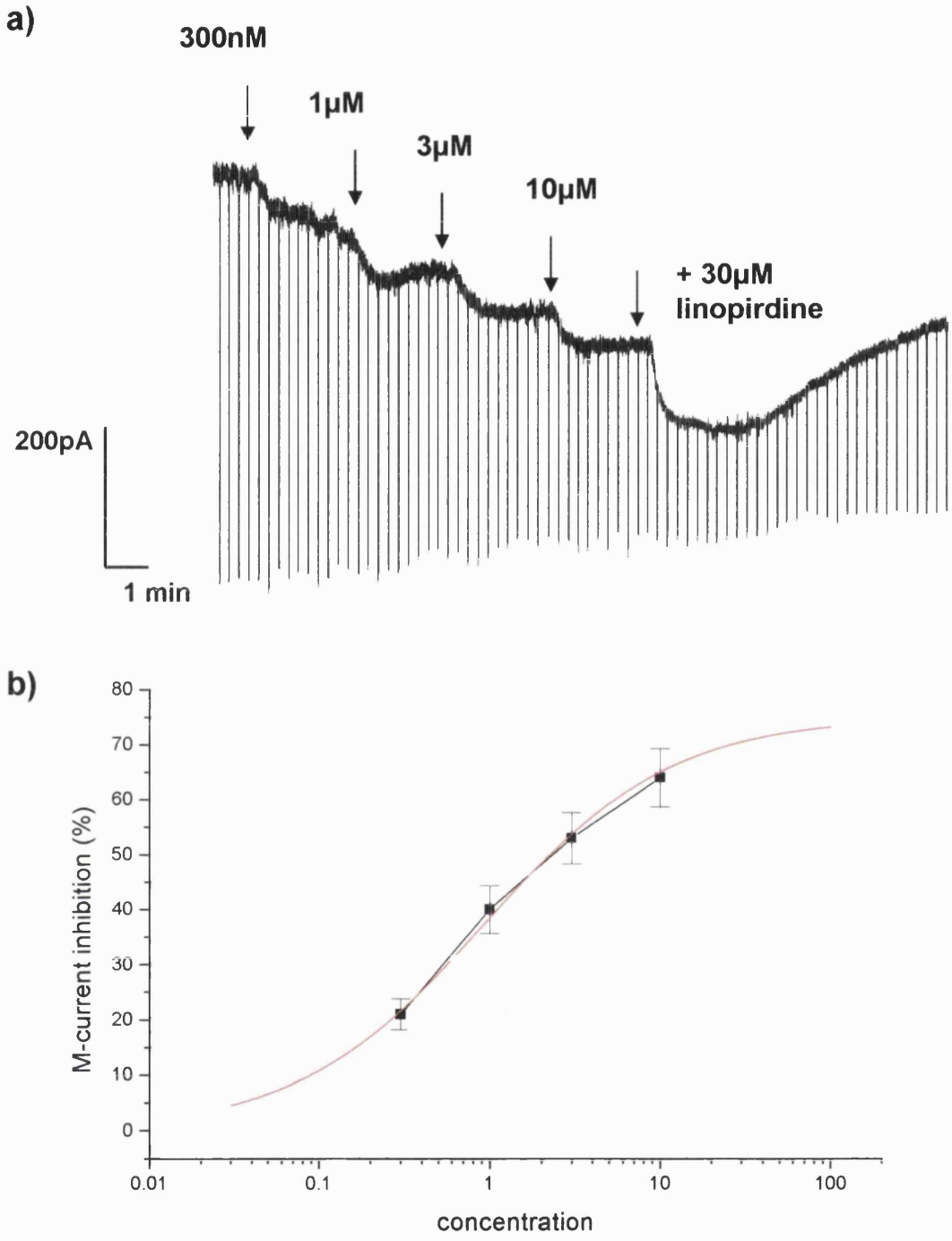

Figure 3.8. a) Concatenated trace of M-current recording showing outward holding current decreases in response to cumulatively increasing doses of oxotremorine M, starting at 300nM and finishing at 10μM. b) Averaged dose-response curve of inhibition of the M-current in rat SCG neurons by oxotremorine M. The curve is fitted with a Langmuir Hill equation, IC_{50}= 0.936 ± 0.03; max = 75%.

induces inhibition of the M-current in rat SCG neurons. Figure 3.9 shows a bar chart with the average inhibitions produced by 10μM oxotremorine M in control SCG neurons and in SCG neurons after 10 minutes perfusion with 5μM pirenzipine (the very small amount of inhibition which remains in the presence of pirenzipine could simply be due to slight rundown of the current over the time taken to apply oxotremorine M and wash it off).

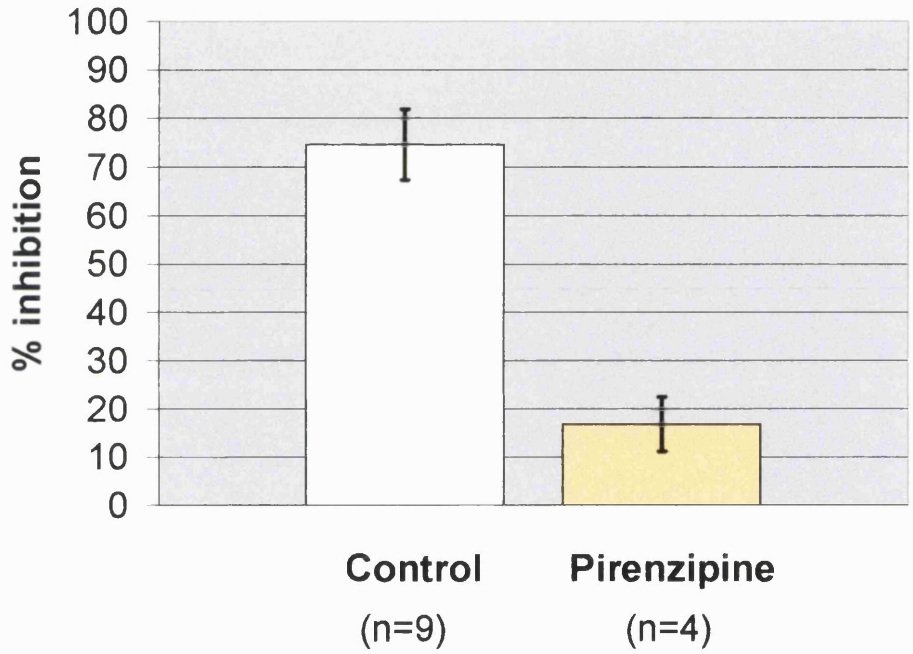

Figure 3.9. Bar chart showing average inhibition of M-current by 10μM oxotremorine M in control and pirenzipine-treated cells.

3.2.3 Inhibition of the M-current by the peptide bradykinin

The peptide bradykinin is reported to inhibit the M-current in rat sympathetic ganglia via its activation of bradykinin B_2 receptors (Jones et al., 1995). Bradykinin was applied to neurons in the same way as oxotremorine M, at room temperature and via addition to the extracellular solution. Bradykinin, like oxotremorine M, was applied for 30 seconds. Cells responded fairly rapidly to bradykinin; the average time from the onset of the response to the peak was around 35 seconds, similar to oxotremorine M, but unlike oxotremorine M, after 175 seconds, when most cells had fully recovered from inhibition by oxotremorine M, the current had only recovered to around 50% of its pre-inhibition amplitude, and recovery was not always complete. The average amount of inhibition produced by a maximal dose, 100nM, was around 50% but was quite variable, as shown in Figure 3.10a (bar chart). Bradykinin also often activated another inward current, which switched off on washout of the agonist – this current was believed to be a chloride current (Marsh et al., 1995). The inhibition of I_M by bradykinin was not repeatable, with rapid desensitisation produced by even a low concentration of the agonist. Figure 3.10b shows a concatenated trace showing changes in the outward holding current on application and washout of 100nM bradykinin – note the long recovery time. The pictures below are individual M-current traces showing the amplitudes of both the outward holding current and the M-current deactivation tail at the points in the recording indicated with arrows.

Average amplitude of response = 43.4 ± 7.1 % (n=8)

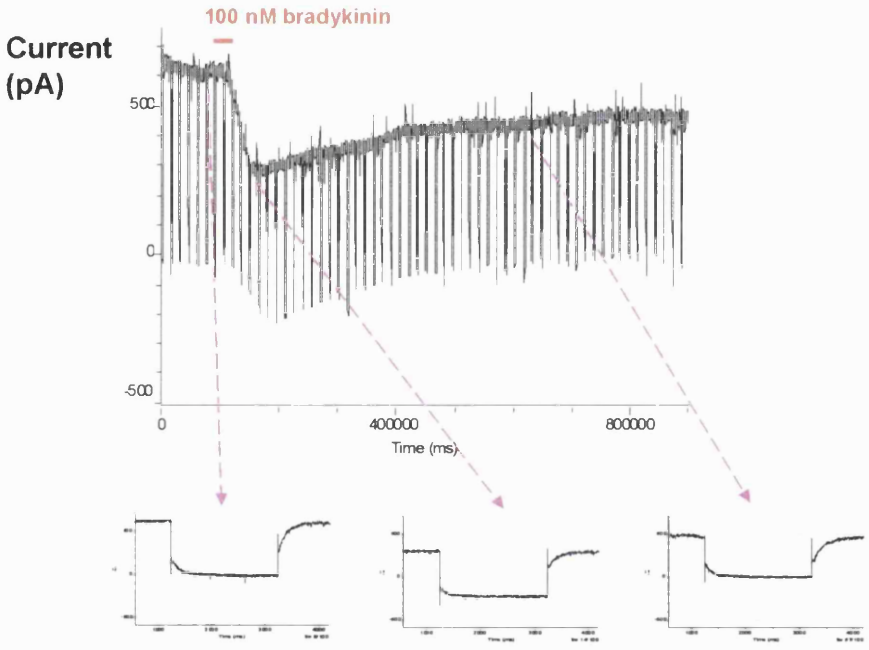

Figure 3.10. Concatenated trace showing changes in outward holding current amplitude on application and washout of 100nM bradykinin. The small figures below are individual M-current traces showing the amplitudes of both the outward current and the M-current deactivation tail – note the partial inhibition and slow recovery time.

3.2.4 Summary of the similarities and differences between inhibition of the M-current by oxotremorine M and by bradykinin

Inhibition of the M-current by both agonists had a similarly fast onset time, but in terms of the dynamics of the responses, it appears that that is where the similarity between the two ends. Oxotremorine M produced on average more of an inhibition at a maximal dose than did bradykinin (≈ 75% as opposed to ≈ 50%), and the inhibition by oxotremorine M was repeatable, whereas the bradykinin response desensitises readily. For this reason it was not possible to add cumulative doses of bradykinin to construct a dose-response curve, although the inhibition by bradykinin has been shown to be dose dependent (Jones et al., 1995). Also, the M-current recovered much more quickly after inhibition by oxotremorine M than by bradykinin, and the recovery after bradykinin-induced inhibition was not always complete whereas after oxo M-inhibition the current nearly always recovered fully.

3.3 Measurement of PLC activity with the green fluorescent protein-tagged pleckstrin homology domain of phospholipase Cδ$_1$ (GFP-PLC-δ PH)

3.3.1 Localisation of the GFP-PLC-δ PH construct in the quiescent SCG neuron.

PIP_2 levels in the plasma membrane can be monitored with the GFP-PLC-δ PH construct via fluorescence microscopy (see Introduction). SCG neurons were transfected with the construct via intranuclear injection of cDNA (Methods, section 2.1.2) and were then incubated for at least 12 hours to allow the protein to express. Neurons were then excited at a wavelength of 475nm and observed under a 40 X oil-immersion objective. Fluorescent neurons were digitally imaged using Openlab software, and the exposure time of the camera adjusted with each neuron so that the brightest points were just below camera saturation. Images were captured and saved, and those selected were enhanced using digital deconvolution, which uses a mathematical algorithm to reduce image blurring (see Methods, section 2.3.1.3).

In the resting SCG, fluorescence was localised mainly to the plasma membrane, with low levels throughout the cytosol. Figure 3.11a) shows an SCG neuron expressing the GFP-PLC-δ PH construct and Figure 3.11b) shows the same image after digital deconvolution to remove blurring.

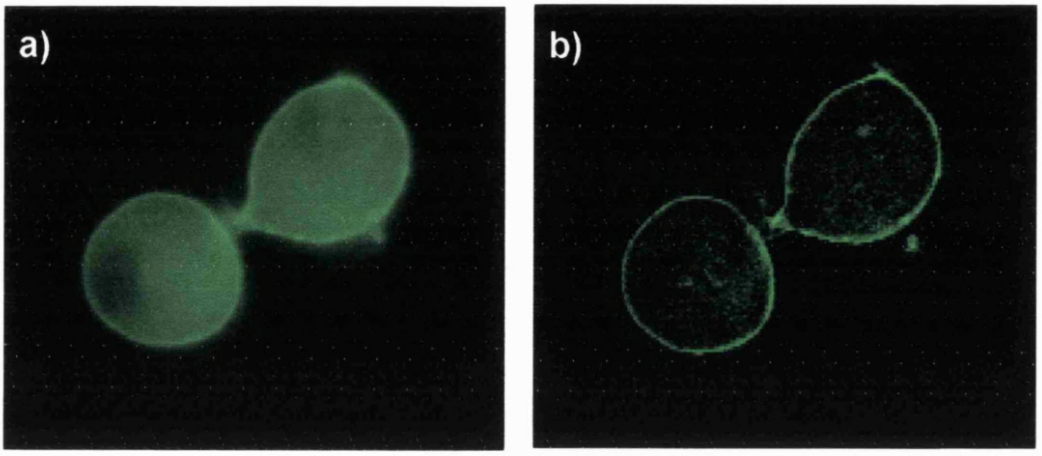

Figure 3.11. a) SCG neuron expressing the GFP-PLCδ PH construct, showing membrane localisation of fluorescence b) The same image after digital deconvolution to remove blurring.

3.3.1 Agonist-induced transiocation of the GFP-PLC-δ PH construct

G-protein-coupled receptors can induce hydrolysis of PIP_2, via activation of phospholipase C. This hydrolysis of PIP_2 would be expected to cause translocation of the fluorescent construct away from the membrane. The two agonists described in the previous section as inhibitors of the M-current, oxotremorine M and bradykinin, were applied to neurons expressing the GFP-PLC-δ PH construct in the same way as they were applied to voltage-clamped neurons to inhibit the M-current. Both agonists did indeed cause translocation of the construct. Neurons were photographed as before and images recorded, with the time between images set to minimum delay, with an image taken approximately every second. Loss of membrane PIP_2 (or synthesis of IP_3 – see Introduction) was measured as a rise in cytosolic fluorescence intensity, and resynthesis of PIP_2 as a fall in cytosolic fluorescence intensity. A region (of roughly $1\mu m^2$) within the cytosol was chosen, and the averaged intensity of light in this area plotted for each image to produce a trace of changes in cytosolic fluorescence intensity throughout the experiment. Figure 3.12 shows an example of such a trace, with the three pictures above it showing the localisation of the fluorescence in the cell before, during and after agonist addition. Before agonist addition the fluorescence is localised mainly to the membrane, as shown in the example of a resting cell in Fig 3.12; the fluorescence intensity (as measured inside the white box on the picture) is stable and low. When the agonist is added the intensity of light in the cytosol starts to rise as the GFP-PLC-δ PH construct translocates from membrane to cytosol – the middle picture in

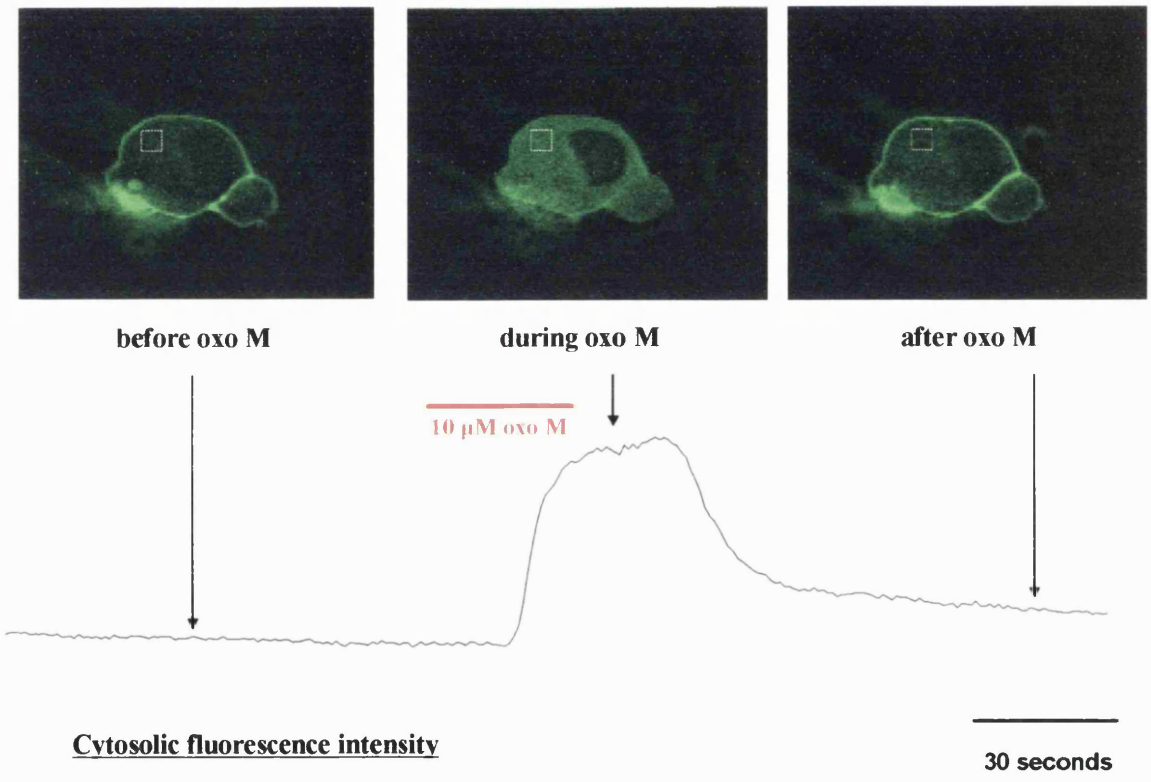

Figure 3.12. Changes in fluorescence localisation within an SCG neuron on addition and washout of a concentration of agonist (in this case oxotremorine M) which inhibits the M-current in these cells. Top three pictures show deconvolved images of the cell before, during and after agonist application and trace below shows corresponding rise and fall in cytosolic fluorescence intensity measured within the white square.

the series of three above the trace shows the localisation of the fluorescence at the peak of the agonist response i.e. it is fairly uniformly distributed throughout the cytosol and shows no specific membrane localisation. The third picture shows the cell after washout of the agonist, where the fluorescent construct has returned to the membrane and the trace of cytosolic fluorescence intensity has returned to its original level, indicating the resynthesis of PIP_2 at the membrane (Varnai and Balla, 1998).

In order to analyse whether various treatments are having any effect on the translocation response by either agonist, it is necessary to identify the features of the control responses, and have a reliable way of analysing them. There are a few problems associated with the quantification of the translocation response, and I shall discuss them below.

3.3.1.1 Problems with the quantification of the translocation response

1) Neuronal size

Even if the amount of protein expressed per unit area is the same in every cell, the magnitude of the rise in cytosolic fluorescence intensity produced by complete translocation of the GFP-PLC-δ PH construct would differ with the size of the cell, because the volume of the cytosol, into which the construct will diffuse is larger. Assuming the thickness of membrane does not change significantly between cells, the ratio of membrane volume to cytosolic volume will decrease as

the diameter of the cell increases. The simple example given below illustrates this difference for two cells differing in size, one with a diameter of 10μm and another with twice that diameter at 20μm. The model assumes that the cells are spherical and that the membrane is 1μm thick (membranes of real cells are probably closer to10nm in thickness, but this figure has been used in the example for simplicity).

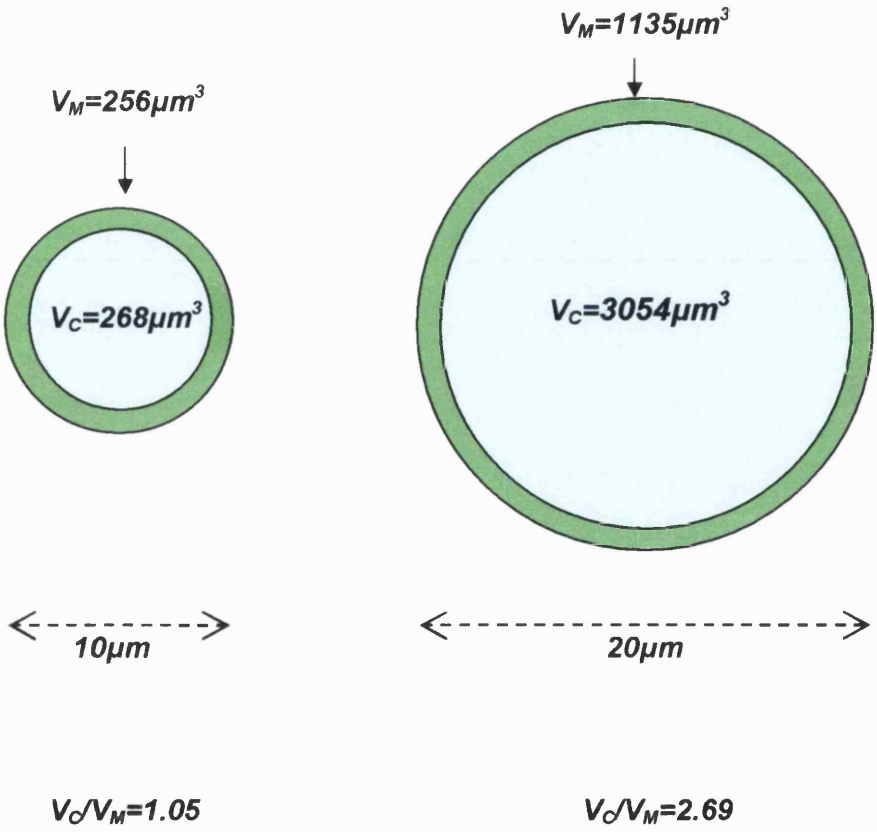

Figure 3.13. Model showing how the ratio of cytosolic to membrane volume differs with cell diameter.

From the figure above we can see that the volume of cytosol in the cell with the diameter of 10μm is $4/3\ \pi\ (4)^3 = 268\mu m^3$, whereas the volume of the membrane in this cell is $\{4/3\ \pi\ (5)^3\} - \{4/3\ \pi\ (4)^3\} = 524 - 268 = 256\mu m^3$. This gives us a membrane to cytosol ratio of 1 : 1.05, meaning that if the fluorescence intensity in the membrane at rest was 10 units (arbitrary units), then the florescence intensity in the cytosol after all of the construct had translocated (and assuming none remains in the membrane) would be 10/ 1.05 = 9.5 units. For the cell with the diameter of 20μm however, the cytosolic volume would be $4/3\ \pi\ (9)^3 = 3054\mu m^3$, whereas the volume of the membrane would be $\{4/3\ \pi\ (10)^3\} - \{4/3\ \pi\ (9)^3\} = 4189 - 3054 = 1135\mu m^3$, which gives us a membrane to cytosol ratio of 1 : 2.69. If the initial membrane fluorescence intensity was again 10 units, then the fluorescence intensity in the cytosol after full translocation of the construct would be only 10/ 2.69 = 3.72 units. This simplified model shows us that, if the initial level of fluorescence in the membrane is the same for each cell, full translocation of the fluorescent construct in a larger cell will produce less of a rise in cytosolic fluorescence intensity.

3) Amount of protein expressed per unit area of membrane

If the amount of protein expressed per unit area of the cell differs between cells, then this is another factor that will cause problems when it comes to quantification of the translocation response. Using the 20μm diameter cell from the model above, we can illustrate how a difference in the initial membrane fluorescence intensity can cause a large difference in the amplitude of the cytosolic

fluorescence intensity rise produced by full translocation of the construct. The ratio of membrane volume to cytosolic volume for this cell was given as 1 : 2.69. If the intensity of fluorescence in the membrane was initially 10 units, it was calculated above that the cytosolic intensity resulting from full translocation of the construct would be 3.72 units. If, however, in another cell of the same size, the initial membrane fluorescence intensity was only 7 units, the cytosolic intensity resulting from a full translocation response would only be 7/ 2.69 = 2.60 units. Assuming that all of the fluorescence was located to the membrane before the agonist was applied i.e. the intensity in the cytosol was zero, this gives us rises of 2.69 units and 3.72 units in cells of the same size. These two responses can clearly not be compared.

Some groups have attempted to circumvent the above problems by taking a line intensity scan of each cell and working out the changes in the ratio of membrane localised fluorescence to cytosolic fluorescence caused by application of agonists or calcium ionophores (e.g. Varnai and Balla 1998; Zhang et al 2002). The ratio $Intensity_{membrane}$ (I_m)/ $Intensity_{cytosol}$ (I_{cyt}) is then plotted with time. This analysis technique throws up problems of its own. Fluorescence intensity is rarely uniform throughout the membrane when the cell is at rest, which makes it difficult to choose the best area for a line scan. Also, the initial ratio between the intensity in the membrane and that in the cytosol differs rather a lot between cells. The technique is also extremely laborious when images are taken with a frequency of up to 10 per second, depending on the exposure of the camera.

The method of analysis I have chosen is to calculate the percentage rise in cytosolic fluorescence intensity over the resting level. In fact, this technique has yielded remarkably consistent results at the maximum dose of both oxotremorine M and bradykinin. When investigating the difference between the translocations caused by both agonists i.e. their differing sensitivities to various treatments, I have applied both agonists in the same cell and used one as the control for changes in the other (as fully explained later).

I have not used the GFP-PLC-δ PH construct as an absolute measure of how much PIP_2 is depleted, but purely as an indicator as to whether various treatments increase, decrease of block this translocation response altogether.

3.3.2 Methods of analysis

As stated above, I have measured the amplitude of the rise in cytosolic fluorescence intensity (CFI) as a percentage of the value of the cytosolic intensity of the cell at rest. Figure 18 below shows a recording of the changes in CFI on addition of bradykinin followed by washout and recovery, and subsequent addition of oxotremorine M. Both agonists were applied at doses which cause maximum inhibition of the M-current (see earlier in this chapter), 100nM and 10μM respectively. There follows an explanation of how this trace would be analysed according to my methodology.

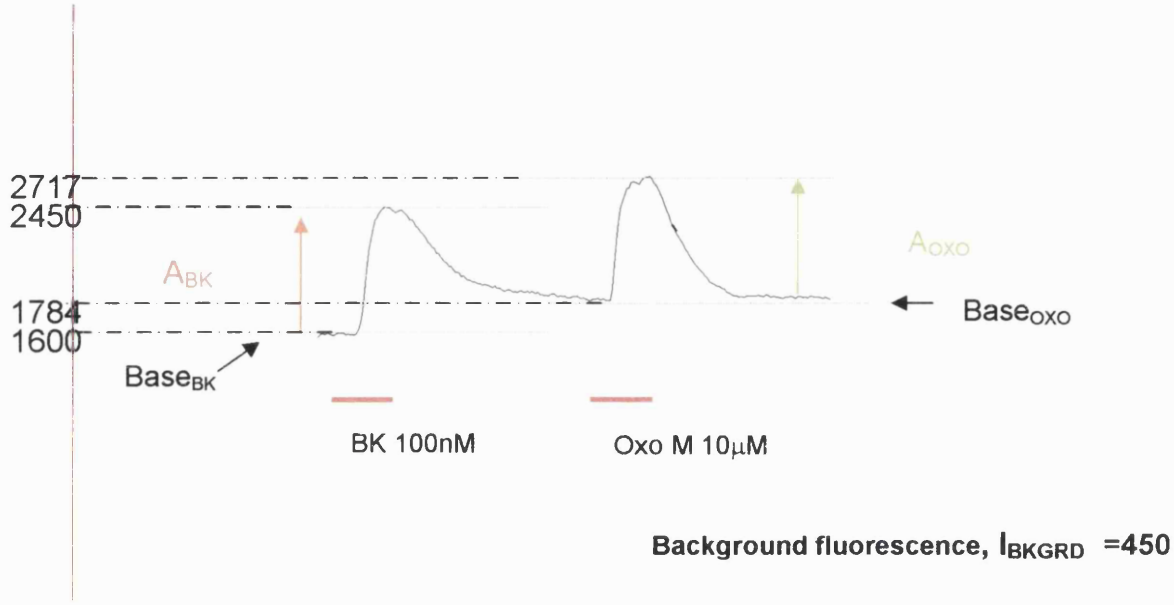

Figure 3.14. Model to illustrate method of analysing agonist-induced rises in cytosolic fluorescence intensity.

The numbers on Figure 3.14 are merely examples to help illustrate a typical calculation of the percentage rise in cytosolic fluorescence intensity resulting from application of the agonist. In the above example, the intensity of light in the cytosolic region of interest at the beginning of the experiment is measured at 1600 units (on a scale of 0 to 4096 units for a 12-bit image) – this value will be called

"$Base_{BK}$" as it is the "resting" cytosolic fluorescence before bradykinin is added. At the peak of the bradykinin response the cytosolic fluorescence intensity has been measured at 2450 units, giving us a value of 2450-1600=850 units for the amplitude of the bradykinin-induced rise, $A_{BK.}$ The background intensity (I_{BKGRD}) in this example however, has been measured at around 450 units (this is the average intensity of the area containing no cells in the field of view and can vary according to exposure time of the camera etc). This value must be subtracted from the resting value, so the real resting cytosolic fluorescence value will be 1600-450=1150. The amplitude of the rise in intensity on application of the drug is now expressed as a percentage of the resting value ie in this example the amplitude of the rise is 850 units, and the resting level is 1150 units. 850 as a percentage of 1150 is 100 (850/1150) =73.9%. Therefore, the equation for the calculation of the bradykinin-induced rise as a percentage of the resting level is as follows :-

$$100 \text{ X } \left(\frac{\text{Peak}_{BK} - \text{Base}_{BK}}{\text{Base}_{BK} - I_{BKGRD}} \right) = \text{BK rise,\% of resting}$$

The procedure is the same for the oxotremorine M-induced rise :-

$$100 \text{ X } \left(\frac{\text{Peak}_{OXO} - \text{Base}_{OXO}}{\text{Base}_{OXO} - I_{BKGRD}} \right) = \text{OXO rise,\% of resting}$$

3.3.3 Both oxotremorine M and bradykinin induce transiocation of the GFP-PLC-δ PH construct from membrane to cytosol

Oxotremorine M (10μM) and bradykinin (100nM) caused reversible translocation of the GFP-PLC-δ-PH construct from membrane to cytosol. Like the inhibition of the M-current by both of these agonists however, some of the features of these translocations differed somewhat.

The maximal increase in cytosolic fluorescence intensity was similar for 10μM oxotremorine M and 100nM bradykinin (Fig 3.15a). These rises both correspond to full translocation of the construct as observed by taking deconvolved images at the peak of the response and noting the uniform distribution of fluorescence in the cytosol with no specific membrane localisation (see Fig 3.12). The amplitudes of the rises produced by both agonists can be compared with each other as they were measured in the same cell. As mentioned above, this negates any problems with quantification associated with neuronal size, density of the construct expressed etc. One agonist was applied to the cell, washed off, and when the baseline had returned to resting levels (or near enough) the second agonist was applied. Agonists were applied in either order, to make sure that one did not desensitise the response to the other, but there was in fact no cross-desensitisation and the order in which the agonists were applied did not affect the magnitude of the translocation responses to them.

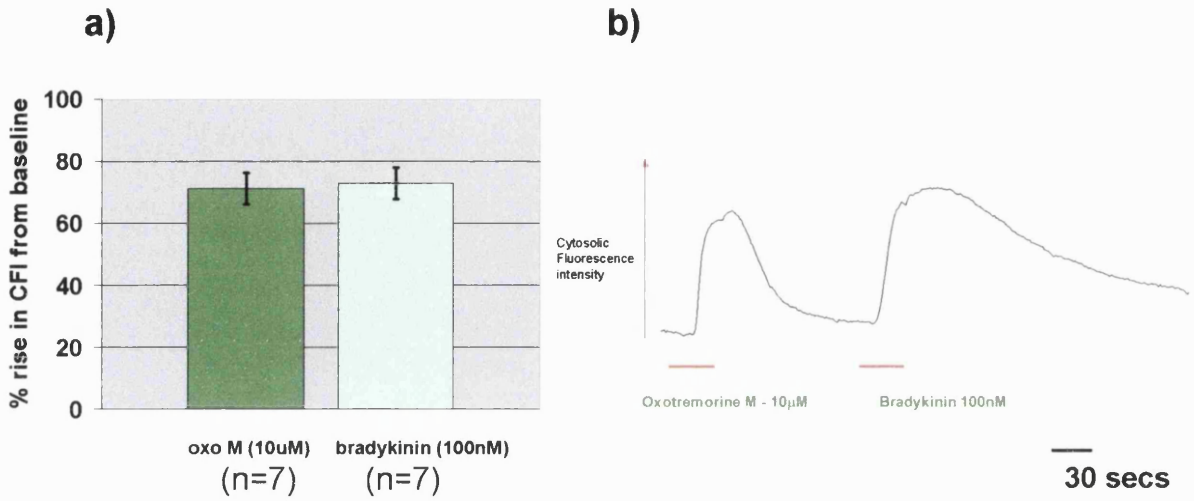

Figure 3.15.a) Average rise in cytosolic fluorescence intensity (CFI) produced by a maximal dose of both agonists (measured as percentage increase in resting CFI). b) Typical trace of response to oxotremorine M followed by response to bradykinin in the same cell.

Although the rate of rise of the cytosolic fluorescence intensity was similar for oxotremorine M and bradykinin, the time courses of the relocation of the fluorescence to the membrane differs between the two agonists, as do the time courses of recovery of the M-current from inhibition. Figure 3.16 shows a reconstruction of the average responses to both agonists, constructed by measuring the time from 1) the onset of the response to 50% of the maximum amplitude 2) onset of the response to the peak amplitude 3) peak amplitude to 25% recovery 4) peak amplitude to 50% recovery 5) peak amplitude to 75% recovery and 6) peak amplitude to 100% recovery.

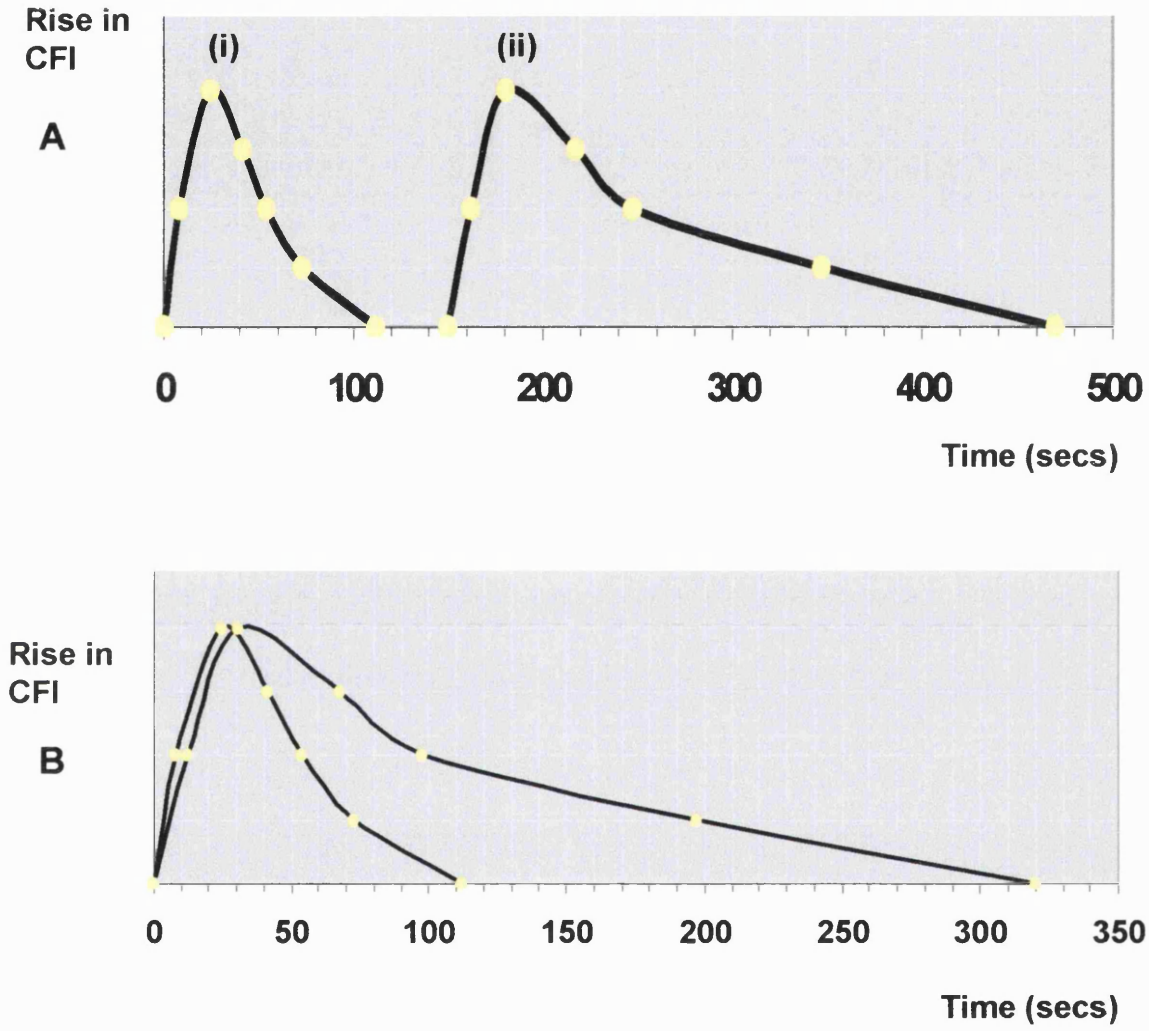

Figure 3.16.A. Reconstruction of average GFP-PLC-δ PH translocation responses to (i) oxotremorine M (10μM) and (ii) bradykinin (100nM). Points plotted are onset of response, time to 50% amplitude, time to peak amplitude, time to 25% recovery, time to 50% recovery, time to 75% recovery and time to full recovery. B. Responses to both agonists overlaid.

As Figure 3.16 shows, the bradykinin-induced GFP-PLC-δ PH translocation takes longer to relocate to the membrane on washout than the oxotremorine M-induced translocation. On average, the time from the onset of the translocation response to the peak is similar for both agonists, at 24 seconds for oxotremorine M and 30 seconds for bradykinin. The recovery phases for both agonists differ considerably however. Membrane relocation of the construct after translocation by both agonists appears to take on a biphasic pattern, with the second, slow phase of recovery being the phase that differs markedly between agonists. The average times taken from peak to 25% recovery are 16 and 38 seconds for oxotremorine M and bradykinin respectively. The times from peak to 50% recovery are 29 and 67 seconds, from peak to 75% recovery are 48 and 167 seconds and the times taken from peak to full recovery are 88 seconds for oxotremorine M and an extrapolated value of 290 seconds for bradykinin (this value was obtained by extrapolating forward from the 75% recovery point as not enough bradykinin-induced translocations recovered fully to obtain a real average value for this point).

3.3.3.1 Translocation of the construct by oxotremorine M is repeatable but the bradykinin-induced translocation desensitises

As described for M-current inhibition (earlier in this chapter), the response to oxotremorine M is repeatable but the response to bradykinin desensitises rapidly, allowing only one response. As soon as the construct has relocated to the membrane after translocating in response to10μM oxotremorine M, reapplication of

the agonist will cause another translocation response (an example is shown in Figure 3.17). Several consecutive responses to oxotremorine M are possible. This is not the case for bradykinin which responds only once, even if the first application of the agonist is washed out for some time.

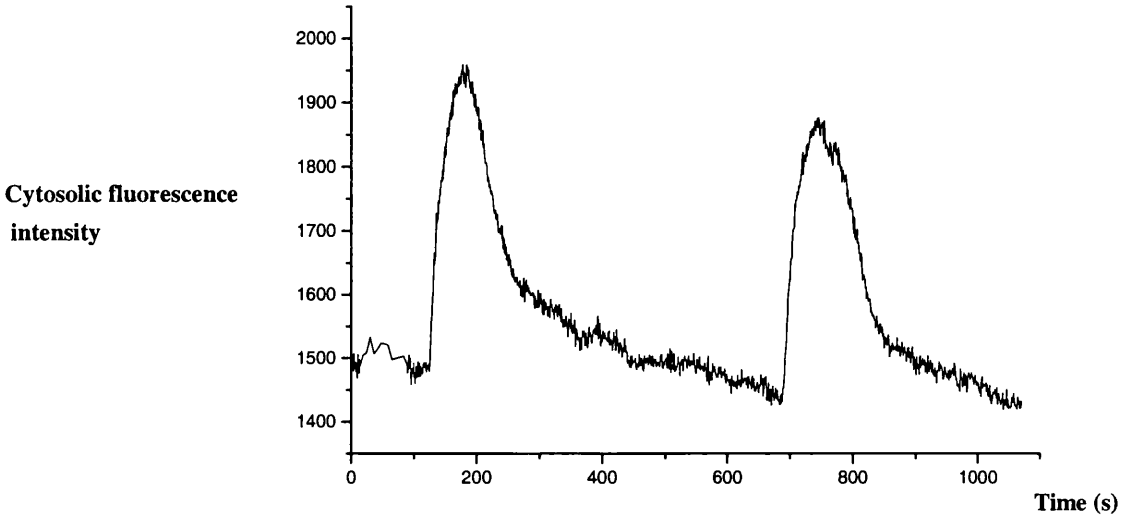

Figure 3.17. Example of two consecutive translocation responses to oxotremorine M. it is not possible to obtain multiple responses to bradykinin as the response desensitises.

3.3.3.2 Translocation of PLC delta PH by oxotremorine M is dose-dependent

The degree of translocation of the GFP-PLC-δ PH construct by oxotremorine M is, like the inhibition of the M-current by this agonist, dependent on the dose of the agonist. It is difficult to quantitate these results, but Figure 3.18 shows the typical changes in cytosolic fluorescence intensity which are the result of cumulative applications of oxotremorine M. The level of cytosolic fluorescence intensity is allowed to stabilise before the next dose is added.

a)

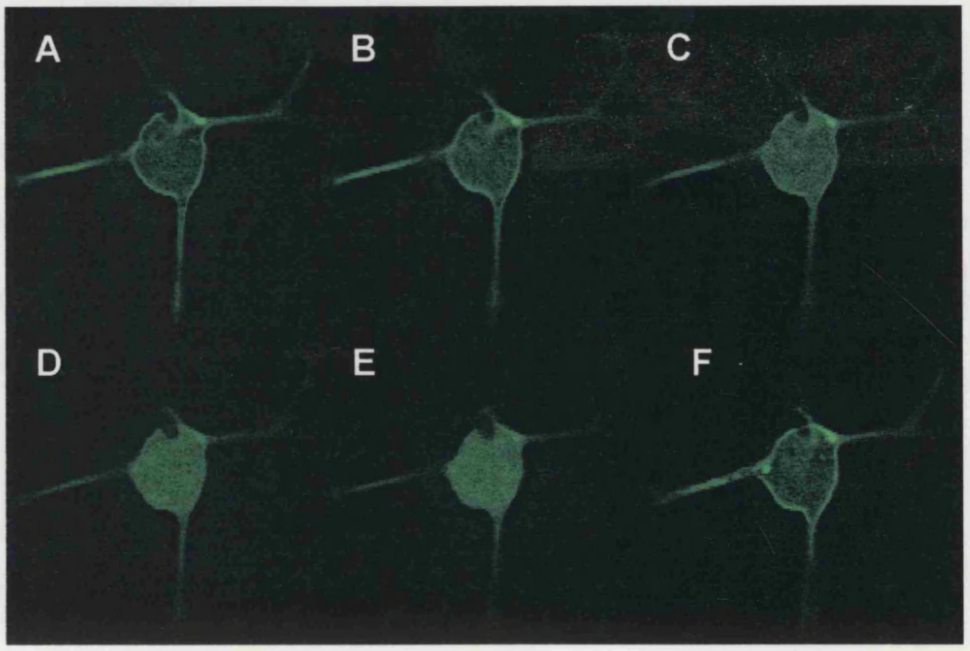

b)

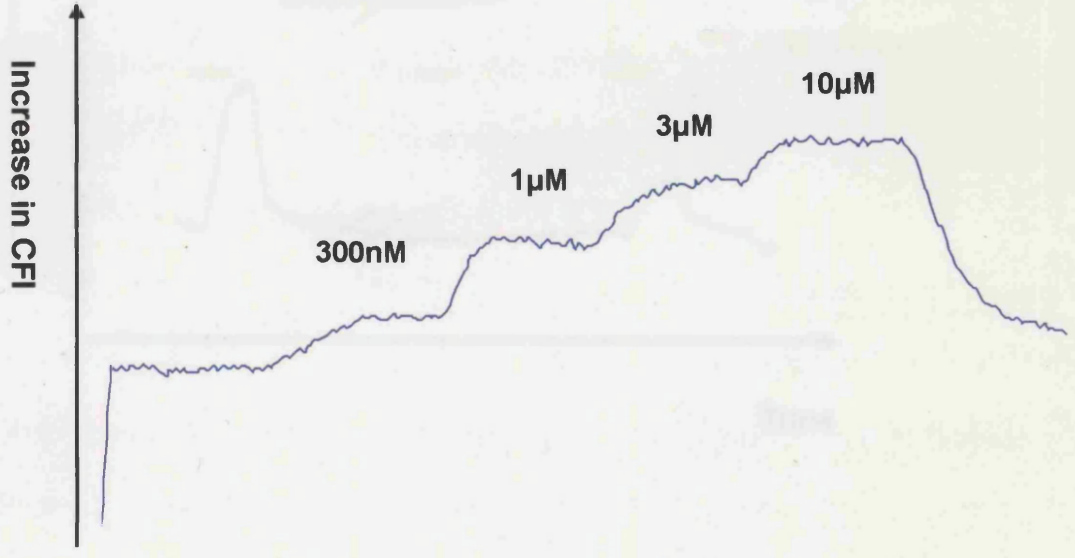

Figure 3.18 a). Deconvolved pictures showing GFP-PLC-δ PH localisation in SCG cell in A. control, B. 300nM oxo M, C. 1μM oxo M, D. 3μM oxo M, E. 10μM oxo M and F. After recovery. b) Corresponding plot of Increases in CFI.

3.3.3.3 *Translocation by oxotremorine M is via the M_1-mACh receptor*

The specific M_1 muscarinic acetylcholine receptor antagonist pirenzipine was used to test whether, like inhibition of the M-current, the GFP-PLC-δ PH translocation induced by oxotremorine M was also mediated via the M1 receptor. The cells were perfused with 5 μM pirenzipine for 10 minutes and then stimulated with 10μM oxotremorine M. Pirenzipine prevented the translocation response as shown in Figure 3.19. On washout of pirenzipine the response to oxotremorine M showed partial recovery.

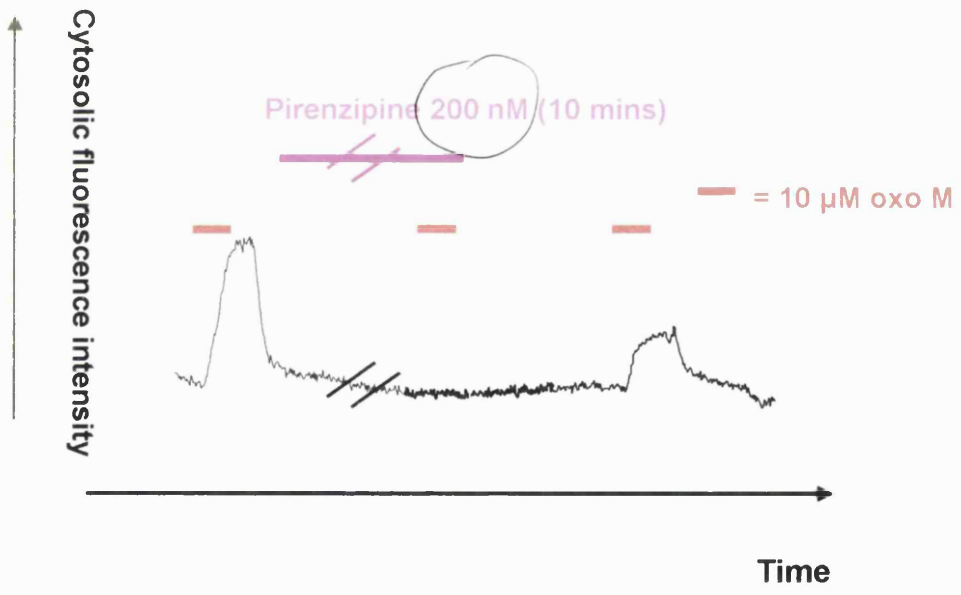

Figure 3.19. Bath perfusion with 5μM pirenzipine (a selective M_1 receptor antagonist) blocks oxotremorine M-induced GFP-PLC-δ PH translocation.

3.4 The M-current in GFP-PLC-δ PH-expressing cells

If the presence of PIP_2 is indeed necessary to hold M-channels in their open configuration, then something which binds to it may have an effect on the M-current. If the binding of the GFP-PLC-δ PH construct were, for example, to affect the binding of PIP_2 to M-channels, this could result in a reduced amplitude of M-current.

The amplitude of the M-current was measured in both uninjected SCGs and SCGs expressing the GFP-PLC-δ PH construct. This was done using the whole-cell voltage-clamp recording technique and measuring the current deactivation tail amplitude directly after break-through before rundown had occurred. The perforated-patch recording method was not used as expression of the GFP-PLC-δ PH construct after 2 or more days caused the perforation process to be very slow and incomplete, making it hard to assess the amplitude of the current as the access resistance remained too high (over 40MΩ).

Current amplitudes in the injected/ uninjected cells are shown in Figure 3.20. The amplitude of the current in the GFP-PLC-δ PH-expressing SCGs does not change significantly between 1 and 3 days after injection. The M-current amplitude in the uninjected cells however *increases* significantly between the 1 and 3 day time points, so that when current amplitudes between transfected and non-transfected cells are compared three days after injection (four days after culture), they are significantly different. This indicates that when the amount of the protein expressed in the cell reaches a certain level, it does interfere with the amplitude of

the M-current. Cells used for experiments in this thesis are always used either one or two days after transfection, when the M-current amplitude is not significantly different between injected and uninjected cells.

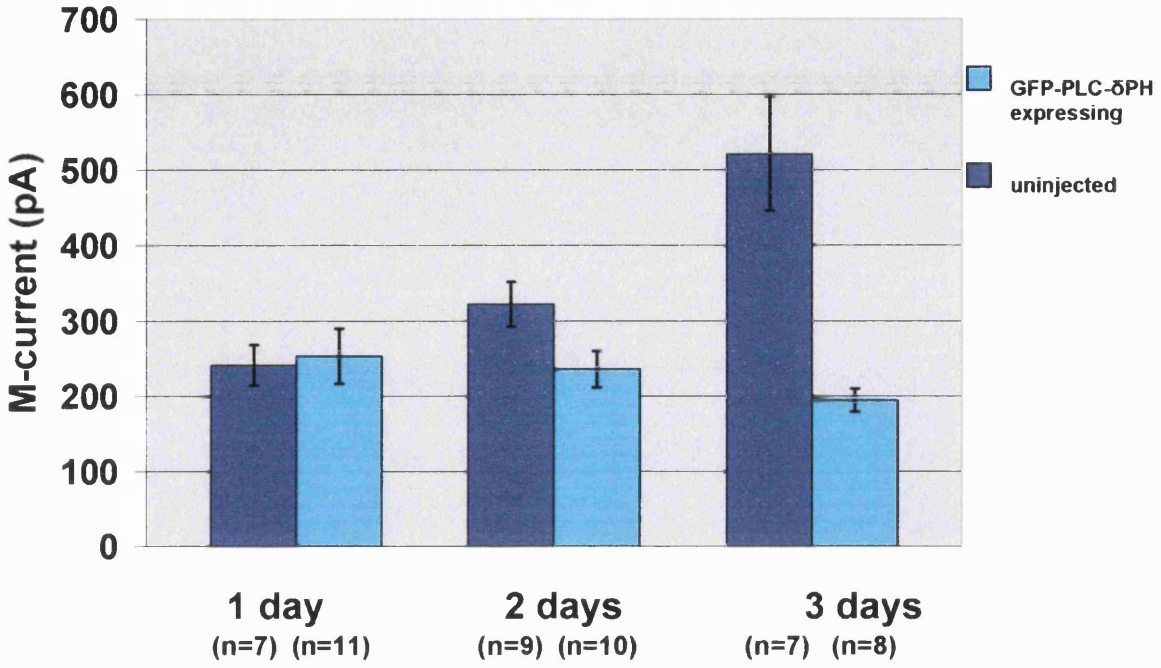

Figure 3.20. Amplitudes of M-current deactivation tail in GFP-PLC-δ PH-expressing SCG neurons (pale blue)1,2 and 3 days after transfection compared with uninjected neurons (dark blue) from the same culture

This chapter so far has examined the similarities and differences between inhibition of the M-current by oxotremorine M and by bradykinin, and also between the membrane to cytosol translocation, and subsequent relocation, of the GFP-PLC-δ PH construct by both of these agonists. Although it is still arguable,

evidence has been provided that the translocation of the fluorescent construct in response to agonist stimulation represents the depletion and resynthesis of membrane PIP_2 (Varnai and Balla, 1998; also see Chapter Four). The fact that the GFP-PLC-δ PH translocation responses by the two agonists differ in very similar ways to the ways in which the M-current inhibition by these two agonists differ, suggests that the two responses may be connected in some way. If current theory is to be believed, this is because the M-current inhibition is due to the depletion of PIP_2 levels, and the recovery of the M-current is due to the replenishment of this phospholipid (Suh and Hille, 2002). If this theory holds, then the model depicted in Figure 3.21 should be correct; at rest, PIP_2 is bound to the M-channels, allowing them to remain open (obviously assuming that the cell is held at a potential within the activation range for the M-current). On application of the agonist, phosholipase C should be activated, causing hydrolysis of PIP_2, resulting in simultaneous closure of the M-channels and translocation of the fluorescent construct from the membrane to the cytosol.

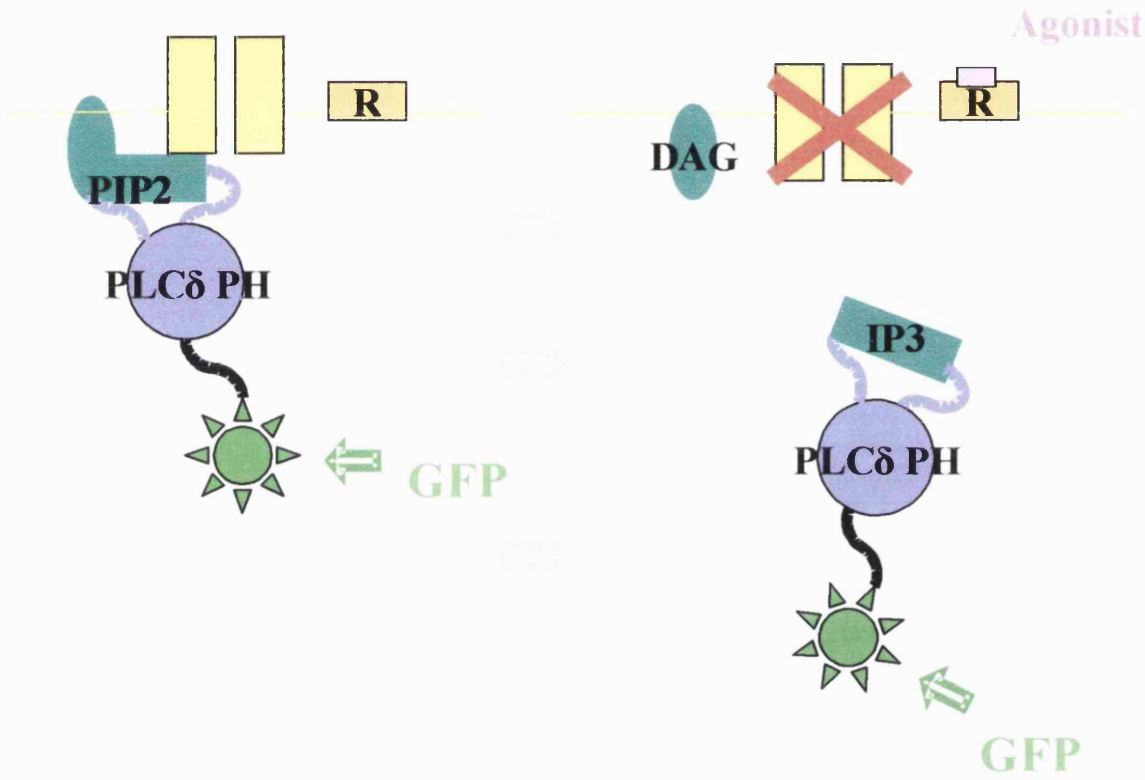

Figure 3.21. Model depicting theorised simultaneous translocation of the GFP-PLC-δ PH construct and closure of M-channels.

3.4.1 Simultaneous recording of the M-current and agonist-induced translocation of the GFP-PLC-δ PH construct

M-currents were recorded in GFP-PLC-δ expressing cells with the perforated patch-clamp method as described before. Location of the fluorescent construct (and changes in the cytosolic fluorescence intensity) were measured simultaneously with M-current. Figure 3.22 shows a simultaneous recording of the M-current and the changes in CFI on addition of 10μM oxotremorine M.

As Figure 3.22 shows, the similarity between the time courses of the M-current inhibition and the translocation response is rather striking. The patterns of onset and offset for both responses are also very similar, with the recoveries of both showing a biphasic pattern. Figure 3.23 shows the time courses of both responses more clearly, with the inverted trace of CFI changes (in red) superimposed on top of the M-current trace.

It is noticeable from the superimposed traces in figure 3.23 that the inhibition of the M-current and the translocation of the fluorescent construct from membrane to cytosol are more or less synchronised, but that the recovery of the M-current precedes the relocation of fluorescence to the membrane. If the construct does indeed have a higher affinity for IP_3 than for PIP_2 (Nash et al., 2001), this could be due to the fact that there is still some IP_3 left in the cytosol to which the construct is bound, and that the concentration of PIP_2 at the membrane has to reach a certain level before the construct will return to the membrane (again, see Chapter Four).

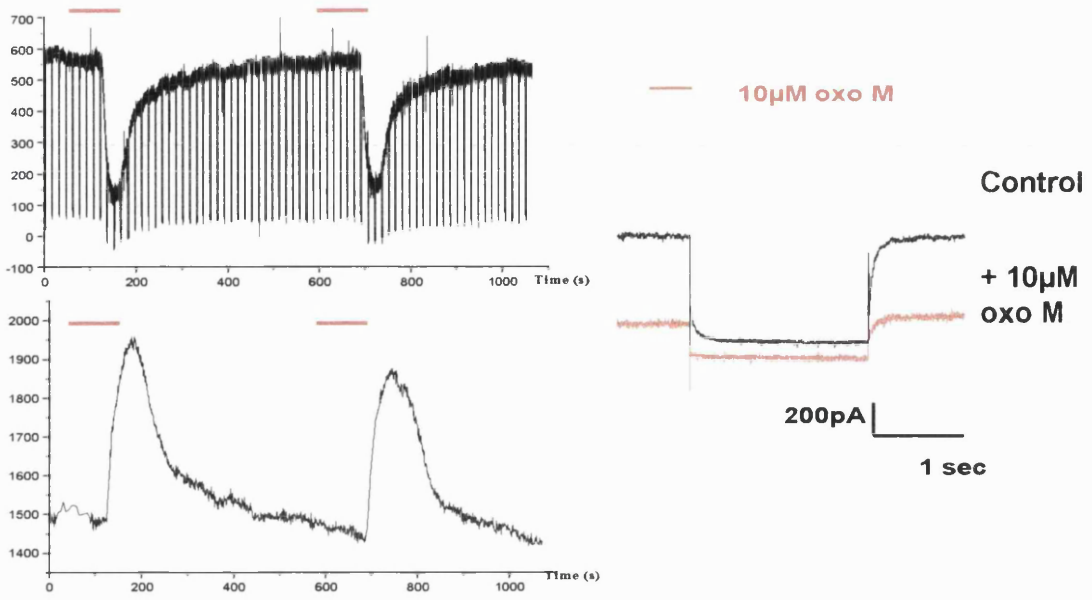

Figure 3.22. Simultaneous recording of inhibition of the M-current, and the changes in cytosolic fluorescence intensity due to translocation of GFP-PLC-δ PH, elicited by two applications of 10μM oxotremorine M.

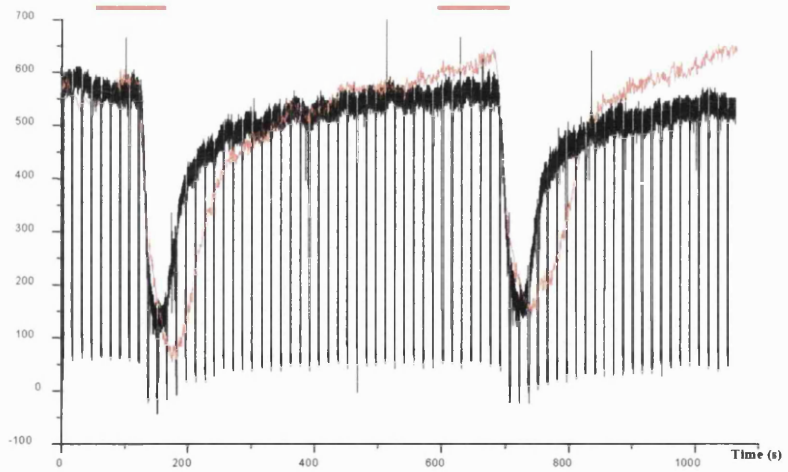

Figure 3.23. Trace of changes in CFI, inverted and superimposed over M-current trace from the same cell, showing relationship between the timecourses of inhibition of the M-current and translocation of the GFP-PLC-δ PH construct by oxotremorine M.

As mentioned earlier, both the extent of the oxotremorine M-induced inhibition of the M-current and the extent of the membrane to cytosol translocation of the GFP-PLC-δ PH construct by this agonist are dependent on the concentration of agonist. Figure 28 shows the changes in outward holding current at -20mV and the cytosolic fluorescence intensity in response to cumulatively increasing doses of oxotremorine M. The patterns of increase and decrease are remarkably similar, particularly the shapes of the increase/ decrease at a concentration of 1μM oxotremorine M.

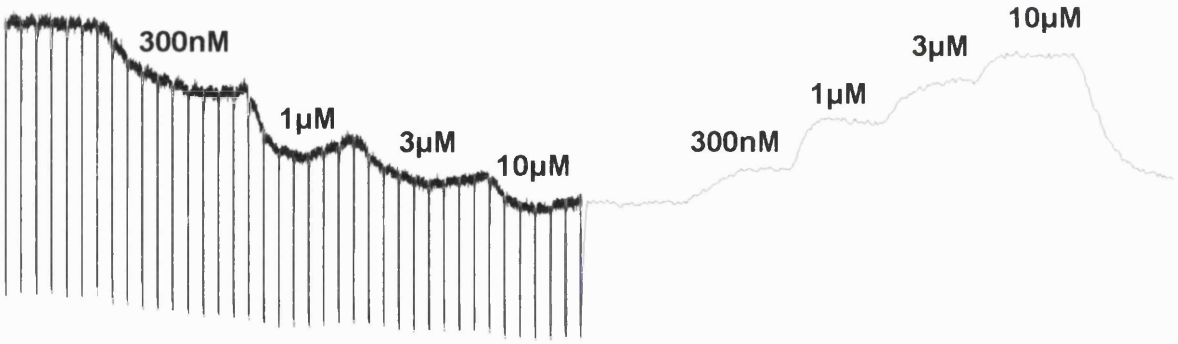

Figure 3.24. Concatenated trace showing stepwise decrease in holding M-current due to cumulative increases in oxotremorine M, and trace of simultaneous changes in CFI in the same cell in response to these doses of oxotremorine M.

3.5 Summary of Chapter

In this chapter I have described the main features of the M-current and of its inhibition by the agonists bradykinin and oxotremorine M. I have also shown that both of these agonists cause reversible membrane to cytosol translocation of the fluorescent PIP_2/ IP_3 indicator GFP-PLC-δ PH and that this translocation and concurrent inhibition of the M-current can be recorded simultaneously. The similarities between the timecourses and patterns of onset and offset of both of these responses to agonist stimulation are remarkably similar, but this does not prove that the depletion of PIP_2 is the event which causes closure of M-channels. It shows us that the depletion of PIP_2 and the inhibition of the M-current are both consequences of receptor activation, but not necessarily that they are connected events. Manipulation of both responses with pharmacological agents and with expressed proteins would help to prove a link between the two. This chapter has introduced the technique of simultaneously monitoring PLC activity and M-current inhibition, and the next chapter will show how this technique is utilised to establish whether the two responses are linked or merely separate consequences of receptor activation.

CHAPTER FOUR

Manipulations of the phosphoinositide cycle and their effect on M-current inhibition and GFP-PLC-δ PH translocation

This chapter investigates the effects of altering the activity of various key players in the phosphoinositide cycle, on the inhibition of the M-current and the translocation of the GFP-PLC-δ PH construct. A simplified diagram of the phosphoinositide cycle is repeated below.

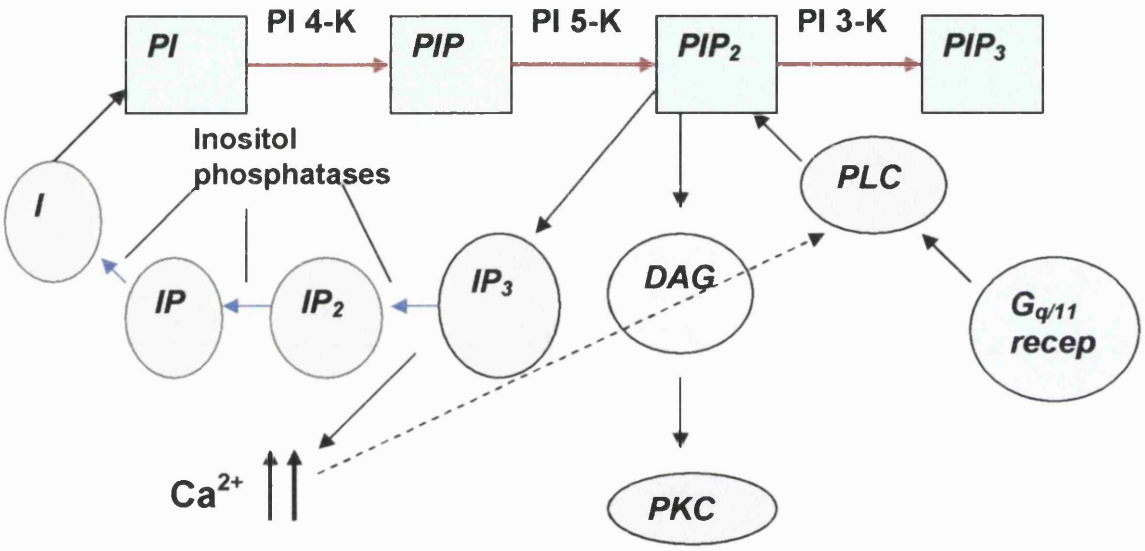

Figure 4.1. Simplified diagram showing the various stages in the phosphoinositide cycle.

I have investigated the involvement of phospholipase C, PI 4-kinase, PI 5-kinase and IP_3 in I_M inhibition and localisation of the GFP-PLC-δ PH construct.

4.1 ROLE OF PHOSPHOLIPASE C and/ or IP_3.

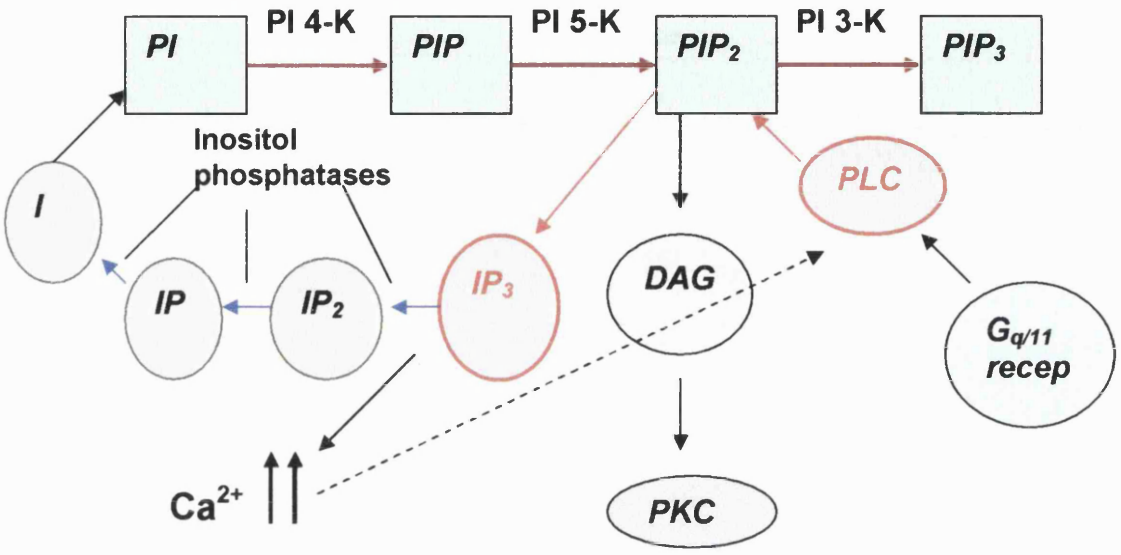

Figure 4.2. Phosphoinositide cycle with phospholipase C and IP_3 highlighted.

The previous chapter shows the simultaneous translocation of the GFP-PLC-δ PH construct and inhibition of the M-current by oxotremorine M and bradykinin. Although these experiments do not conclusively prove a link between activation of phospholipase C and inhibition of the M-current, the similarity of the time-courses, dose-dependence etc of both reactions suggests that they may be related. In this section I have inhibited PLC activity with the aminosteroid U73122, which is reported to block bradykinin-induced calcium transients in dorsal root ganglion neurons via its inhibitory action on phospholipase C (Jin et al, 1994).

I have also looked at the effect of dialysing the cell with IP_3 on rundown of the M-current and on translocation of the GFP-PLC-δ PH construct. I have carried out experiments to test the concentration of IP_3 that is required to cause translocation of the GFP-PLC-δ PH construct when dialysed into the cell via the patch pipette. Accompanying these experiments is a model, based on the affinities of the construct for PIP_2 and IP_3, showing the percentage of the construct expected to be bound to IP_3 and that expected to be bound to PIP_2 as the concentration of each changes, as happens in response to agonist stimulation.

RESULTS

4.1.1 Effect of the aminosteroid U73122

When the effect of U73122 on the inhibition of the M-current was tested, a 20 minute treatment with 1μM of this compound was reported to block only bradykinin-induced I_M inhibition; oxotremorine M-induced inhibition of the M-current was unaffected (Cruzblanca et al., 1998). Two years later, Bofill-Cardona et al. tested the compound again and found that treatment of cells with 1μM for 15 minutes did indeed greatly reduce bradykinin-induced I_M inhibition, and also UTP-induced inhibition, but only mildly reduced oxotremorine M-induced inhibition (from around 80% to around 52%; Bofill-Cardona et al., 2000); the inactive analogue U73343 had no effect on I_M inhibition by any agonist. In 2002, Suh and Hille increased the concentration of the aminosteroid from 1μM to 3μM, and found that

this concentration did significantly reduce oxotremorine M-induced inhibition of the M-current (while the same concentration of the inactive analogue U73343 had no effect; Suh and Hille, 2002).

I have tested the effects of a 10 minute treatment with 3μM U73122 on the oxotremorine M-induced inhibition of the M-current and on the translocation of the GFP-PLC-δ PH construct by this agonist.

Inhibition of the M-current by 10μM oxotremorine M was significantly reduced by treatment with the aminosteroid. Figure 4.3 shows the pooled data, showing that the control inhibition of 66± 2.5% (SEM) has been reduced to 23.5± 4.2% (SEM) by treatment with U73122. During treatment with the compound however, the amplitude of the M-current was running down, in the absence of the agonist. This suggests that U73122 is not entirely specific for phospholipase C, but may be having other effects within the cell. Suh and Hille stated that they did not use concentrations of U73122 higher than 3μM because of this effect on the amplitude of the M-current (Suh and Hille, 2002).

Figure 4.4a shows a typical effect of U73122 on the changes in cytosolic fluorescence intensity induced by 10μM oxotremorine M. At the beginning of the trace is a control response to the agonist, showing a large reversible translocation of the fluorescent construct from the membrane to the cytosol. The aminosteroid is then added and the cell monitored for 10 minutes before another addition of oxotremorine M (it has already been established that repeated translocation responses of the same magnitude are possible with this agonist – data shown, Chapter 3, Figure 3.17). The resting level of cytosolic fluorescence intensity

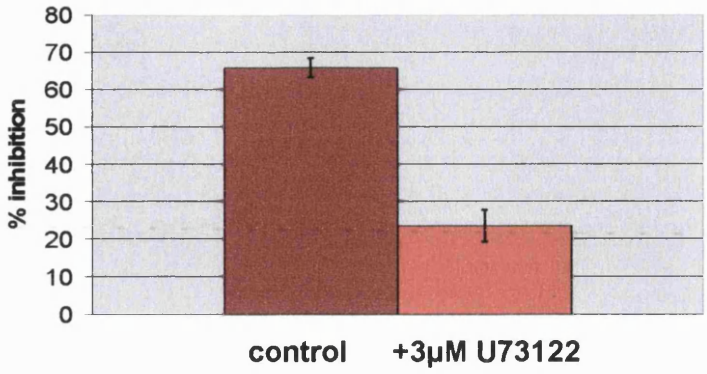

Figure 4.3. Pooled data showing the effect of a 10 minute treatment with the phospholipase C inhibitor U73122 on inhibition of the M-current by 10μM oxotremorine M.

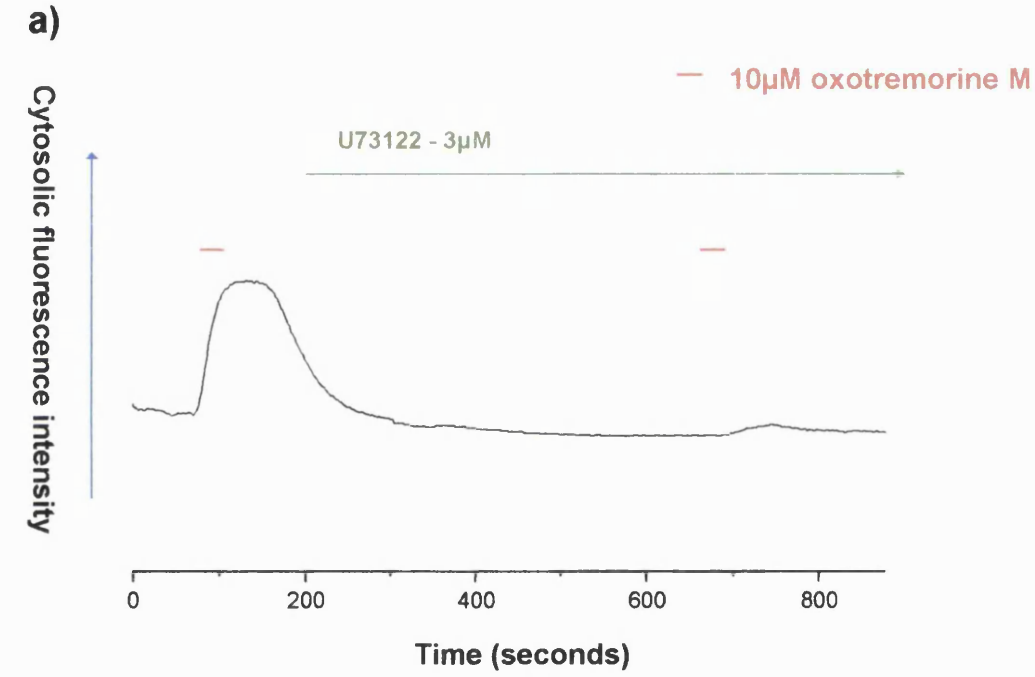

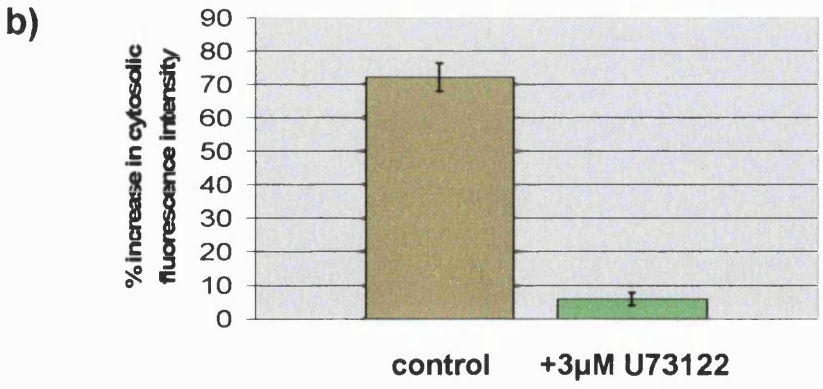

Figure 4.4. Effects of a 10 minute treatment with the phospholipase C inhibitor U73122 on the oxotremorine M-induced translocation of the GFP-PLC-δ PH construct. a) representative trace of changes in CFI b) pooled data.

unchanged by the addition of U73122, which shows that the compound does not induce translocation of GFP-PLC-δ PH in the absence of agonist. After 10 minutes, oxotremorine M is added again and, as Figure 4.4 shows, the extent of translocation of the fluorescent construct is significantly reduced. This was the case in all cells tested, with the average percentage increase from the resting level reduced from 72.2± 4.2% (n=9) to 5.9± 1.9% (n=7) after treatment with U73122; Figure 4.4b shows the pooled data for translocation of GFP-PLC-δ PH.

4.1.2 Effect of dialysing the cell with IP_3

4.1.2.1 Effect of IP_3 on the whole-cell rundown of the M-current

I wanted to test whether IP_3 itself, and not the associated Ca^{2+} rise, affected M-channels. To distinguish between a direct effect of IP_3 on the channels and an effect of the IP_3-induced calcium rise, the cell was dialysed with 100μM IP_3 in a zero calcium solution containing 10mM EGTA to buffer calcium release from intracellular stores. Whole cell rundown of the M-current (Simmons and Schneider, 1998) was observed over a ten minute period and compared between cells dialysed with a standard whole-cell recording solution (see Methods), and cells dialysed with the same solution plus 100μM IP_3. There was no significant difference between the rates of current rundown in the two groups, which indicates that IP_3 does not act directly on M-channels to cause closure. This data is shown in Figure 4.5.

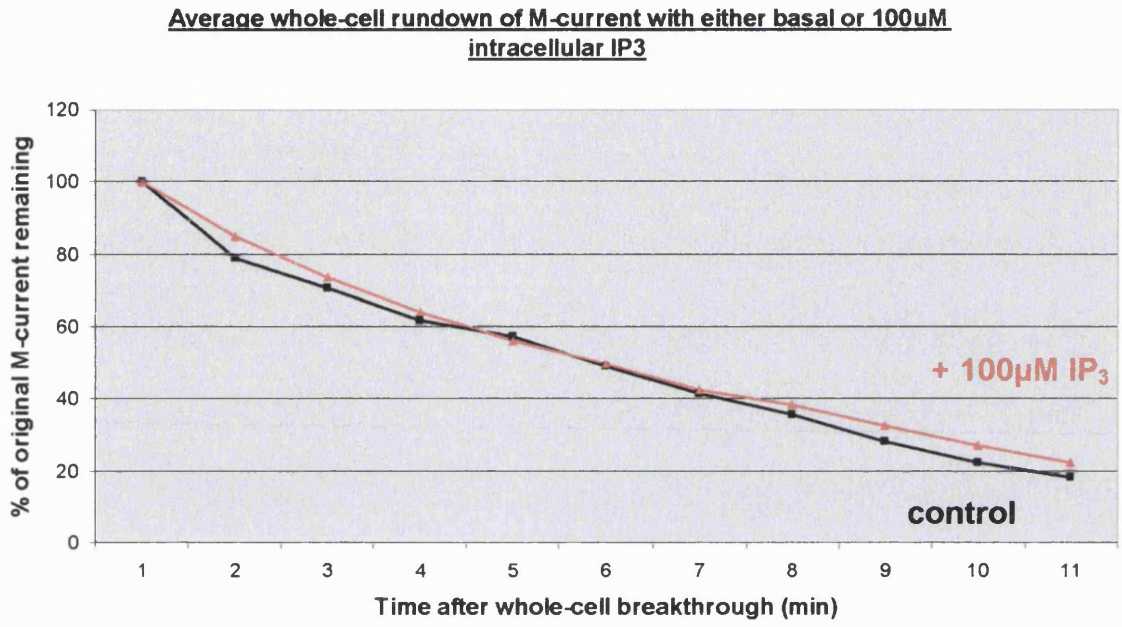

Figure 4.5. Dialysing the cell with 100μM IP_3 in a high EGTA solution (10mM) does not alter the rate of whole-cell M-current rundown.

4.1.2.2 Effect of IP_3 on the translocation of the GFP-PLC-δ PH construct

A model predicting the percentage of the GFP-PLC-δ PH construct bound to either PIP_2 or IP_3, with varying concentrations of each.

As discussed in the Introduction, the relative affinities of the GFP-PLC-δ PH construct for PIP_2 and for IP_3 have been measured as 0.21μM and 1.7μM respectively (Lemmon and Ferguson, 2000). These figures indicate that the affinity of the GFP-PLC-δ PH construct for IP_3 is eight times greater than its affinity for PIP_2. Based on these figures, I have constructed a model which assumes that 8X as many molecules of PIP_2 as of IP_3 need to be present for equal proportions of the construct to be bound to PIP_2 and half to IP_3. The model begins with the assumption that 100% of the molecules initially present are PIP_2, and that for every one molecule of PIP_2 which is hydrolysed, one molecule of IP_3 is formed, until 100% of the molecules present are IP_3 (this is obviously an oversimplification as both are continually synthesised and metabolised during the course of an agonist-induced response, but for the purposes of the model these factors are ignored). The following equations have been used to construct the model.

$$\% PIP_2 \text{ bound} = 100 X \left(\frac{\left[1/(1+8) \times \% PIP_2 \right]}{\left[1/(1+8) \times \% PIP_2 \right] x \left[8/(1+8) \times \% IP_3 \right]} \right)$$

$$\% IP_3 \text{ bound} = 100 X \left(\frac{\left[8/(1+8) \times \% IP_3 \right]}{\left[1/(1+8) \times \% PIP_2 \right] x \left[8/(1+8) \times \% IP_3 \right]} \right)$$

where % PIP_2 bound is the percentage of PIP_2 which is bound to the GFP-PLC-δ PH construct, % IP_3 bound is the percentage of IP_3 which is bound to the construct, % IP_3 is the percentage of IP_3 as a percentage of total IP_3 + total PIP_2, and % PIP_2 is the percentage of total IP_3 + total PIP_2 which is made up by PIP_2.

The variation in the percentage of GFP-PLC-δ PH bound to IP_3 and the percentage of the construct bound to PIP_2, as the levels of both molecules vary, are plotted in Figure 4.6.

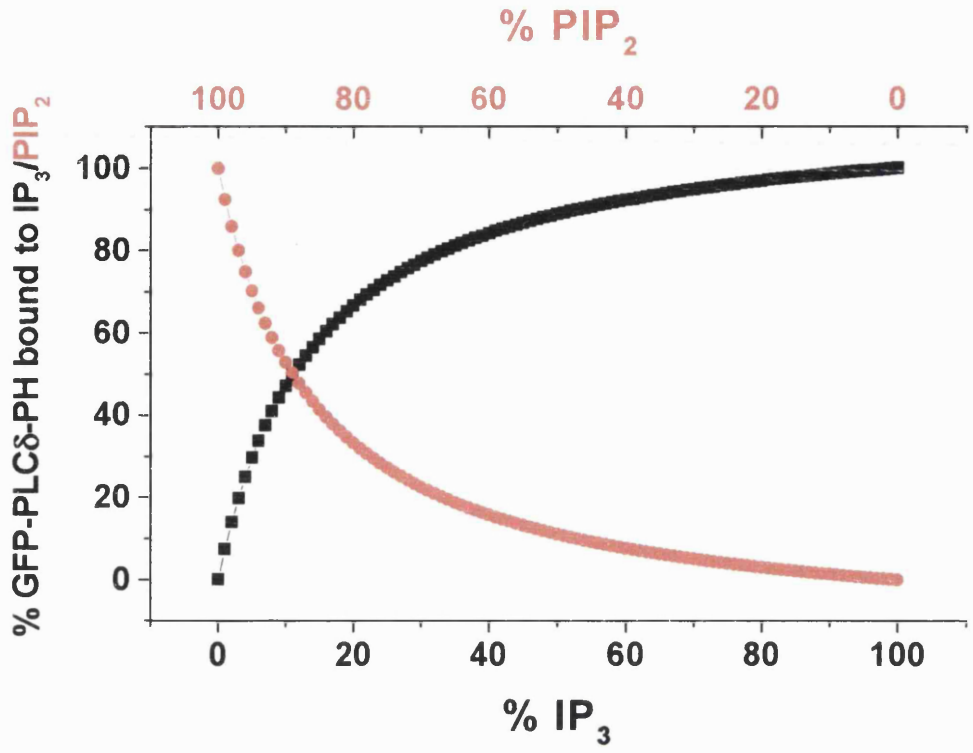

Figure 4.6. Model of predicted distribution of the GFP-PLC-δ PH domain between PIP_2 and IP_3, as the proportions of both of these molecules change. The model is based on the relative affinities of the GFP-PLC-δ PH construct for IP_3 and PIP_2 stated in Lemmon and Ferguson (2000) i.e. 0.21μM and 1.7μM respectively. The model assumes that the combined concentration of IP_3 and PIP_2 is greater than the total concentration of the GFP-PLC-δ PH construct. The model also assumes that, at rest, there is no IP_3 and 100% PIP_2, and that as the cell is stimulated with a PLC-mobilising agonist, PIP_2 is hydrolysed, leading to the production of one IP_3 molecule for every one PIP_2 molecule hydrolysed. Thus, as the response proceeds, the percentage of the total IP_3/PIP_2 pool made up by IP_3 increases and that made up by PIP_2 decreases. The bottom X axis shows IP_3 as a percentage of total IP_3/PIP_2 and the top X axis shows PIP_2 as a percentage of this pool. The Y axis shows the % of each of IP_3 and PIP_2 which should theoretically be bound to the GFP-PLC-δ PH construct as the proportions of both vary. The red trace shows changes in he percentage of bound PIP_2 and the black trace shows changes in the percentage of bound IP_3.

Figure 4.6 predicts that around an 11% decrease in PIP_2 (accompanied by the associated rise in IP_3) should be enough to cause half of the GFP-PLC-δ PH construct to bind IP_3, and hence to translocate to the cytosol. McLaughlin et al (2002) estimate an effective concentration of around 10μM PIP_2 inside a typical mammalian cell; if this estimation is fairly accurate, a rise of approximately 1μM IP_3 should be sufficient to induce translocation of half of the GFP-PLC-δ PH construct, and over 90% should occur for a concentration of around 5μM IP_3. The amount of IP_3 produced during agonist-stimulation of a G-protein-coupled receptor/ PLC pathway has been measured at between 0.1 and 10μM (Varnai et al., 2002), which relates to the model in Figure 4.6, but the decrease in PIP_2 will be similar, so this does not tell us whether the construct is reporting IP_3 levels or PIP_2 levels.

As discussed in the Introduction, Van der Wal et al (2001) tried releasing different amounts of caged IP_3 inside the cell via flash photolysis, and measuring the localisation of the CFP- and YFP-tagged versions of PLC-δ PH via fluorescence resonance energy transfer (FRET). No translocation was seen for 1μM IP_3, very little for 10μM and a large translocation at 100μM IP_3, although even at this very high concentration of IP_3, the translocation was not as complete as it was in response to 1μM bradykinin (Van der Wal et al., 2001). The model in Figure 4.6 cannot be used to predict the amount of PLC-δ PH translocation expected for the release of these concentrations of IP_3 as the model assumes that this IP_3 is being produced by hydrolysis of PIP_2, and that therefore the PIP_2 concentration is changing. I have adapted the model to predict the proportions of GFP-PLC-δ PH that would be bound to IP_3 and PIP_2 (and therefore its subcellular localisation) for

different levels of IP_3, while the amount of PIP_2 remains constant. This revised model is shown in Figure 4.7.

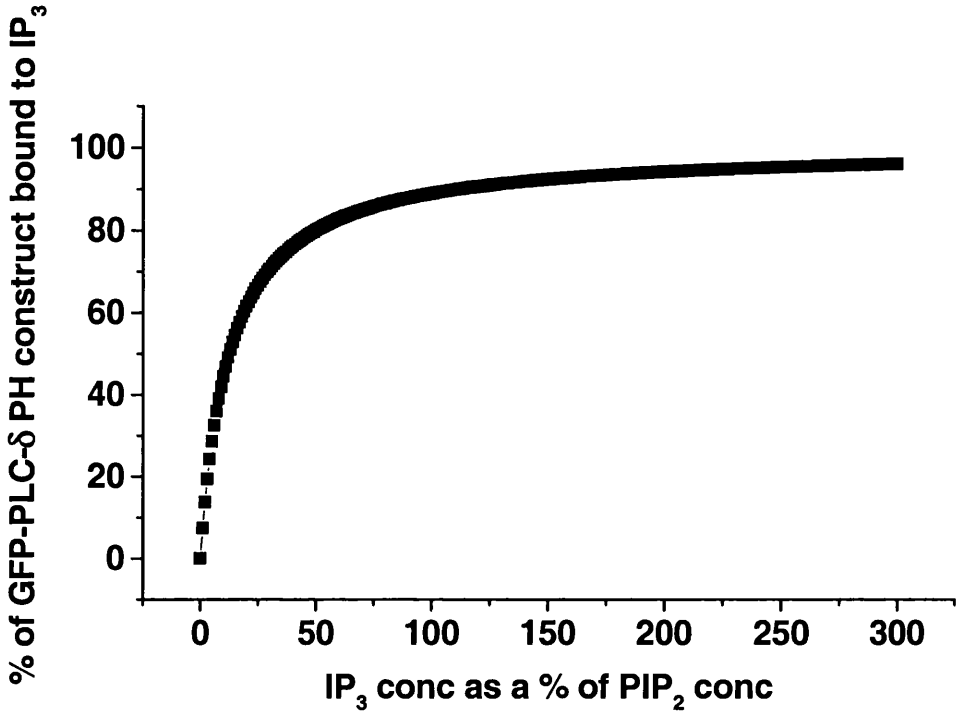

Figure 4.7. Revised version of Figure 34, showing predicted percentage of the GFP-PLC-δ PH construct bound to IP_3 for different concentrations of IP_3,but a constant level of PIP_2.

The revised model shown in Figure 4.7 predicts that, if the intracellular concentration of PIP_2 is indeed around 10μM, release of 1μM IP_3 (10% of the PIP_2 concentration) into the cytosol should induce translocation of around 45% of the GFP-PLC-δ PH construct, and release of 10μM IP_3 should cause translocation of around 89%. These predicted results do not reflect those reported by Van der Wal et al. (2001).

Effect of dialysing SCG neurons with differing amounts of IP_3 on the localisation of the GFP-PLC-δ PH construct.

I have also tested the effect of dialysis of the cell with IP_3 on translocation of the GFP-PLC-δ PH construct

GFP-PLC-δ PH-transfected cells were dialysed with different concentrations of IP_3 via the patch pipette, in a calcium free intracellular solution containing a high concentration of the calcium chelator EGTA (10mM). Cells were initially patched and broken through into the whole-cell configuration with patch pipettes containing 1μM IP_3, as this seemed a comparable concentration to that produced by an agonist response (see above), and as Figure 4.7 predicts that this concentration of IP_3 should produce around a 45% translocation of the GFP-PLC-δ PH construct .

Dialysis with 1μM IP_3 failed to produce any translocation of the GFP-PLC-δ PH construct, so cells were dialysed with 10, 25, 50 or 100μM IP_3, and the localisation of the GFP-PLC-δ PH construct was recorded.

No translocation was seen after dialysis with 1μM IP_3 (n=3), 10μM IP_3 (n=3), or 25μM IP_3 (n=2). A very small amount of translocation was detected when cells were dialysed with 50μM IP_3 (n=2) and full translocation was seen on dialysis with 100μM IP_3 (n=5). These results are similar to those obtained by van der Wal et al (2001) using the FRET technique, and like Van der Wal's results, do not reflect those predicted in the model in Figure 4.7 for the same amounts of IP_3.

The model in Figure 4.6 appears to be a reasonable indicator of the extent of GFP-PLC-δ PH translocation expected for different amounts of IP_3 production when this production is via the hydrolysis, and hence, depletion, of PIP_2. It is still unclear however, whether the translocation of the construct is due to the rise in IP_3 or to the fall in PIP_2. The revised model in Figure 4.7, which predicts GFP-PLC-δ PH translocation for rises in IP_3 *without* the accompanying decrease in PIP_2, does not reflect the translocation induced by these concentrations of IP_3, both in the experiments reported by van der Wal et al. (2001) and in my own experiments reported above.

This result suggests that translocation of the GFP-PLC-δ PH construct may be more accurately reporting depletion of PIP_2 rather than generation of IP_3. Van der Wal et al. also came to this conclusion, and added that high concentrations of IP_3 (i.e. 100μM) could distort the PIP_2-reporting ability of this construct.

Consideration of the difference in volume between the membrane and the cytosol

In fact, another major factor to consider, which may help to explain why the experimental data do not reflect the predicted data in Figure 4.7, is the difference in volume between the membrane and the cytosol. If we assume that, in the average SCG neuron, the thickness of the membrane is around 10nm, and the entire diameter of the cell is around 20μm, using the same model as that shown in Figure 3.13, the entire volume of the cell will be $4/3\ \pi\ (10^3)$=4189μm, the volume of the cytosol would be $4/3\ \pi\ (9.98^3)$=4164μm, and the volume of the membrane would be 4189 - 4164= 25μm. This would give us a membrane volume: cytosolic volume

ratio of 1: 167. As stated earlier, the approximate average concentration of PIP_2 in a typical mammalian cell, when considering the entire cell volume, is around 10μM (McLaughlin et al., 2002), but because PIP_2 is in fact restricted to the membrane, the concentration of this phospholipid is more likely to be around 170 times greater, at roughly 1.7mM. When IP_3 is produced via hydrolysis of PIP_2, this IP_3 is liberated into the cytosol where, because the volume of the cytosol is so much larger than the volume of the membrane, the concentration of IP_3 formed will be around 170 times lower than predicted. Varnai et al (2002) measured production of between 0.1 and 10μM IP_3 in response to a PLC-mobilising agonist; a concentration of 10μM IP_3 in the cytosol would result from the hydrolysis of enough PIP_2 to produce a concentration of around 1.7mM in the membrane. Because of this difference in volume between the membrane and cytosol, and because PIP_2 is found only in the membrane and IP_3 only in the cytosol, the amounts of IP_3 produced and PIP_2 hydrolysed will be the same, but the concentration of IP_3 produced by hydrolysis of PIP_2 will not be the same as the concentration of PIP_2 that has been hydrolysed. Figure 4.7 predicts that a concentration of IP_3 of around 15% of the current concentration of PIP_2 is necessary to produce translocation of around 50% of the GFP-PLC-δ PH construct from membrane to cytosol. If we consider these differences in volume when looking at Figure 4.7, we will notice that, if the thickness of the membrane is 10nm, then a concentration of IP_3 which represents around 15% of the PIP_2 present would be close to 250μM for a cell of diameter 20μm. In my, and Van der Wal's experiments (Van der Wal et al., 2002) a concentration of 100μM IP_3 produced a large translocation of the GFP-PLC-δ PH construct, whereas 50μM IP_3 produced very little, so the concentration which would

produce translocation of half of the construct would be somewhere between 50 and 100μM IP_3. This suggests that the concentration of PIP_2 in the membrane would have been around 100/15 times this amount (as 15% would cause half translocation) – somewhere between 335 and 670μM. This would suggest that the membrane volume: cytosolic volume ratio in the cells tested was between 1:30 and 1: 70 (assuming that the total PIP_2 concentration when dissolved throughout the cell is around 10μM); for a cell of 20μm diameter this would suggest a membrane thickness of around 30nm (total cell volume = 4189μm^3, cytosolic volume ≈ 50/51 x 4189 = 4107 (50 is halfway between 30 and 70, so membrane volume: cytosolic volume is approximately 1:50); cytosolic volume = 4/3 π r^3, so cytosolic radius, r = cube root of 4107/ 4/3 π = cube root of 980 ≈ 9.94; membrane radius = (10-9.94)/2 = 0.03μm = 30nm. A membrane of this thickness is feasible, or alternatively, if the membrane is ruffled rather than smooth, this could also increase its volume.

When the difference between the cytosolic and membrane volumes are considered, and the real concentration of PIP_2 in the membrane is calculated, the results obtained in my and Van der Wal et al.'s experiments appear to reflect those predicted in Figure 4.7. This difference in membrane and cytosolic volume and hence difference in subcellular PIP_2 and IP_3 concentrations suggests that translocation of the GFP-PLC-δ PH construct from membrane to cytosol is likely to be a more accurate indicator of PIP_2 depletion than IP_3 production.

4.1.2.3 Control experiment to test that IP_3 is dialysing into the cells

In order to test whether the IP_3 was actually dialysing into the cells a control experiment was carried out on Chinese Hamster Ovary cells (CHOs). These cells yield a much greater IP_3-induced calcium rise than do SCG neurons, so it is easier to visualise this rise using the ratiometric calcium dye FURA 2. In the presence of 10mM EGTA, used in this solution to buffer the small IP_3-induced calcium rise in SCGs, a small, transient calcium rise was still evident on whole-cell breakthrough with the IP_3 solution in CHO cells (n=3). This transient rise was absent on whole-cell breakthrough with the same solution minus IP_3 (n=3). This result indicates that IP_3 was entering the cells in the desired manner.

4.2 THE EFFECT OF OVEREXPRESSING PHOSPHATIDYLINOSITOL 4 PHOSPHATE 5 KINASE (PI 5-KINASE)

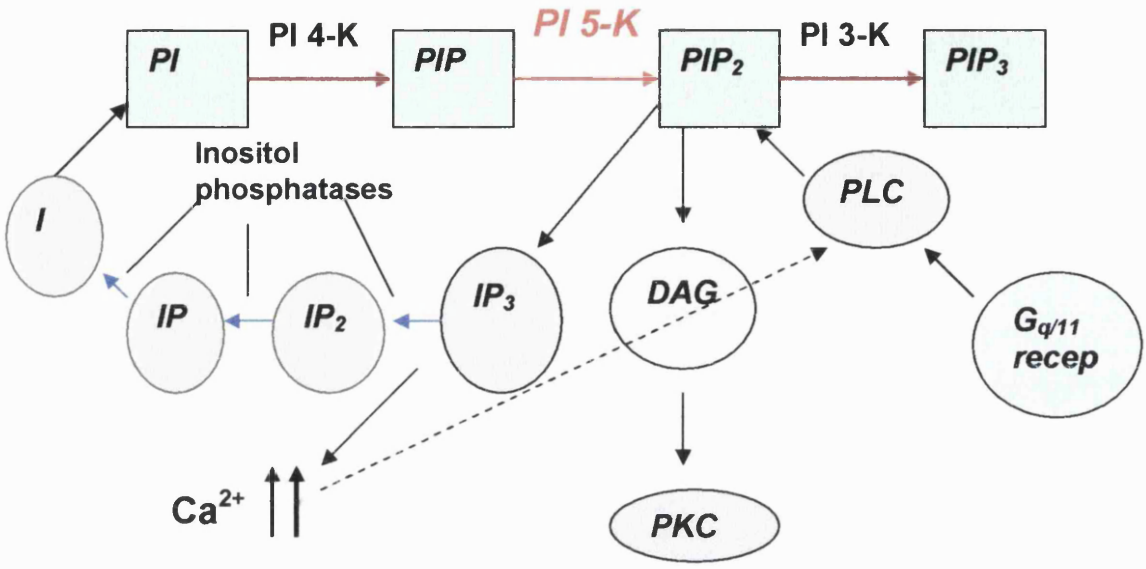

Figure 4.8. Phosphoinositide cycle with PI 5-kinase highlighted.

As discussed in the Introduction, the levels of PIP_2 in the plasma membrane are regulated by a complex system of PI kinases, PI phosphatases and phospholipase C, with most PI 4,5 P_2 generated from PI 4 P by PI 5-kinase. The majority of PIP_2 is formed via PI5-kinase from PI 4 P, although it is suggested that some pools of PIP_2 exist that have been formed from PI5 P via a PI 4-kinase (Tolias and Carpenter, 2000). PI5-kinase activity has been detected in several subcellular compartments, including the plasma membrane, cytosol, endoplasmic reticulum, cytoskeleton and nucleus (Loijens et al., 1996). The activity of this

kinase is enhanced by heparin, spermine and phosphatidic acid (PA), and is inhibited by PIP_2 itself (Loijens et al., 1996). PI 5-kinase activity is also affected by G-proteins *in vivo,* and the non-hydrolysable GTP analogue, GTPγS has been shown to increase PI5-kinase activity (Urumow et al., 1986). Interestingly, this could mean that agonist-stimulation of G-protein-coupled receptors, which leads to hydrolysis of PIP_2 via PLC, would also signal replenishment of this phospholipid by enhancement of PI 5-kinase activity (agonist stimulation of GPCRs could lead to stimulation of PI 5-kinase activity both directly, via G-protein activation, and indirectly via a negative feedback mechanism after depletion of PIP_2).

Disruption of the balance of this system by increasing the activity of PI 5-kinase has been shown cause an increase in PIP_2 levels (Coburn et al., 2002); this activity can be increased by overexpression of the kinase itself. Such overexpression has been shown to affect the sensitivity of PIP_2 –modulated channels to agonist-induced inhibition. Overexpression of PI 5-kinase in a heterologous expression system affected the sensitivity of co-expressed K_{ATP} channels to ATP (Shyng et al., 2000). Overexpression of the α-isoform of PI 5-kinase in adult rat atrial myocytes completely abolished α_{1A}-adrenergic- and ET_A-receptor-mediated inhibition of the endogenous GIRK current (Bender et al., 2002). Both are $G_{q/11}$-coupled receptor subtypes which activate PLC and are believed to cause inhibition of GIRK currents via depletion of PIP_2. This overexpression of PI5-kinase did not affect the density of the ACh-activated GIRK current or its activation rate (Bender et al, 2002). If inhibition of the K_{ATP} channel and the GIRK current mentioned above is due to PIP_2 depletion as reported (Kobrinsky et al, 2000; Lei et al., 2001), then overexpression of PI 5-kinase is likely to block receptor-mediated

inhibition of the currents by increasing the rate of synthesis of PIP_2, and therefore preventing the depletion of this phospholipid from the channels. In order for this increase in the rate of synthesis of PIP_2 to "override" inhibition, the rate of increase must be equal to, or greater than, the rate of decrease on agonist stimulation; thus the net depletion of PIP_2 would be zero and the channels would remain open. If agonist-induced inhibition of the M-current is also mediated via depletion of PIP_2, increasing the rate of synthesis of this phospholipid so that replenishment counteracts PLC-mediated hydrolysis would block this inhibition.

RESULTS

4.2.1 Expression of PI5-kinase and mutant (K179M) PI5-kinase in SCG neurons

SCG neurons were transfected with a GFP-tagged PI 5-kinase, or a GFP-tagged mutant version of this kinase, which is devoid of kinase activity (mutation is K179M). Cells were transfected via intranuclear injection of cDNA, at a concentration of 100ng/µl in the standard injection solution (see Methods, section 2.1.2). Neurons were incubated for 2 days to allow the protein to fully express, and were then observed via fluorescence microscopy (see Methods, section 2.3).

Figure 4.9a shows an SCG neuron transfected with the GFP-tagged PI 5-kinase enzyme. This figure shows the typical membrane-localisation of the enzyme, with the occasional patch of cytosolic fluorescence. Figure 4.9b shows an SCG neuron transfected with the mutant form of this kinase

a)

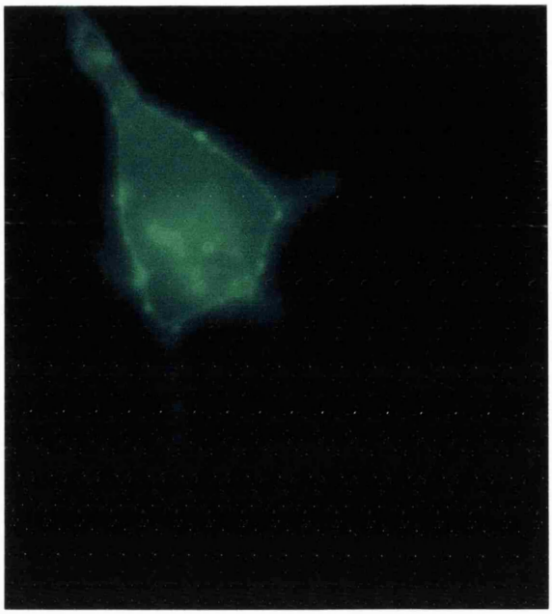

b)

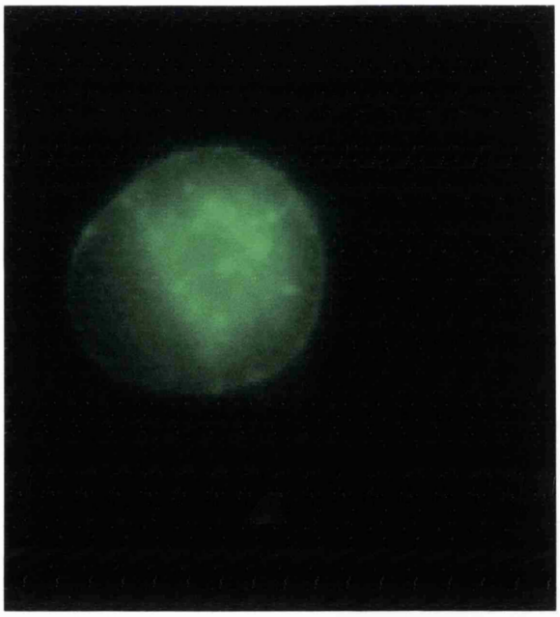

Figure 4.9. a) SCG neuron overexpressing PI 5-kinase (with a GFP tag) and b) SCG neuron overexpressing the PI 5-kinase K179 mutant – note the membrane localisation, but a greater amount of fluorescence in the cytosol than for the wild-type kinase.

4.2.2 The M-current in PI 5-kinase- and mutant PI 5-kinase-overexpressing cells.

Fluorescent neurons were selected and M-currents recorded from them using the perforated patch configuration of the voltage-clamp recording technique. The protocol used for recording M-currents was the same as that described in Chapter 3 (section 3.1.1). The amplitude of the deactivation tail, and also the durations of the fast and slow exponentials (taus) making up this relaxation, were measured and compared between the different cell groups. There was no significant difference between the amplitudes of the deactivation tails between the three groups (Figure 4.10a).

Measurement of the time course of the deactivation tail in the different groups yielded less comprehensive results however, with much variability in the lengths of the slow tau in PI 5 kinase-overexpressing cells (Figure 4.10b).

4.2.3 Inhibition by 10μM oxotremorine M in control and PI5-Kinase-overexpressing SCG neurons.

M-currents recorded from PI 5-kinase- and mutant PI 5-kinase-overexpressing cells were challenged with a maximal dose of oxotremorine M (10μM). Inhibition of the M-current in PI 5-kinase-overexpressing cells was greatly attenuated, from 72.6 ± 3.6% (n=10) in control cells to 14.5 ± 3.2% (n=13) in PI 5-kinase-overexpressing cells. Inhibition was not significantly reduced in the mutant

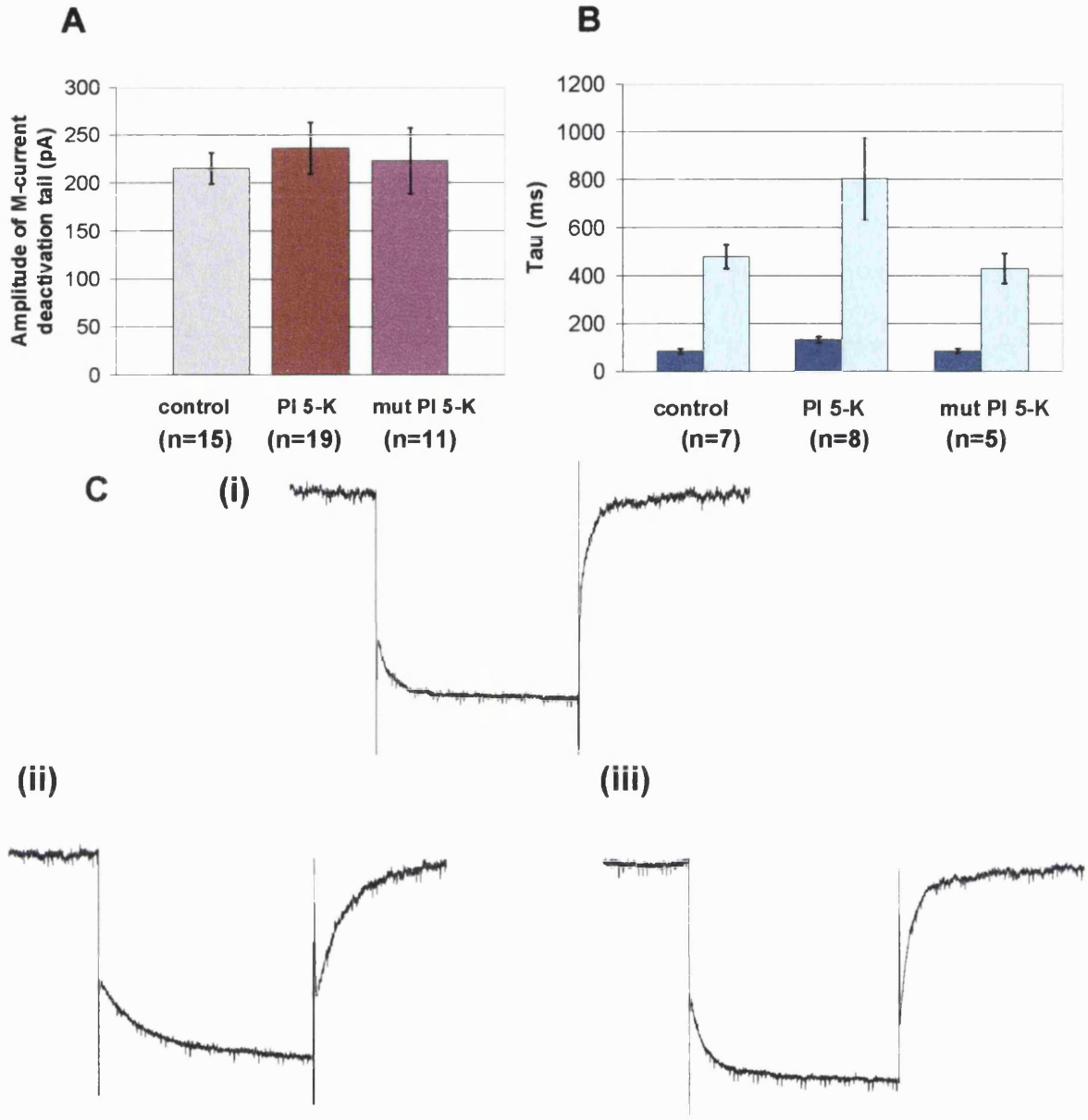

Figure 4.10. A. Amplitudes of M-current deactivation tails are not significantly different in control, PI 5-K-overexpressing or PI 5-K mutant-overexpressing SCG neurons. B. Time course of M-current deactivation tails are not significantly different between control PI 5-K- and mutant PI 5-K-overexpressing cells and C. examples of M-currents from (i) control, (ii) PI 5-K-overexpressing and (iii) mutant PI 5-K-overexpressing cells. NB. The slow tau varied greatly in PI 5-K-overexpressing cells, and the example shown in C (ii) shows a cell with a particularly slow tau – this was evident in about half of the PI 5-K-overexpressing cells.

PI 5-kinase-overexpressing cells when compared to the control group. Figure 4.11a shows these results in bar chart form.

4.2.4 Effect of overexpression of PI 5-kinase and mutant PI 5-kinase on inhibition of the M-current by bradykinin.

Although the focus of the recent publications hypothesising PIP_2 depletion as the "message" for agonist-induced M-current inhibition have focused more on muscarinic agonists, Zhang et al reported that expressed KCNQ2/3 heteromers with a mutation in the KCNQ2 subunit, which lowered the channel's affinity for PIP_2, were much more sensitive to bradykinin-induced inhibition (via co-expressed BK_2 receptors) than wild-type heteromers (Zhang et al., 2002). This is evidence that bradykinin also inhibits M-current via depletion of PIP_2 (although the IP_3-induced Ca^{2+} rise may also activate another pathway; see Gamper and Shapiro, 2002).

M-currents were recorded in control, PI 5-kinase- and mutant PI 5-kinase-overexpressing cells and challenged with 100nM bradykinin. The results obtained were very similar to those obtained for inhibition by oxotremorine M; overexpression of the wild-type PI 5-kinase greatly reduced bradykinin-induced inhibition of the M-current, from 54 ± 7.9% (n= 7) to 8 ± 2.6% (n=8). Overexpression of the mutant form of this kinase reduced bradykinin-induced I_M inhibition to 34 ± 15.2% (n=7), but this was not significantly different to the control. Figure 4.11b shows these results in bar chart form.

These results offer further evidence that both bradykinin- and oxotremorine M-induced inhibition of the M-current is indeed mediated via depletion of phosphatidylinositol 4,5 bisphosphate.

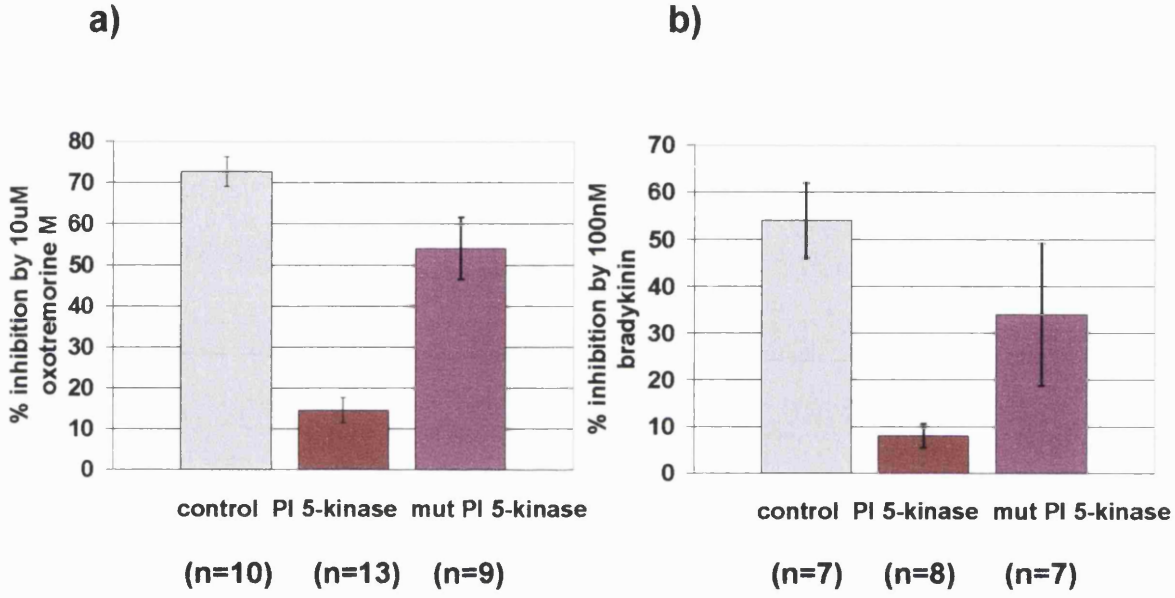

Figure 4.11. Inhibition of the M-current in control, PI 5-K- and mutant PI 5-K-overexpressing SCG neurons by a) 10μM oxotremorine M and b) 100nM bradykinin.

4.2.5 Effect of overexpressing PI 5-kinase on agonist-induced translocation of the GFP-PLC-δ PH construct.

In the preceding section, the method of detection of cells which had been transfected with either PI 5-kinase, or its mutant form, had been via visualisation of the green fluorescent protein attached to them. Obviously, this method of detection is no longer valid when the enzymes are co-expressed with the GFP-PLC-δ PH construct, as visualisation of a green fluorescing cell is not a guarantee that both the enzyme and the PIP_2-binding construct have been expressed. The cDNAs encoding both proteins are not expressed on the same plasmid, merely mixed into the injection solution, so expression of both is not guaranteed in an injected cell. In order to be able to visualize expression of both proteins individually, a construct of PI 5-kinase with a red fluorescent protein (pDSRed) tag incorporated into the vector was used. Transfected cells were observed under conditions for recognising fluorescence in both the green and red parts of the spectrum, and only cells from which fluorescence could be detected under both conditions were used. Figure 4.12 shows pictures of a transfected SCG under both green fluorescence and red fluorescence.

"Bleed-through" - Is light from the red fluorescent protein "contaminating" the green fluorescent protein imaging and vice versa ?

The patterns of expression for overexpressed PI5-kinase and for the GFP-PLC-δ PH construct shown in Figure 4.12 look very similar. I have considered the

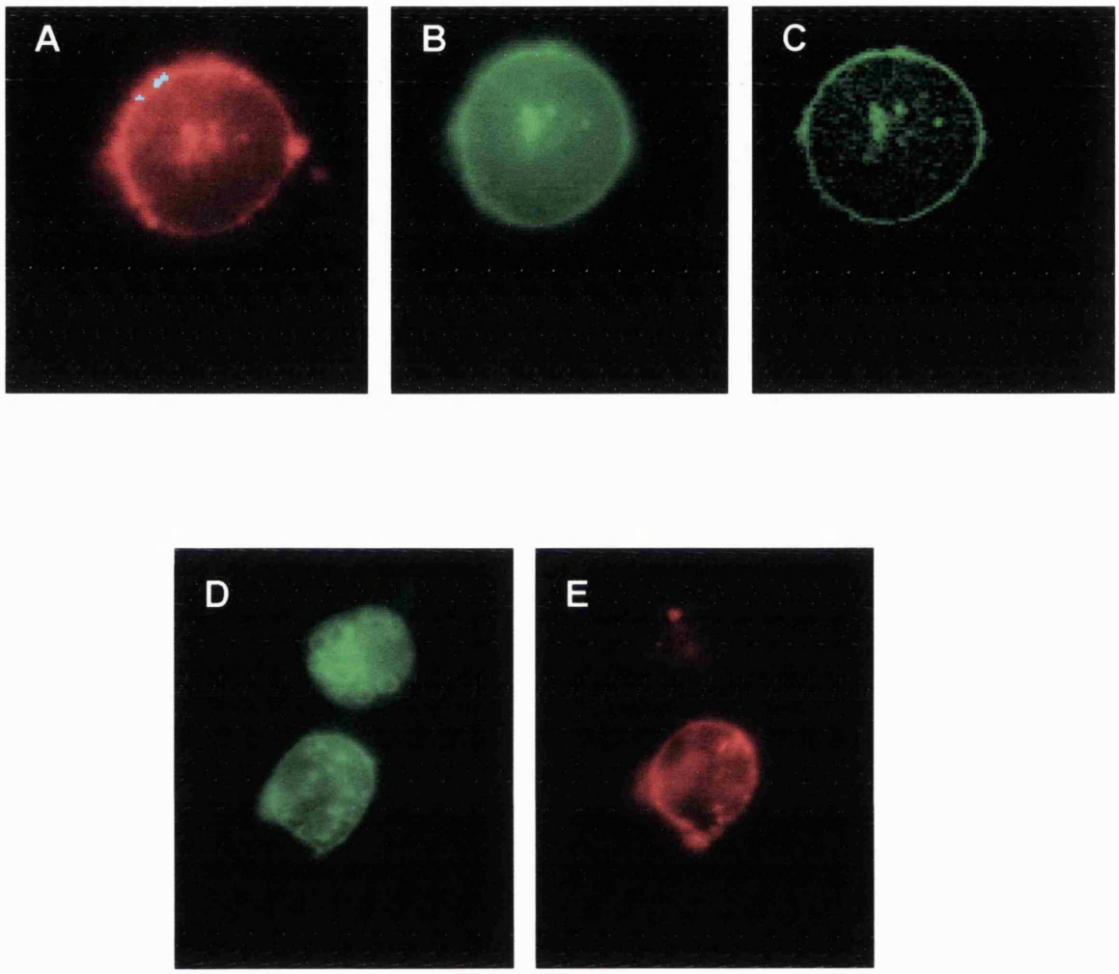

Figure 4.12. A. SCG neuron expressing PI 5-kinase with a pDSRED tag, B. same neuron also expressing GFP-PLC-δ PH construct, C. picture B after digital deconvolution, D. pair of SCG neurons showing green fluorescence indicating localisation of the GFP-PLC-δ PH construct and E. same pair of neurons showing red fluorescence indicating localisation of PI 5-kinase (different localisation than picture D, showing that "bleed-through" is not occurring.

phenomenon of "bleed-through", which is said to occur when light from a fluorophore creates "noise" when another fluorophore with different excitation and emission wavelengths is being visualised. This is unlikely in this case as, for GFP visualisation, excitatory light at a wavelength of 475 nm is passed through a 510 nm dichroic mirror, so that only light of wavelength less than 510 nm would be reflected onto the cells. The red fluorescent protein is excited by light of wavelength 535 nm (a difference of 60 nm from the GFP excitation wavelength), so it is unlikely that red fluorescent protein is being activated by light intended to excite GFP fluorescence. GFP emits light at a wavelength of around 530 nm however, so there is a possibility that light emitted from GFP could be activating the red fluorescence. Before light reaches the camera however, it is passed through a 530 nm bandpass filter (when GFP is being visualised); the red fluorescent protein emits light at around 610 nm, so this light would not pass through the filter.

Alternately, the red fluorescent protein used is excited at a wavelength of 535 nm, which would not excite the GFP. Even if GFP were excited, the light emitted by this green fluorophore at 530 nm would not pass through the 610 nm bandpass filter used in red fluorescent protein imaging.

The fact that the GFP-PLC-δ PH construct is acting as a marker for the product of the overexpressed PI 5-kinase helps to explain the similarity in the expression patterns of the two.

Agonist-induced translocation of the GFP-PLC-δ PH construct

Cytosolic fluorescence intensity was measured in these cells as before, and the changes induced by the addition of oxotremorine M (10μM) and bradykinin (100nM) were compared with those induced in control cells. The oxotremorine M-induced translocation of the GFP-PLC-δ PH construct was almost completely blocked by overexpression of PI 5-kinase; the CFI rise in control cells was 72.2 ± 4.2% (n=9), whereas in PI 5-kinase-transfected cells it was reduced to 9.0 ± 4.2% (n=6). The bradykinin-induced rise was also significantly attenuated, but not as dramatically, falling from 72.9 ± 5.1% (n=7) in control cells, to 33.5 ± 8.1% (n=4) in the PI 5-kinase-overexpressing cells. Figure 4.13 shows these results in bar chart form.

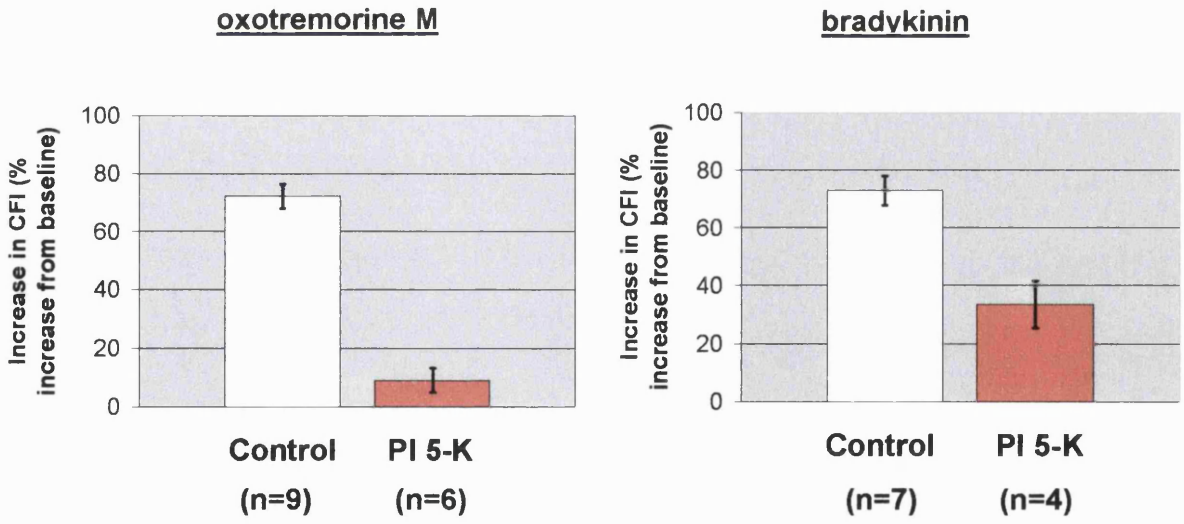

Figure 4.13. Bar charts showing average rise in cytosolic fluorescence intensity, due to translocation of the GFP-PLC-δ PH construct, by 10μM oxotremorine M or 100nM bradykinin in control or PI 5-knase-overexpressing SCG neurons.

The data in this section adds to the evidence that PIP_2 levels are able to influence the sensitivity of the M-current to inhibition by both oxotremorine M and bradykinin. The fact that the GFP-PLC-δ PH translocation by both of these agonists is also reduced lessens the possibility that overexpression of PI 5-kinase is acting in some other way to reduce M-current sensitivity to inhibition.

4.3 EFFECTS OF ALTERING PI 4-KINASE ACTIVITY

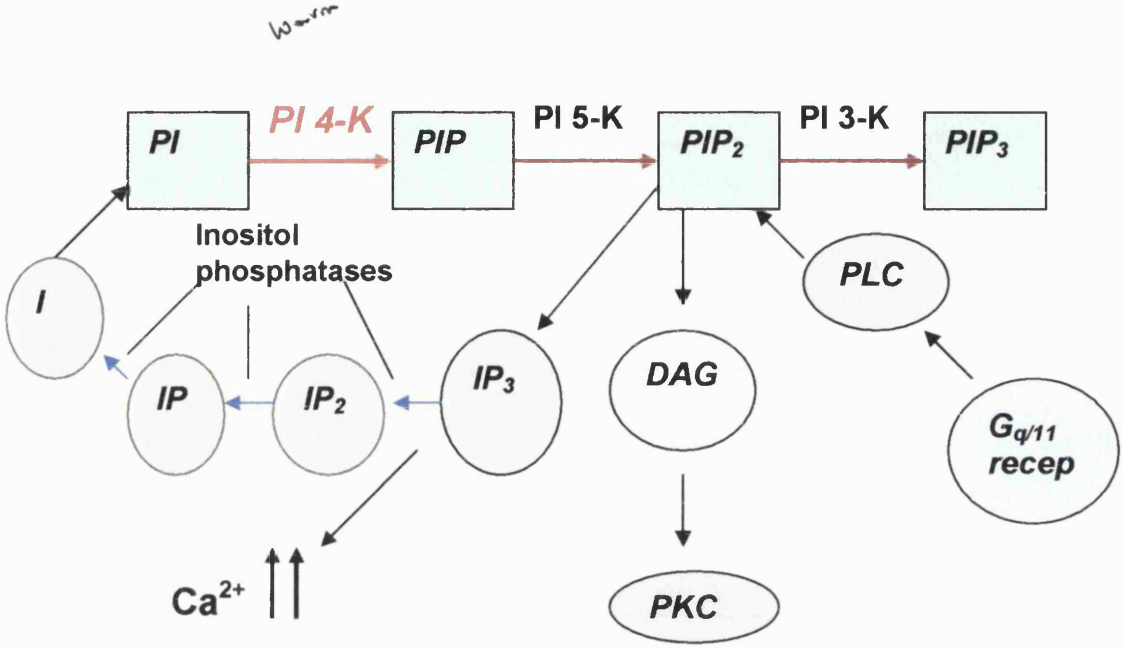

Figure 4.14. Phosphoinositide cycle with PI 4-kinase highlighted.

PI 4-kinase is the enzyme which phosphorylates phosphatidylinositol (PI) to produce phosphatidylinositol 4 phosphate (PIP), the precursor of PI 4,5 P_2. PI 4-kinases are ubiquitously expressed enzymes which associate with celluar membranes such as the endoplasmic reticulum, Golgi, plasma membrane, nuclear envelope, lysosomes and a variety of intracellular vesicles (Pike, 1992). I have tested the effects of inhibiting this enzyme with wortmannin, which has been

shown, at micromolar concentrations, to block the activity of most PI 4-kinases (Nakanishi et al., 1995), and therefore to block the replenishment of PIP_2 after its hydrolysis.

Wortmannin is reported to prevent recovery of M-current after inhibition by oxotremorine M (Suh and Hille 2002; Zhang et al., 2002) and it is also reported to considerably slow the membrane relocation of the GFP-PLC-δ PH construct in M_1-mACh receptor-transfected Chinese Hamster Ovary (CHO) cells, after translocation by acetylcholine (Zhang et al., 2002). Varnai and Balla however, report that treatment of NIH-3T3 cells with 10μM wortmannin failed to inhibit the relocalisation of the GFP-PLC-δ PH construct in response to calcium chelation, after translocation by ionomycin; in the same experiment wortmannin did, however, partially inhibit PIP_2 resynthesis as measured by mass assay (Varnai and Balla, 1998).

I have also used Neuronal Calcium Sensor protein 1 (NCS-1) in this section, because of its reported interaction with, and enhancement of the activity of PI 4-kinase (Hendricks et al, 1999; Koizumi et al, 2002; Zhao et al., 2001; Pan et al., 2002).

RESULTS

4.3.1 Effects of inhibiting PI 4-kinase with wortmannin

4.3.1.1 Effect of treatment with wortmannin on M-current amplitude and magnitiude of agonist-induced inhibition

Treatment with 20μM wortmannin for 10minutes caused a reduction in the amplitude of the M-current of 28.7 ± 4.7% (SEM; n=6); a likely explanation for this reduction in current amplitude would be that wortmannin is causing a reduction in the levels of PIP_2 in the plasma membrane. Basal activity in the phosphoinositide cycle with a certain amount of phospholipase C activity would gradually reduce PIP_2 levels. These levels would normally be replenished, but in the presence of wortmannin a vital stage in the regeneration pathway is inhibited, leading to a gradual reduction in PIP_2 levels and consequently, a reduction in M-current amplitude. This possible reduction in PIP_2 however, is not reflected by any change in localisation of the GFP-PLC-δ PH construct, the levels of which, both in the membrane and in the cytosol, remain constant throughout the treatment of the cell with wortmannin.

Despite this reduction in amplitude, the percentage inhibitions of the M-current by either oxotremorine M or bradykinin in the presence of wortmannin were not significantly different from those in control cells – see Figure 4.15.

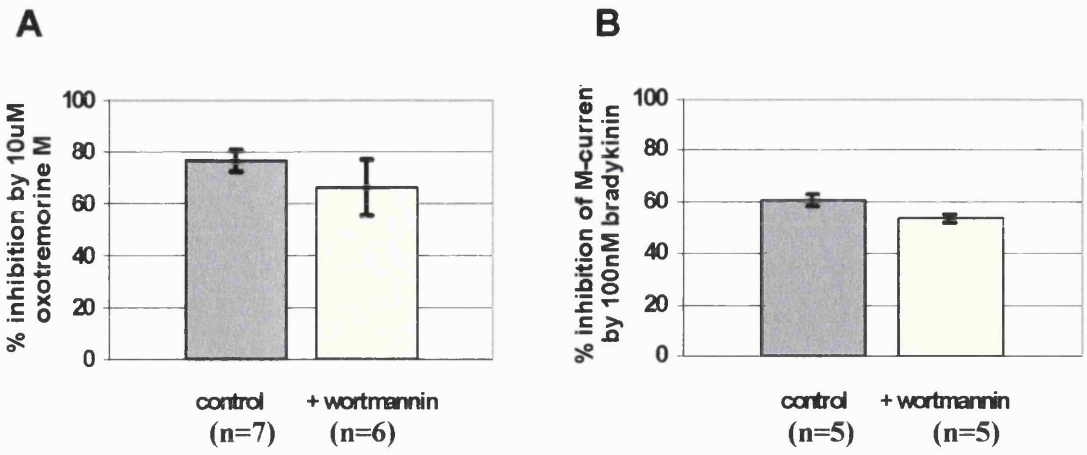

Figure 4.15. Comparison of the percentage of M-current inhibition in control cells and cells treated with 20μM wortmannin for 10 mins, induced by A. 10μM oxotremorine M and B. 100nM bradykinin. Treatment with wortmannin did not significantly alter the sensitivity of the M-current to inhibition by either agonist, according to an unpaired t-test at the 95% confidence level.

4.3.1.2 Effect of wortmannin on recovery of the M-current from agonist-induced inhibition

Treatment of SCG neurons for 10 minutes with 20μM wortmannin dramatically slowed recovery of the M-current after inhibition by 10μM oxotremorine M.

A control response to oxotremorine M was always recorded in the same cell before the wortmannin was added, and often two responses, to ensure that the second response was of the same magnitude and time-course as the first. After the control response(s), 20μM wortmannin was added to the bath solution and neurons were superfused with this solution for 10 minutes, after which 10μM oxotremorine M was added again. Figure 4.16 shows an example of the inhibition of the M-

current by 10μM oxotremorine M in the presence of wortmannin, and the lack of recovery from this inhibition.

For a 30 second application of oxotremorine M to a cell not treated with wortmannin, around 50% of the outward current amplitude had recovered at 80 seconds after the peak of the response. For an application of oxotremorine M of the same duration in a cell treated with wortmannin however, at the same time point after the peak of the response, only about 15% of the current amplitude had recovered. The average percentages of the holding current to have recovered at 50, 100, 150 and 200 seconds after the peak of the inhibition response, for both control and wortmannin-treated SCG neurons, is shown in Figure 4.17.

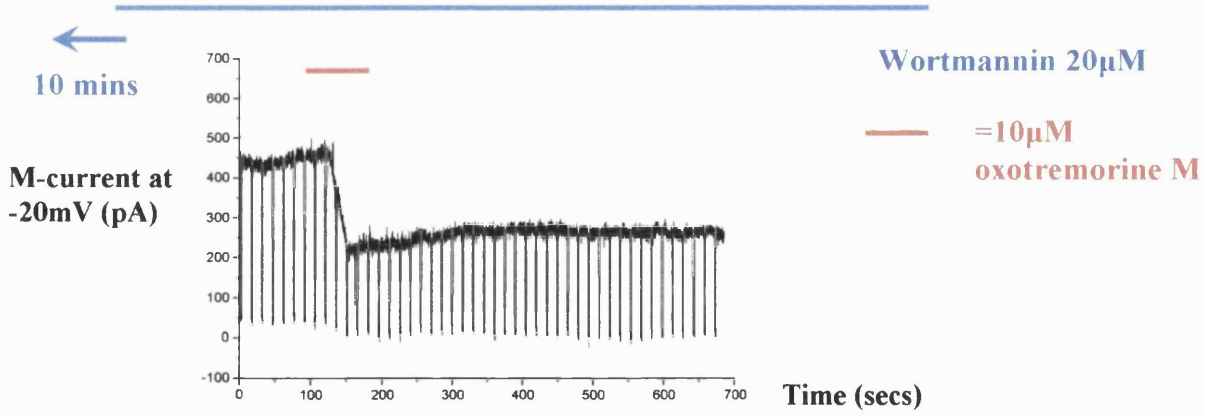

Figure 4.16. Example of oxotremorine M-induced M-current inhibition/ recovery in the presence of wortmannin.

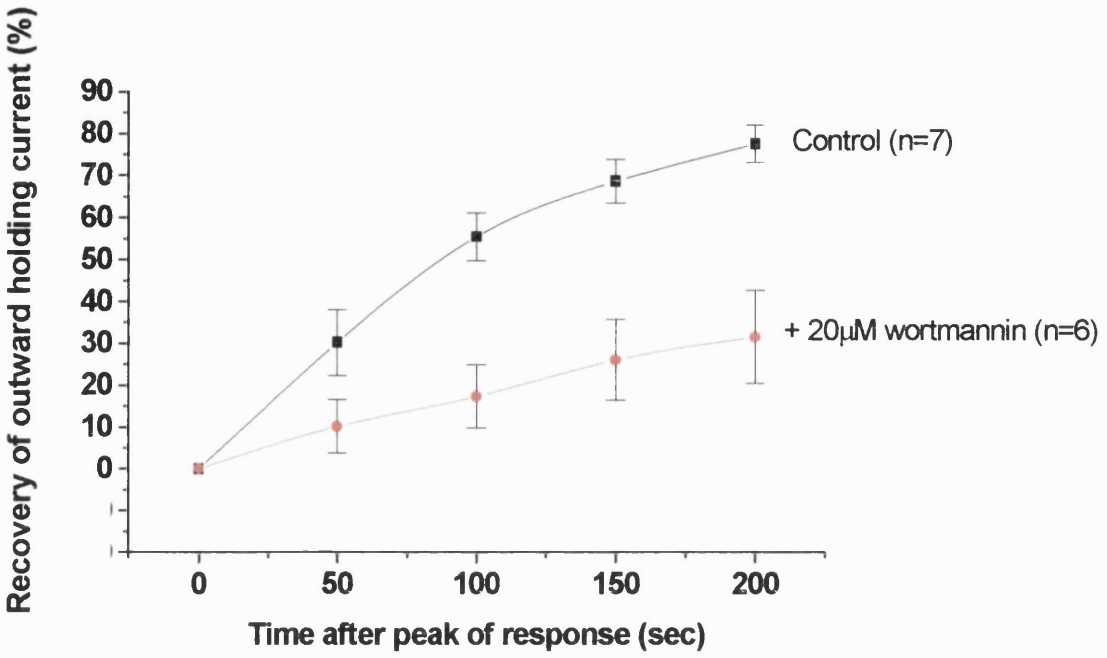

Figure 4.17. Average percentage of outward holding current (M-current) to have recovered after 50, 100, 150 and 200 seconds after the peak of the inhibition response to 10μM oxotremorine M (applied for 30 seconds at room temperature), in control SCGs and in SCGs treated with 20μM wortmannin for 10 minutes

The recovery of the M-current after inhibition by bradykinin was also tested, but the variability of the recovery time of the M-current after inhibition by this agonist, and the sometimes very slow or incomplete recovery, made it rather difficult to measure an effect of wortmannin on the time course of this recovery.

4.3.1.3 Effect of wortmannin on agonist-induced translocation/ relocation of the GFP-PLC-δ PH construct

The effect of treatment with wortmannin on the relocation of the GFP-PLC-δ PH construct after oxotremorine M-induced translocation was not as conclusive as the effect on the recovery of the M-current, and very variable results were obtained.

In four out of the nine cells tested wortmannin did not affect the timecourse of relocation at all, with the construct returning fully to the membrane. In four cells, the first, fast phase of relocation was intact but the second phase was slowed, to varying degrees (see Figure 4.18), and in one cell the first, fast phase was not present and the relocation took on a slow monophasic timecourse.

The amplitude of the translocation response was reduced in the presence of wortmannin (see Figure 4.19). This reduction was shown to be significant, according to an unpaired t-test, at the 95% confidence level.

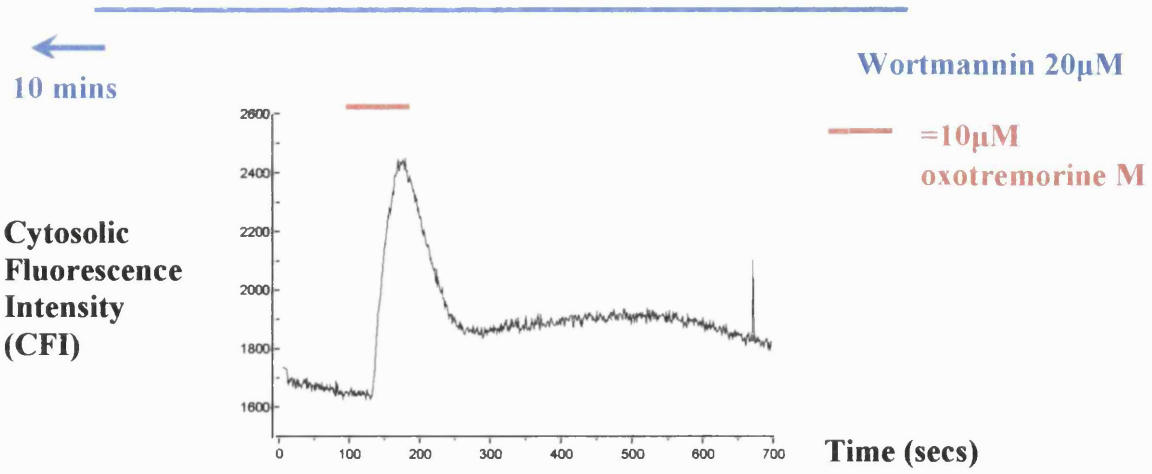

Figure 4.18. Example of GFP-PLC-δ PH translocation/ relocation by oxotremorine M in the presence of wortmannin. Note the inhibition of the second, slow phase of relocation. Four cells out of nine shared this pattern of GFP-PLC-δ PH relocation to the membrane.

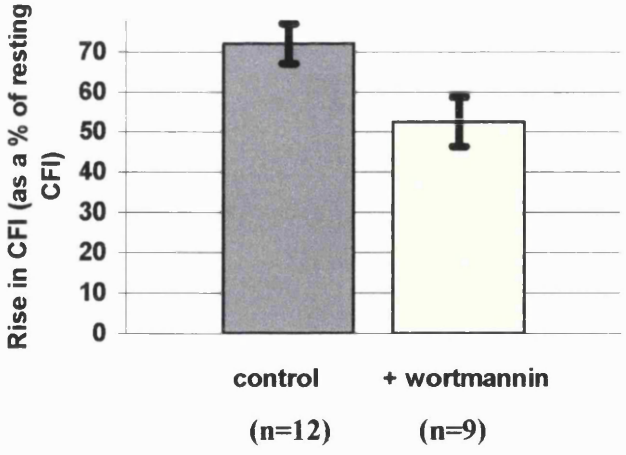

Figure 4.19. The rise in cytosolic fluorescence intensity (expressed as a percentage of the resting CFI) induced by 10μM oxotremorine M was significantly reduced in cells treated with 20μM wortmannin for 10 mins, when compared with untreated cells. The reduction is statistically significant at the 95% confidence level according to an unpaired t-test.

The reduction in amplitude of the rise in CFI induced by oxotremorine M-induced translocation of the GFP-PLC-δ PH construct is likely to be due to the levels of PIP_2 being reduced before the agonist-response. A reduction in steady-state PIP_2 levels by treatment with wortmannin would also explain the reduction in M-current amplitude seen, but one might expect to see higher levels of fluorescence in the cytosol if this were the case, due to some translocation of the GFP-PLC-δ PH construct in response to depletion of PIP_2. The fact that such translocation is not seen in the absence of agonist-stimulation of PLC is surprising, as there appears to be less of the construct available for translocation judging by the reduction in amplitude of the response.

IP_3 K_5?

4.3.2 Effect of enhancing PI 4-kinase activity with Neuronal Calcium Sensor protein 1 (NCS-1)

Neuronal Calcium Sensor protein (NCS-1) belongs to a family of EF-hand-containing Ca^{2+} sensor proteins that are mainly expressed in neurons. It was originally identified in Drosophila, in which it is referred to as "frequenin". Frequenin is just one of a variety of related small Ca^{2+}-binding proteins expressed mainly in neuronal and neuroendocrine cell types (others including recoverin/ S-modulin, visinin, visinin-like protein, neurocalcin and hippocalcin; Hendricks et al., 1999). NCS-1 was believed to be specific to neurons until it was discovered in glial cells of the central nervous system (Olafsson et al., 1997).

NCS-1 is a 22kDa protein with a higher affinity for calcium than that of calmodulin (3×10^{-7M} verses $4\text{-}20 \times 10^{-6}$M; Schaad et al., 1996) which could therefore provide an effective switch mechanism within neurons in response to slight variations in calcium concentration. The calcium binding properties of NCS-1 come from its four EF-hand domains, although the first EF-hand is non-functional (Cox et al., 1994). NCS-1 has been shown to bind to cell membranes, and some of its substrates, in a calcium independent manner, and to undergo two calcium-dependent conformational changes, one at a low calcium concentration (range 0.1 to 1.0μM) due to binding at two sites with high cooperativity, and one at a much higher concentration due to the third, low affinity, calcium binding site (McFerran et al., 1999).

Frequenin has been shown to enhance synaptic efficacy in Drosophila motor neuron (Pongs et al 1993; Rivosecchi et al, 1994) and Xenopus embryonic spinal

neuron (Olafsson et al, 1995). More recently, overexpression of NCS-1 has been shown to cause an alteration of exocytotic activity in bovine chromaffin cells (Pan et al, 2002; Mc Ferran et al.,1998) and PC12 cells (Koizumi et al, 2002; Mc Ferran et al.,1998), a potentiation of transmitter release via the enhancement of Ca^{2+} currents in neuromuscular synapses (Wang et al, 2001), modulation of Kv4-encoded K^+ currents in the mammalian myocardium (Guo et al, 2002), enhanced synapse formation and neurotransmission in NG108-15 cells (Chen et al, 2001) and inhibition of insulin-stimulated GLUT4 translocation in 3T3L1 adipocytes (Mora et al, 2002). NCS-1 appears to be a multi-functional protein, playing a role in several different intracellular pathways. NCS-1 has been shown to be able to substitute for the ubiquitous calcium binding protein calmodulin (Schaad et al., 1996), but perhaps a more publicised action of NCS-1 is its role in the regulation of phosphoinositide turnover via its direct interaction with phosphatidylinositol 4-kinase, the enzyme which catalyses the formation of PIP from PI.

4.3.2.1 Interaction between NCS-1/ Frequenin and PI 4-kinase and enhancement of PI 4-kinase activity

This interaction was first shown in yeast, where Frq1 and Pik 1 (the yeast homologues of frequenin and PI 4-kinase respectively) coimmunoprecipitate; it is the binding of Frq1 to the N-terminus of Pik1 which stimulates the enzyme's catalytic activity (Hendricks et al, 1999). Koizumi et al provided evidence that these proteins similarly interacted in mammalian cells by showing that overexpression of NCS-1 in PC12 cells resulted in an increase in the levels of downstream signals of

PI 4-K following stimulation of receptors by UTP or bradykinin (both calcium mobilising agonists). They measured the levels of PI, PIP and PIP_2 as relative percentages of the total phosphoinositide pool in control and NCS-1-overexpressing PC12 cells, and found no significant difference in the levels of PI between the two cell groups at rest. The levels of PIP and PIP_2 were significantly higher in the NCS-1 cells however, with the percentage of PIP rising to 2.2% from 1% in the control, and the percentage of PIP_2 rising from 2.2% to 3.7%. They also measured the accumulation of IP_3 against a lithium block (lithium inhibits inositol phosphatases which dephosphorylate IP_3) on stimulation of both groups of cells with UTP, and found that the accumulation in NCS-1 cells was 198% over basal at 20 min compared with 83% over in control cells (Koizumi et al, 2002). This increase in the percentage of the phosphoinositide pool made up by PIP and PIP_2, along with the marked increase in magnitude of the IP_3 response to UTP in NCS-1 cells, against a lithium block, (caused by more available PIP_2) is consistent with NCS-1 causing an enhancement in the activity of PI4-kinase.

It has also been shown recently that overexpression of NCS-1 in bovine chromaffin cells leads to an enhancement of histamine-induced exocytosis, due to a greater Ca^{2+} release from stores by elevated levels of IP_3 (Pan et al., 2002). Combined with immunocytochemistry, which showed a similar intracellular distribution of endogenous NCS-1 and PI4Kβ, and co-immunoprecipitation which showed a direct interaction of the two (Zhao et al., 2001; Pan et al., 2002), this result again indicates an enhancement of PI4-kinase activity by NCS-1.

It was observed by Rajebhosale et al. (2002) that overexpression of NCS-1 in PC-12 caused an enhancement of ATP-induced secretion. Evidence that this

effect of NCS-1 was via the enhancement of PI 4-kinase activity includes measurement of enhanced PIP_2 synthesis, and also that overexpression of NCS-1 caused a shift in the dose-response curve of inhibition of this secretion by the PI 4-kinase inhibitor phenylarsine oxide (PAO), indicating that NCS-1 antagonises the effect of this inhibitor (Rajebhosale et al., 2003).

This section looks at the effects of overexpressing NCS-1 on the properties of the M-current, the agonist-induced inhibition of this current, and the agonist-induced translocation of the GFP-PLC-δ PH construct in SCG neurons.

RESULTS

4.3.2.2 Immunocytochemistry using anti-NCS-1 antibody in uninjected and NCS-1-overexpressing SCG neurons.

Plasmids containing cDNA encoding the NCS-1 wild-type protein, expressed in the pcDNA 3.1 vector (see Methods, section 2.1.3) were injected into the nuclei of SCG neurons the day after culture; the neurons were then incubated for a further 2 days to allow the proteins to express.

Figure 4.20 shows immunocytochemistry in a control SCG neuron and in one transfected to overexpress NCS-1. Cells transfected with either the pcDNA 3.1 vector only (control) or the NCS-1 plasmid were incubated for two days to allow the protein to express and then fixed and stained with anti-NCS-1 antibody (see Methods, section 2.4 for full procedure). Figure 4.20c shows the same image as in 4.20b after it has undergone deconvolution to remove blurring. Note the membrane localisation of the expressed protein (see Scalettar et al., 2002).

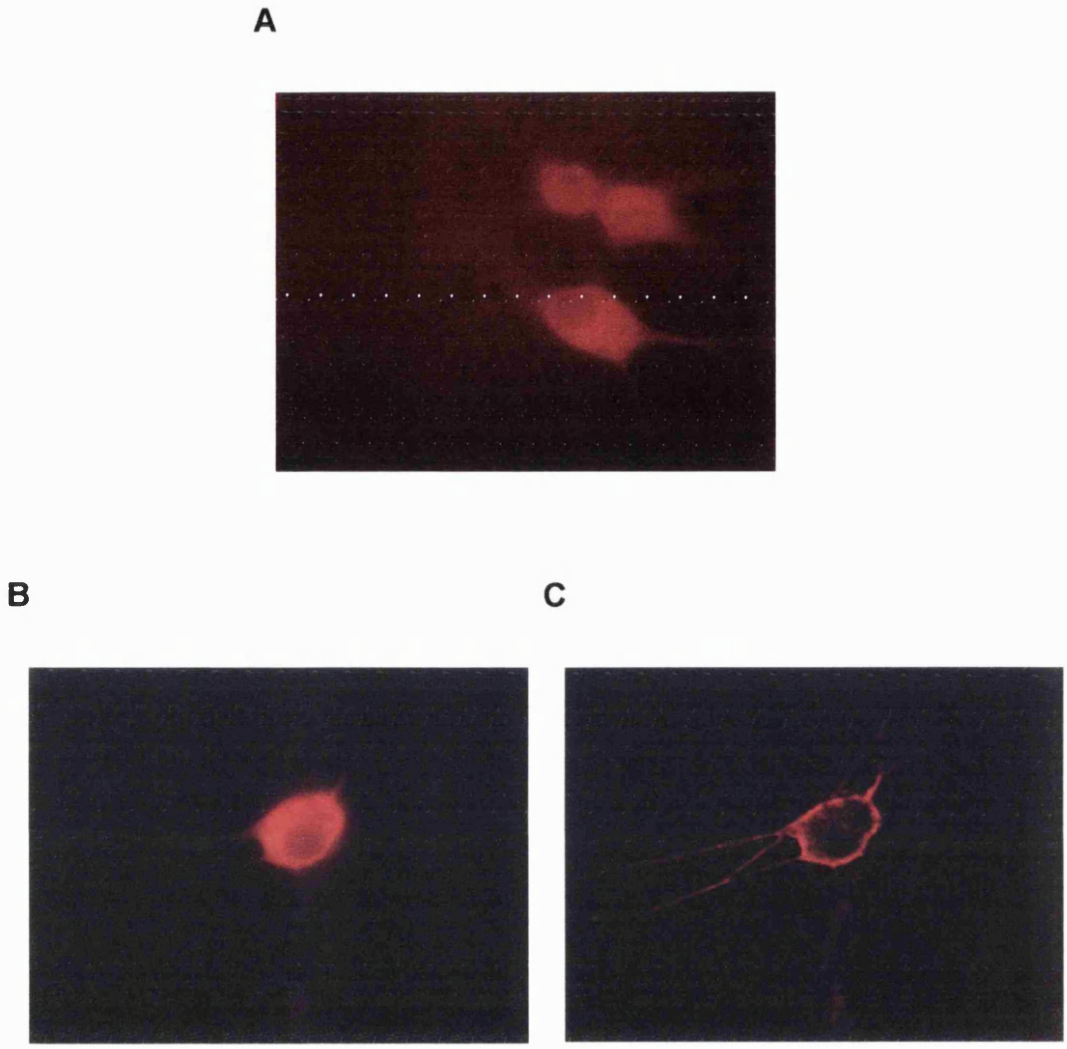

Figure 4.20. Immunocytochemistry with anti-NCS-1 antibody, showing A. staining for endogenous NCS-1 protein in uninjected SCG nerons, B. staining for NCS-1 protein in SCG neurons transfected with NCS-1 via intranuclear injection of cDNA plasmid and C. the same image as B. after undergoing digital deconvolution (see Methods) to reduce blurring and to show the membrane localisation of the expressed NCS-1 protein.

4.3.2.3 M-currents in uninjected, sham- and NCS-1-transfected cells

M-currents were recorded using the perforated patch-clamp configuration of the voltage clamp technique, with the standard solutions (see Methods, section 2.2.4.2), and the properties of these M-currents were compared between control (sham-injected with the pcDNA 3.1 vector) and NCS-1-transfected cells.

Amplitude

The average amplitude of the current deactivation relaxation on hyperpolarisation to –50mV was measured for each group, and the results are shown in Figure 4.21a.These average amplitudes were not significantly different according to an ordinary ANOVA test ($p>0.05$). Cells of a similar size were chosen for recordings in each cell group, so as to remove the possibility that current amplitudes were differing because of the size of the cells (larger cells tend to produce larger currents).

Kinetics of deactivation relaxation

The kinetics of the deactivation relaxation at -50mV were next compared between the different groups. The fast and slow components making up the deactivation tail were measured and compared in uninjected, NCS-1-

overexpressing and sham-injected SCG (shown in Figure 4.21b) and were found not to be significantly different according to an ordinary ANOVA test.

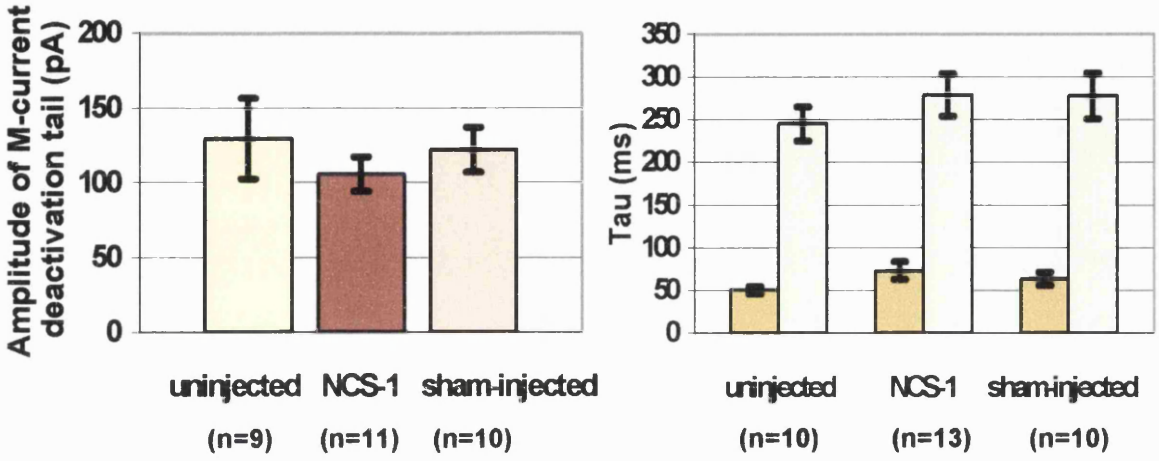

Figure 4.21. A. Overexpression of NCS-1 does not significantly alter the amplitude of the M-current deactivation tail or B the timecourse of the deactivation tail.

4.3.2.4 Agonist-induced inhibition of the M-current in uninjected, sham-injected (pcDNA 3.1 vector only) and NCS-1-injected SCGs.

M-currents were recorded from each cell group as before, and challenged with 1μM oxotremorine M or 100nM bradykinin. 1μM oxotremorine M was used here as this dose is reported to be on the steepest part of the dose-response curve for inhibition of the M-current, and would therefore show the most variation if this dose-response curve were shifted by expression of NCS-1.

Overexpression of the NCS-1 protein did not significantly alter the average inhibition of the M-current by 1μM oxotremorine M. The average inhibition by 100nM bradykinin however, was altered from 43% ± 9.0% SEM (n=5) in sham-injected cells to 14% ± 4.4% SEM (n=6), which is significantly reduced according to an ordinary ANOVA test. Figure 4.22 shows these results in bar chart form, with "*" indicating a result which is significantly different (at the 0.05 probability level) according to an ordinary ANOVA test.

It is clear from the data in Figure 4.22 that overexpression of the NCS-1 protein greatly reduces the sensitivity of the M-current to inhibition by bradykinin.

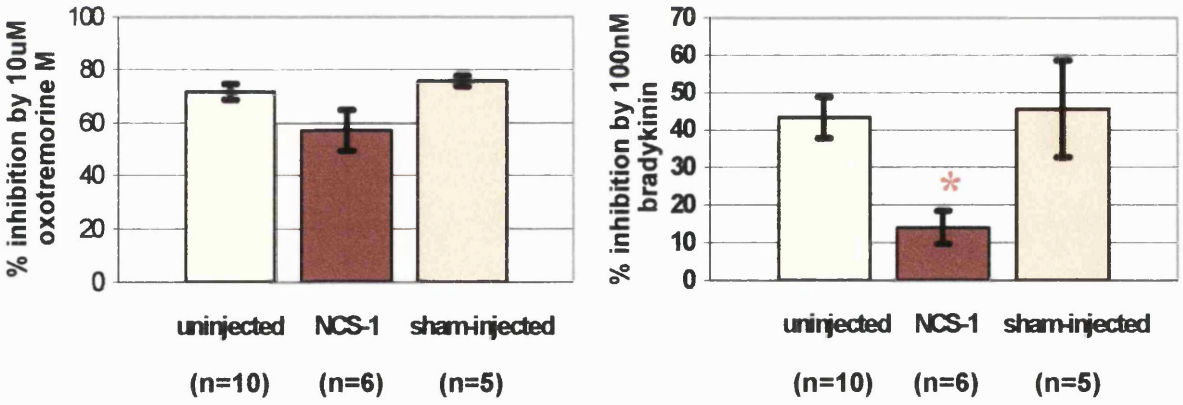

Figure 4.22. A Overexpression of NCS-1 does not alter the sensitivity of the M-current to inhibition by oxotremorine M, but B does significantly reduce the sensitivity of the M-current to inhibition by bradykinin (statistically significant according to an ordinary ANOVA test).

4.3.2.5 Is NCS-1 acting as a calcium buffer ?.

Although NCS-1 has been used in this section by virtue of its ability to interact with and enhance the activity of PI 4-kinase, it does have other possible functions within the cell. One fundamental property of NCS-1 which must be considered when investigating the effect of overexpressing the protein on the sensitivity of the M-current to inhibition by oxotremorine M and bradykinin, is its calcium binding ability. Rajebhosale et al. suggest that NCS-1 may buffer depolarisation-induced Ca^{2+} entry because of its plasma membrane localisation; a mutant form of the protein with reduced calcium-binding ability due to a non-functional third EF hand (E120Q mutation; Weiss, Archer and Burgoyne, 2000) does not buffer this calcium entry, even though it is also located to the plasma membrane (Rajebhosale et al., 2002). There is a chance that the reduction in sensitivity of the M-current to inhibition by bradykinin could be due to a calcium buffering effect.

A proportion of the M-current inhibition by bradykinin has been shown to be calcium-dependent (as has a small proportion of the oxotremorine M-induced inhibition of the M-current; Cruzblanca et al., 1998), and the proportion which is calcium-dependent seems to correlate with the amount by which the overexpression of NCS-1 wild-type overexpression has reduced the inhibition. Cruzblanca et al. showed that buffering intracellular calcium via the inclusion of 20mM BAPTA in the pipette solution reduced muscarinic inhibition of the M-current (by 10μM oxotremorine M) from 74.1 ± 3.8% SEM to 58.6 ± 3.2% SEM. The bradykinin-induced inhibition of I_M under these conditions was reduced from 44.4 ± 3.4% SEM to 10.3 ± 1.3% SEM (Cruzblanca et al., 1998). As shown above,

overexpression of wild-type NCS-1 reduced inhibition by bradykinin from 43% to 14%, a very similar reduction to that obtained by Cruzblanca with 20mM BAPTA. The small reduction in oxotremorine M sensitivity seen by Cruzblanca is also possibly mimicked in my experiment, but as the difference in oxotremorine M sensitivity of the M-current between NCS-1-overexpressing and control cells is not statistically significant, this cannot really be considered.

a) Does NCS-1-overexpression alter the resting calcium levels in an SCG ?

In order to investigate a possible calcium chelating effect of the NCS-1 protein, resting calcium levels were measured in uninjected, sham- and NCS-1-injected cells using the dual excitation calcium-sensing dye FURA 2 (see Methods, section 2.3.2). The results are shown in Figure 4.23.

According to an ordinary ANOVA test, there was no significant difference in the resting calcium levels between the different cell groups, indicating that the NCS-1 protein is not acting as a calcium chelator in the resting cell.

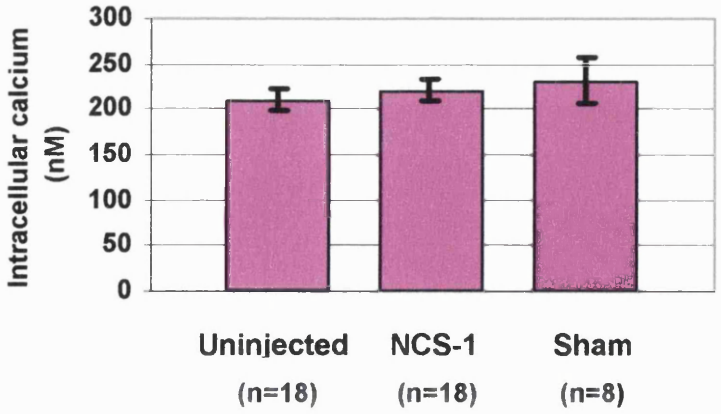

Figure 4.23. Overexpression of NCS-1 does not alter resting Ca^{2+} levels in the SCG neuron

b) Measurement of the calcium buffering capacity of control and NCS-1-overexpressing cells

The calcium rises elicited by oxotremorine M and by bradykinin are fairly small in SCG neurons, and are thus not easy to accurately measure by whole-cell imaging with FURA 2 (the rises may also be partly localised to the submembrane shell, which would not be detectable with this method). This makes measurement and comparison of the bradykinin-induced Ca^{2+} rise in control and NCS-1-overexpressing cells very difficult with the technology available.

Another method for measuring the calcium buffering capacity of a cell however, is to activate voltage activated calcium currents and simultaneously measure the associated calcium rise within the cell with FURA 2. The integral of the calcium current, and thereby the total concentration of Ca^{2+} entering the cell can be calculated, and compared to the amount which remains free to bind to the FURA 2 (calculated from the measured Ca^{2+} rise). The proportion of calcium which is entering the cell, which is then free to bind to FURA 2, can be compared between cells to see if their buffering capacity differs.

SCGs were transfected with cDNA encoding NCS-1 and a red fluorescent protein (pDSRed) via intranuclear injection. Red fluorescent protein was used as a transfection marker rather than GFP as FURA 2 was to be used to measure calcium rises and the excitation/ emission wavelengths for GFP and FURA 2 are very similar. Fluorescence from GFP would interfere with the FURA 2 signal. Cells

were then incubated at 37˚C for 30 mins with 5μM FURA 2 AM. After 30 mins cells were transferred to the microscope stage and superfused for at least 10 min with the standard extracellular solution (Methods, section 2.2.4.1).

Recording voltage-activated Ca^{2+} currents

Ca^{2+} currents were recorded from both uninjected (control) or NCS-1-overexpressing cells in the perforated-patch configuration with a Cs^{+}-based intracellular solution (Methods, section 2.2.4.2) containing amphotericin B.

Neurons were voltage-clamped at -70mV and calcium currents were elicited with depolarising steps to 0mV for 200ms. Ca^{2+} currents were obtained after digital subtraction of the current recorded with the same voltage protocol in the presence of $CoCl_2$. $CoCl_2$ blocks all calcium currents, so subtraction of the current remaining in the presence of $CoCl_2$ should ensure that the currents recorded mainly represented Ca^{2+} influx through the plasma membrane.

Translation of calcium current recordings into total calcium entry

Total calcium entry $[Ca^{2+}]_{total}$, given as a Molar concentration, is calculated from the following equation:

$$[Ca^{2+}]_{total} = Q_{Ca}/ zFV$$

where Q_{Ca} is the total charge which enters the cell during a calcium current, measured as the integral of the current, $\int I_{Ca}\, dt$, z is the valency of a Ca^{2+} ion (i.e. 2), F is the Faraday constant (96485 $C.mol^{-1}$) and V is the volume of the cell (cells are assumed spherical and have a radius of roughly 10µm).

The net variation in intracellular calcium concentration, as calculated by the FURA 2-measured Ca^{2+} rise, was then plotted against the calculated total calcium entry, $[Ca^{2+}]_{total}$. Figure 4.24A shows this data for control cells, 4.24B shows this data for NCS-1-overexpressing cells, and 4.26 shows the two graphs in A and B superimposed. The solid lines in Figure 4.24 A and B and Figure 4.25 represent the best fit obtained from a linear regression.

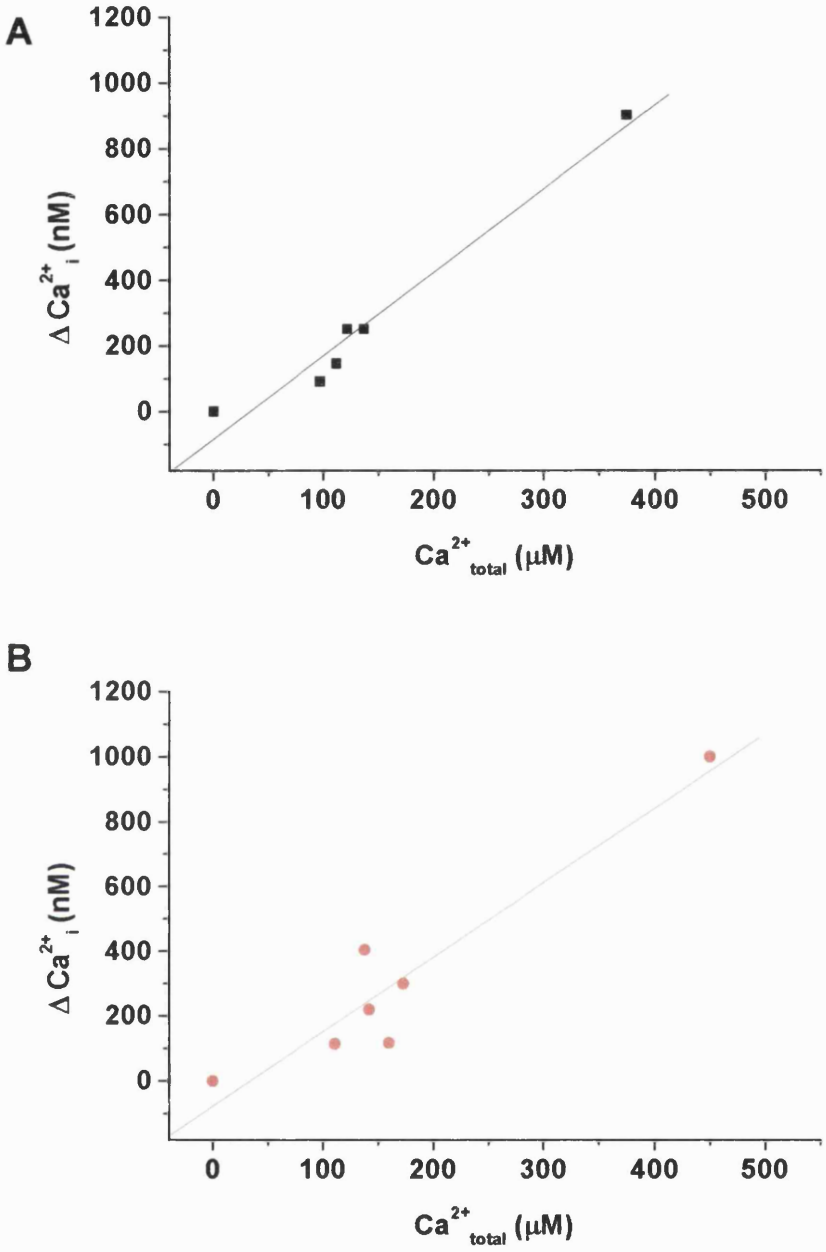

Figure 4.24. Relationship between total Ca^{2+} entry and the associated Ca^{2+} rise as measured with FURA 2 in A. Control SCG neurons and B. NCS-1-overexpressing SCG neurons. Solid lines represent the best fit obtained from a linear regression.

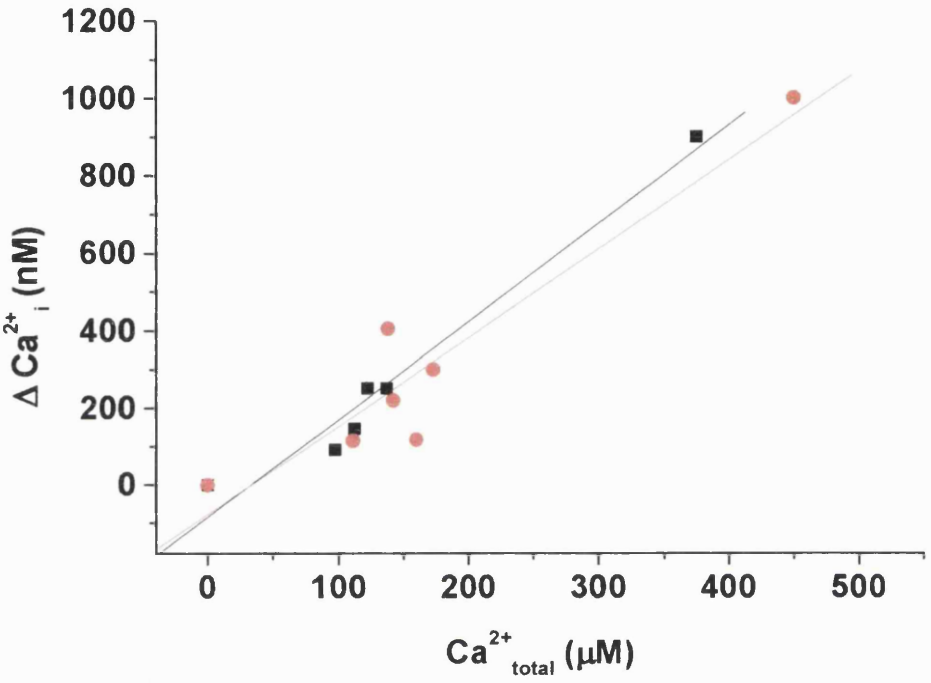

Figure 4.25. Plots in Figures 4.25 A and B superimposed.

Endogenous calcium binding ratio (κ) in control and NCS-1-overexpressing SCG neurons

The calcium binding ratio (κ) is defined at a particular $[Ca^{2+}]_i$ (Neher and Augustine, 1992) by the following equation.

$$K = \frac{\Delta [Ca^{2+}]_{bound}}{\Delta [Ca^{2+}]_i}$$

where $\Delta[Ca^{2+}]_i$ is the FURA 2-measured change in intracellular concentration and $[Ca^{2+}]_{bound} = [Ca^{2+}]_{total} - [Ca^{2+}]_i$.

The calcium binding ratio for each control cell and for each NCS-1-overexpressing cell were calculated, and the averaged values are plotted in Figure 4.26.

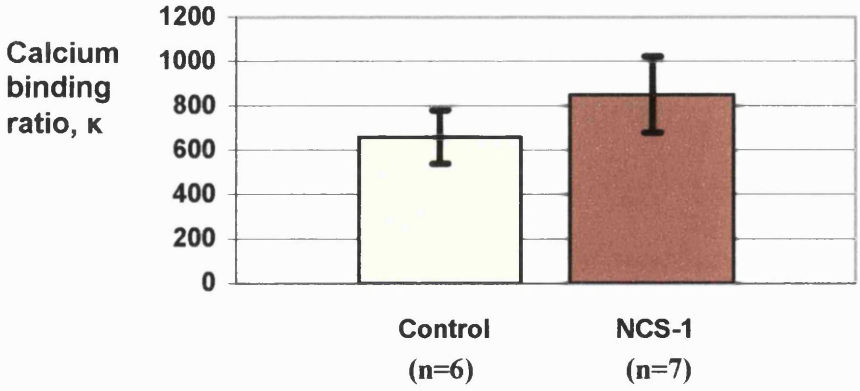

Figure 4.26. Average calcium binding ratios (κ) in control and NCS-1-overexpressing SCG neurons – the values are not significantly different at the 95% confidence interval, according to an unpaired t-test.

The calcium binding ratios in control and NCS-1-overexpressing cells are not significantly different according to an unpaired t-test, indicating that NCS-1 is not reducing the sensitivity of the M-current to inhibition by bradykinin via a calcium buffering effect.

4.3.2.6 Does translocation of the GFP-PLC-δ PH construct reflect the change in M-current inhibition by bradykinin in NCS-1-overexpressing cells ?.

SCG neurons were transfected, via intranuclear injection, with plasmids containing cDNA encoding either the GFP-PLC-δ PH construct alone, or this construct plus the NCS-1 protein. Cells were incubated for two days to allow the proteins to express, and then observed under X40 magnification via fluorescence microscopy. The distribution of the GFP-PLC-δ PH construct is unchanged by co-expression of the NCS-1 protein, as shown in Figure 4.27.

Increases in cytosolic fluorescence intensity in response to agonist application were recorded and measured. As Figure 4.28 shows, the effect of overexpressing NCS-1 on the translocation of the GFP-PLC-δ PH construct by bradykinin does reflect the effect that overexpressing this protein has on the bradykinin-induced inhibition of the M-current. The average increase in cytosolic fluorescence intensity induced by 100nM bradykinin is less in an NCS-1-overexpressing cell than in a control cell. Figure 4.28 shows representative traces of changes in cytosolic fluorescence intensity in response to addition of 100nM bradykinin, followed by 10μM oxotremorine M, in a control cell and in an NCS-1 overexpressing cell. Below these traces are bar charts showing the average increases induced by both agonists in the control and NCS-1-overexpressing cells.

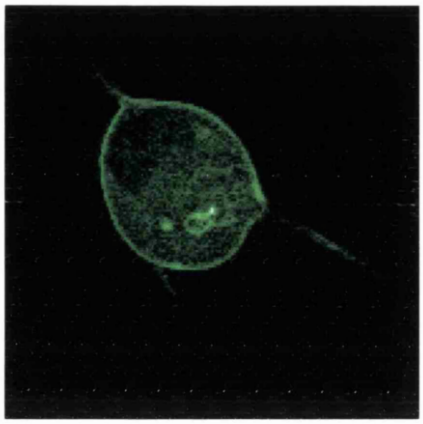

Figure 4.27. SCG neuron overexpressing NCS-1 and expressing GFP-PLC-δ PH construct – NCS-1 does not alter the localisation of the GFP-PLC-δ PH construct.

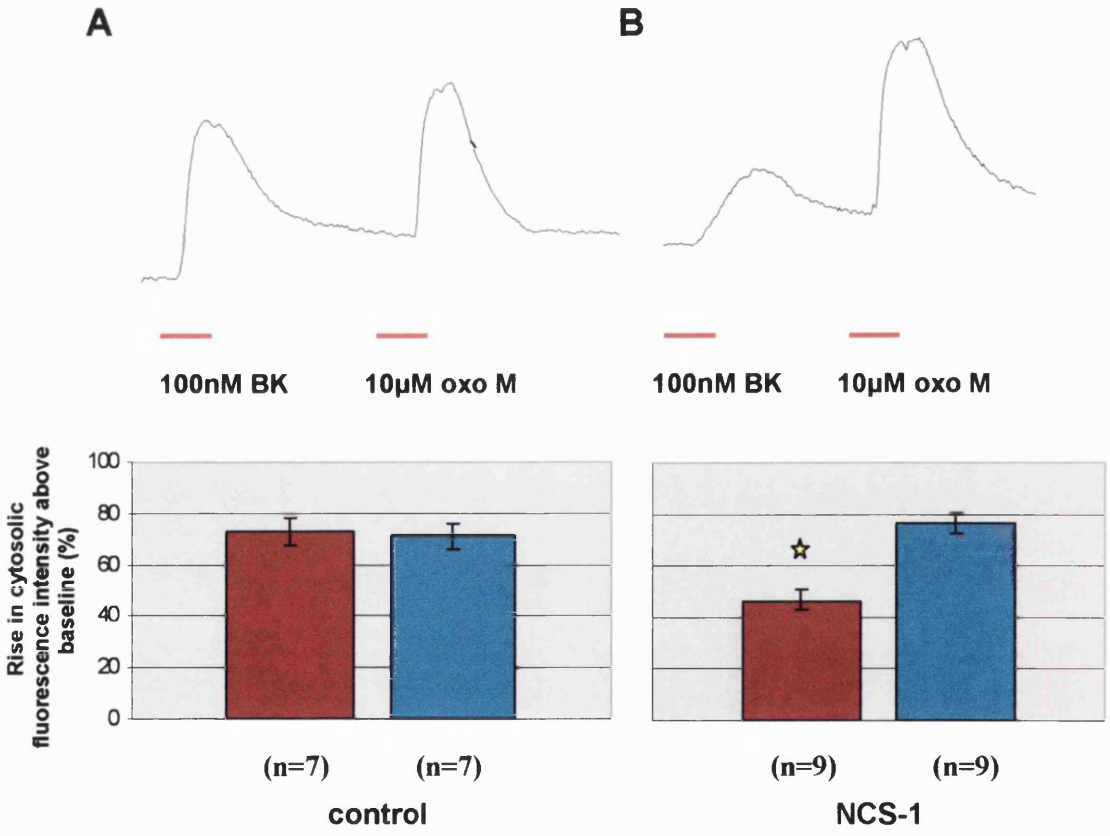

Figure 4.28. Typical trace of CFI changes on application of bradykinin followed by oxotremorine M, accompanied by a bar chart showing the average rises induced by each agonist in A. control cells and B. NCS-1-overexpressing cells.

Quantification of GFP-PLC-δ PH translocation response

Note that, in the cytosolic fluorescence intensity traces in Figure 4.28, the rises in response to oxotremorine M look similar in amplitude between the two cell types, but the bradykinin-induced rise is obviously smaller in the NCS-1-overexpressing cell. When the methods for analysing and attempting to quantify the translocation of GFP-PLC-δ PH were discussed in Chapter 3, it was mentioned that, due to various factors, responses could not accurately be compared between cells. It is obviously not possible to obtain a control response and an NCS-1-overexpressing response in the same cell, so a control had to be found. Both oxotremorine M and bradykinin have been applied to each cell; if the translocation of GFP-PLC-δ PH by oxotremorine M were not altered by NCS-1 (as the M-current inhibition by this agonist was not altered), the translocation by this agonist could be used as a control to measure any alterations in bradykinin-induced translocation by NCS-1. In control cells, injected only with the GFP-PLC-δ PH construct, the average percentage rise in CFI induced by oxotremorine M is 71 ± 5.1% (n=7), whereas in NCS-1 cells it is 76.4 ± 3.7% (n=9). Although rises in individual cells cannot be compared, two averages taken from similar populations of cells, i.e. with similar variations in size etc, are more reliable; thus it appears that overexpression of NCS-1 does not alter the amount of translocation induced by oxotremorine M. The fact that the average rise induced by bradykinin in NCS-1 cells is smaller than that induced by oxotremorine M can therefore be attributed to there having been a reduction in the amplitude of the bradykinin response rather than an increase in the amplitude of the oxotremorine M response.

This result indicates that overexpression of NCS-1 results in less M-current inhibition and also less translocation of the GFP-PLC-δ PH construct in response to bradykinin, but that both of these responses are not significantly altered by NCS-1 when induced by oxotremorine M.

Taken together with recent published work showing that NCS-1 directly interacts with, and enhances the activity of PI4-kinase, these data indicate that NCS-1 may be reducing the sensitivity of M-current inhibition to bradykinin by reducing the agonist's ability to deplete PIP_2. This theory was tested using the PI 4-kinase inhibitor wortmannin (as used in the previous section). If NCS-1 is producing its effect via stimulation of PI 4-kinase, resulting in enhanced PIP_2 production, inhibition of this kinase by wortmannin should oppose the effect of NCS-1. It has been reported that another PI 4-kinase inhibitor, phenylarsine oxide (PAO), can antagonise the effect of overexpressing NCS-1 on the ATP-induced secretion; NCS-1 shifts the dose-response curve of inhibition of this ATP-evoked secretion by PAO (Rajebhosale et al., 2002).

4.3.2.7 Effect of wortmannin on NCS-1-induced reduction of M-current sensitivity to bradykinin.

Cells were injected with plasmids containing NCS-1 or the pcDNA 3.1 vector only, as before. Two days later, M-currents were recorded and the inhibition of these currents by 100nM bradykinin was tested in both cell types in the presence of, and without, wortmannin. Cells were perfused with the normal bath solution with 20μM wortmannin added (or not added for the controls) for at least 15 minutes

before currents were recorded. The results are shown in the bar chart in Figure 4.29.

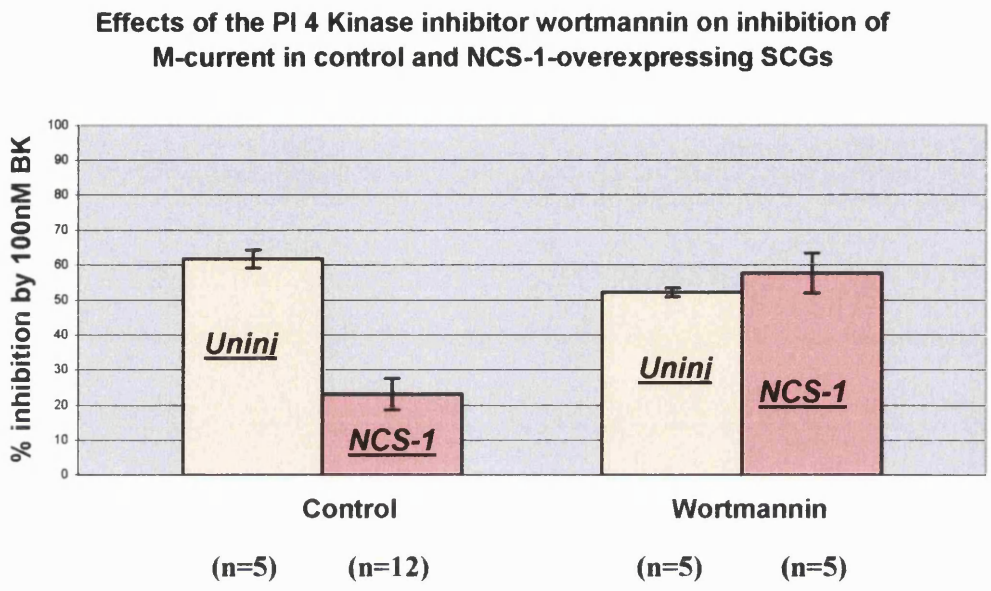

Figure 4.29. Effect of the PI 4-kinase inhibitor wortmannin on bradykinin-induced inhibition of the M-current in control and NCS-1 overexpressing SCG neurons.

Figure 4.29 shows that treatment of the cells with wortmannin is able to reverse the effect of NCS-1 on M-current inhibition. The control group of cells (those not treated with the PI 4-kinase inhibitor) are split into uninjected and NCS-1 overexpressing cells; the NCS-1 cells clearly showing reduced I_M inhibition by bradykinin. The inhibition of M-current by bradykinin is not significantly different in uninjected cells with or without wortmannin treatment, which indicates that the PI 4-

kinase inhibitor itself is not having a marked effect on M-current inhibition by this agonist. The difference in the sensitivity of the M-current to bradykinin-induced inhibition in the NCS-1 cells however is marked, between cells treated with wortmannin and cells not treated with wortmannin. These inhibitions are significantly different according to an ordinary ANOVA statistical test ($p<0.05\%$).

The above result suggests that wortmannin is working to antagonise the action of NCS-1 by slowing the rate of PIP production by PI 4-kinase. This will slow the rate of PIP_2 production to a manageable rate which enables PLC hydrolysis to deplete the channels of this phosphoinositide.

I have applied wortmannin to cells transfected with both NCS-1 and GFP-PLC-δ PH, in an attempt to see whether the reduced translocation of the construct by bradykinin in NCS-1-overexpressing cells can also be antagonised by treatment with wortmannin. Unfortunately, it was very difficult to gain reliable results using this technique as the translocation of the construct by bradykinin in the presence of wortmannin was rather inconsistent.

4.4 Summary of Chapter

The results shown in this chapter elaborate on those shown in Chapter Three, and indicate further that closure of M-channels could be linked to translocation of the GFP-PLC-δ PH construct and therefore to depletion of PIP_2.

The work with the phospholipase C inhibitor U73122 has confirmed the work of Suh and Hille (2002), who also used this compound to show that phospholipase C was involved in the muscarinic inhibition of the M-current as well as the bradykinin-induced inhibition.

The experiments with IP_3 have indicated that IP_3 does not affect M-channels directly, and also and probably more importantly, that very high concentrations of IP_3 (≈ 100μM) are needed to pull the GFP-PLC-δ PH construct out of the membrane (and off PIP_2) and into the cytosol. The levels required are between 10 and 1000-fold higher than the concentration of IP_3 produced during an agonist response (Varnai et al., 2002), so this suggests that the construct does not simply detach from PIP_2 to bind preferentially to IP_3, but that its localisation is determined by the ratio of IP_3 to PIP_2 (as theorised in section 4.1.2.2 of this Chapter). This theory would also help to explain why the agonist-induced translocation of the GFP-PLC-δ PH construct is less in cells overexpressing PI 5-kinase (overexpression of which has been shown to lead to higher levels of PIP_2; Coburn et al., 2002). One would imagine that in a cell with higher than normal levels of PIP_2, the amount hydrolysed during an agonist response, and therefore the amount of IP_3 produced, would be at least as high as in a control cell, and possibly higher. If translocation of the GFP-PLC-δ PH construct were purely an indicator of IP_3

production, translocation would also be as great as it is in a control cell. The fact that this is not the case indicates that the raised levels of PIP_2 are able to compete with IP_3 for possession of the construct.

The same explanation can be applied to the result obtained with translocation of the GFP-PLC-δ PH construct by bradykinin in NCS-1-overexpressing cells. PC12 cells overexpressing this calcium sensor protein have been shown to yield higher levels of IP_3 on stimulation with UTP, as PIP_2 levels in these cells are higher (Koizumi et al., 2002). If this result translates to SCG neurons, again one would expect to see full translocation of the GFP-PLC-δ PH construct in response to agonist if the construct were an indicator of IP_3 production. That we do not see full translocation of the construct by bradykinin in cells overexpressing NCS-1 suggests again, that translocation is reporting PIP_2 levels rather than levels of IP_3.

CHAPTER FIVE

GENERAL DISCUSSION

The evidence presented in the Introduction and Results chapters of this thesis provides a strong case for the depletion of PIP_2 as a signal for agonist-induced closure of M-channels, by both oxotremorine M and bradykinin.

Both agonists induce simultaneous, reversible translocation of the GFP-PLC-δ PH construct and M-current inhibition, with very similar time-courses for onset and offset of both responses. This fact alone does not prove the involvement of the depletion of PIP_2 in channel closure; rather it merely indicates that PLC is activated by both agonists and suggests a possible connection due to the similarity of the time-courses. Chapter Four however, does build on this possibility, with alteration of the activity of various components in the cycle bringing about changes in the sensitivity of both M-current inhibition and GFP-PLC-δ PH translocation. The fact that these two consequences of receptor activation are similarly affected by each alteration of a component in the phosphoinositide cycle suggests a link between them.

5.1 Phospholipase C activity

The interpretation of the results obtained with the aminosteroid U73122 is fairly straight forward – inhibition of PLC with this compound renders both M-current inhibition and the translocation of GFP-PLC-δ PH much less sensitive to both oxotremorine M and bradykinin, indicating that PLC is indeed involved in both pathways. What is interesting however, is the fact that the bradykinin-induced inhibition/ translocation is more sensitive to this analogue than the oxotremorine M responses, with 1μM U73122 being enough to block the response to a maximal concentration of bradykinin (100nM) – the same

concentration of the aminosteroid having virtually no effect on the oxotremorine M-induced inhibition/ translocation (Suh and Hille 2002). The lack of effect by the inactive analogue U73343 makes the possibility that U73122 is having some kind of non-specific effect on the cell rather than specifically targeting PLC less likely. Possible reasons for this difference in sensitivity between the agonists is discussed in section 5.4.

5.2 Experiments with PI 5-kinase

The data gained with the overexpression of PI 5-kinase enzyme indicates that, like the GIRK current (Bender et al., 2002) and the K_{ATP} current (Shyng et al., 2000), increasing the levels of plasma membrane PIP_2 decreases the sensitivity of the M-current to agonist-mediated inhibition. This has been shown to be true for both oxotremorine M- and bradykinin-induced inhibition. The reduction in the agonist-induced translocation of the GFP-PLC-δ PH construct caused by overexpression of PI 5-kinase was perhaps less predictable. One would imagine that, if the amount of membrane PIP_2 is increased, or at least if synthesis of it is faster, the amount of PIP_2 which is hydrolysed by phospholipase C during the agonist response would be the same as usual, or perhaps even more. This would mean that the amount of IP_3 produced would be the same or greater than in control cells, and therefore, if the affinity of the GFP-PLC-δ PH construct for IP_3 is so much higher than it is for PIP_2, one would expect it to translocate in the normal way; that it doesn't is perhaps an indication that the amount of PIP_2 generated in the PI 5-kinase overexpressing cells exceeds the amount of IP_3 produced by enough to overcome this difference in

affinity, allowing the construct to remain at the membrane, bound to PIP_2 (see the model in section 4.1.3.2).

The fact that overexpression of PI 5-kinase greatly reduces the sensitivity of the M-current to inhibition by either oxotremorine M or bradykinin suggests that depletion of PIP_2 is involved in the transduction pathways by both agonists.

5.3 PI 4-kinase experiments

5.3.1 Experiments with wortmannin

The experiments with the PI 4-kinase inhibitor wortmannin did not provide such "clear cut" answers as one would hope with regards the simultaneous measurement of M-current inhibition/ GFP-PLC-δ PH translocation. The slowing of recovery of the M-current after oxotremorine M-induced inhibition was robust, but the effect on the relocation of the fluorescent construct to the membrane was less conclusive.

Other instances of wortmannin having little or no effect on the time-course of the relocation of the GFP-PLC-δ PH construct have been reported. Treatment of NIH-3T3 cells with 10μM wortmannin failed to inhibit the relocalisation of the GFP-PLC-δ PH construct in response to calcium chelation, after translocation by ionomycin; in the same experiment wortmannin did, however, partially inhibit PIP_2 resynthesis as measured by mass assay (Varnai and Balla, 1998). Varnai and Balla explain this discrepancy by hypothesising that certain PIP_2 pools that bind PH domains may be synthesised by wortmannin-insensitive PI 4-kinases.

Another possible explanation for the results I have seen is that all of the IP_3 produced by the agonist-induced hydrolysis of PIP_2 had been broken down by inositol phosphatases, and that not all of the PIP_2 in the membrane was hydrolysed by the agonist, or that some was replenished from the pool of PIP that remained in the membrane (wortmannin inhibits the enzyme that synthesises PIP not PIP_2, so there would be a residual pool of PIP present in the membrane ready for phosphorylation by PI 5 kinase to form PIP_2). If the localisation of the GFP-PLC-δ PH construct is dependent on the ratio of IP_3 to PIP_2, it would return to the membrane in this case. If the amount of PIP_2 synthesised at the membrane is below the threshold needed for opening of M-channels, this would explain why the channels remain closed even though the fluorescent construct relocates to the membrane. Of course, there is also the possibility that, in the absence of sufficient PIP_2 or IP_3 to bind to, the GFP-PLC-δ PH construct could, in theory, bind to PIP_3 in the membrane. The construct has a relatively low affinity for this phospholipid, as the presence of a phosphate group at the "3" position interferes with the binding (Lemmon and Ferguson, 2000), but in the absence of a more favourable target, it is possible that PIP_3 binding could account for the return of the construct to the plasma membrane.

Also, when slowing of the relocation of the construct did take place, it was most usually the second, slow phase of relocation that was slowed or inhibited; the first, fast phase of relocation could represent the resynthesis of PIP_2 from the residual pool of PIP, and the slower phase could represent the more time-consuming resynthesis of PIP_2 from stages further back in the phosphoinositide cycle. Any variation in the magnitude and duration of the initial fast phase of GFP-PLC-δ PH relocation could be due to variation in the amount

of PIP still available for phosphorylation by PI 5-kinase to form PIP_2. One would imagine that if this were the case, subsequent agonist-induced translocations of the construct whilst in wortmannin would have gradually slower relocation timecourses and gradually smaller amplitudes as the residual pool of PIP were used up (as less PIP_2 were available for hydrolysis and IP_3 production with each subsequent response). This experiment is an important one for the future if we are to ascertain why wortmannin does not always have the anticipated response on relocation of the fluorescent construct.

These experiments with wortmannin add to previous findings that the activity of PI 4-kinase is necessary for the recovery of the M-current after agonist-induced inhibition (Zhang et al., 2002; Suh and Hille, 2002). I have attempted to explain the unexpected result with the relocation of the GFP-PLC-δ PH construct to the membrane, but further experiments would help to clarify my theory.

5.3.2 Experiments with Neuronal Calcium Sensor 1 (NCS-1)

Although used in this thesis by virtue of its ability to interact with and enhance the activity of PI 4-kinase, NCS-1 does have several other possible functions within the cell. Hence, there are a few different avenues to explore when investigating why overexpression of this protein should reduce the sensitivity of the M-current to inhibition by bradykinin.

One of the properties of NCS-1, mentioned earlier, that could be of interest to us with regard to its effect on the sensitivity of I_M to inhibition by bradykinin, is the fact that it has been shown to substitute for calmodulin

(Schaad et al., 1996). In Gamper and Shapiro's publication on the possible role of calmodulin in bradykinin-induced I_M inhibition however, overexpression of wild-type calmodulin greatly reduced the M-current density in SCGs – NCS-1 does not do this (Figure 4.21); also it was the dominant-negative mutant of calmodulin which was reported to reduce bradykinin inhibition of the M-current, with the wild-type protein proposed to be in some way necessary for the inhibition (Gamper and Shapiro., 2002). If NCS-1 were directly substituting for calmodulin, one would expect overexpression of the wild-type protein to *increase* the bradykinin-induced inhibition. I have considered the possibility that NCS-1 could be competing with calmodulin for its target, due to its far greater abundance in the transfected cells, but not activating this target (NCS-1 has been reported only to activate some of calmodulin's targets; Schaad et al., 1996); this would render NCS-1 a kind of "dominant-negative" of calmodulin, and in this case, overexpression of the wild-type could possibly reduce bradykinin-induced M-current inhibition.

However, the similar alterations to the sensitivity of the translocation of GFP-PLC-δ PH to bradykinin and to the sensitivity of the M-current to inhibition by this agonist in NCS-1-overexpressing cells, suggests that NCS-1 may indeed be having its effect somewhere within the phosphoinositide cycle, and most likely at PI 4-kinase. As discussed previously in this chapter, overexpression of PI 5-kinase almost abolished oxotremorine M- and bradykinin-induced inhibition of the M-current and also greatly reduced the amount of translocation of the GFP-PLC-δ PH construct by both agonists, so a reduction in both M-current inhibition AND GFP-PLC-δ PH translocation could be indicative of increased PIP_2 synthesis. If my theory that NCS-1 is affecting the bradykinin-induced

inhibition of the M-current via its interaction with PI 4-kinase is correct, overexpression of NCS-1 should reduce translocation of the GFP-PLC-δ PH construct by bradykinin but not by oxotremorine M, to reflect the selectivity between the agonists shown in I_M inhibition. As seen in section 4.2.2.6, this is the case, with GFP-PLC-δ PH translocation by bradykinin in NCS-1-overexpressing cells significantly less than in control cells, and with no difference between the oxotremorine M-induced responses in transfected or control cells.

It is likely, considering the effect of NCS-1 on the GFP-PLC δ PH translocation (as well as the effect of overexpression of PI 5-kinase on the M-current inhibition/ GFP-PLC-δ PH construct translocation – see Chapter Four), that NCS-1 could be enhancing the activity of PI 4-kinase in my system, and so increasing the amount of plasma membrane PIP_2. This will reduce the sensitivity of the channel to inhibition via PLC-induced PIP_2 depletion (see previous chapter and Bender et al., 2002). Increased activity of PI 4-kinase would lead to higher levels of the polyphosphoinositide intermediary PIP, but increased production of PIP_2 would also depend on an enhanced activation of PI 5-kinase. This enhanced activity of PI 5-kinase would appear to occur as a result of PI 4-kinase enhancement, as levels of PIP_2 as well as levels of PIP are reported to be increased in PC12 cells overexpressing NCS-1 (Koizumi et al., 2002; Rajebhosale et al., 2002).

The fact that the PI 4-kinase inhibitor wortmannin is able to antagonise the effect of overexpressing NCS-1 on the bradykinin-induced I_M inhibition, suggests that NCS-1 was indeed interacting with PI 4-kinase to enhance its activity and raise PIP_2 levels. The effect on ATP-induced secretion in PC-12

cells produced by enhancing PI 4-kinase activity via overexpression of NCS-1 can be antagonised with an inhibitor of PI 4-kinase (phenylarsine oxide, PAO, was used here; Rajebhosale et al., 2002). Combined with the data obtained with PI 5-kinase in the previous chapter, this adds more evidence in favour of PIP_2 depletion being a process which leads to M-channel closure.

Is it the Ca^{2+}-mobilising properties of bradykinin which cause NCS-1 to have an effect on bradykinin-induced M-current inhibition/ GFP-PLC-δ PH translocation and not oxotremorine M-induced responses ?

It has already been established, through the experiments in section 4.2.2.5, that NCS-1 is not acting as a calcium buffer, therefore it is not reducing the bradykinin-induced M-current inhibition and GFP-PLC-δ PH translocation by buffering the bradykinin-induced Ca^{2+} rise. The differentiator however, between the effect on the bradykinin-induced inhibition/ translocation and the lack of effect on the oxotremorine M-induced responses appears to be the calcium rise, or lack of it, elicited by these agonists.

The different Ca^{2+}-mobilising capabilities of bradykinin and oxotremorine M have been cited as the reason for the different effects of overexpressing calmodulin or its dominant-negative mutant on M-current inhibition by these two agonists (Gamper and Shapiro, 2002). Neither overexpression of wild-type calmodulin, nor its dominant-negative mutant form, had any effect on the muscarinic I_M inhibition in Gamper and Shapiro's publication; this is believed to be because oxotremorine M did not produce a large enough calcium rise to activate calmodulin, whereas bradykinin did. NCS-1, like calmodulin, is a

calcium binding protein (albeit with a higher affinity for calcium than that of calmodulin), so the need for a calcium rise in order to activate NCS-1 could be the factor which differentiates between the bradykinin- and oxotremorine M-induced I_M inhibitions. The bradykinin-induced Ca^{2+} rise could activate NCS-1, which is already bound to PI 4-kinase, stimulating it to produce more PIP, and hence more PIP_2, which would counteract the PLC-mediated hydrolysis of PIP_2, resulting in less net depletion of PIP_2, and therefore less M-channel closure.

The above could theoretically be tested in two ways; one would be to try to buffer the Ca^{2+} rise produced by bradykinin, and see whether this buffering would prevent activation of NCS-1, and therefore prevent its effect. Theoretically, this could be attempted by incubating the cells with a high concentration of the calcium buffer BAPTA AM, to see whether this removes the difference between the two agonists. Conversely, a calcium rise could be elicited in cells before stimulation with oxotremorine M, to see if this results in activation of NCS-1 and a consequent reduction in the sensitivity of the M-current inhibition/ GFP-PLC-δ PH translocation due to increased PI 4-kinase activity. Practically though, there would be problems associated with manipulating intracellular calcium in this way; buffering the bradykinin-induced Ca^{2+} rise with high levels of BAPTA AM greatly reduces the sensitivity of M-current inhibition to bradykinin (Cruzblanca et al., 1998), and raising intracellular Ca^{2+} levels can cause activation of PLC and hydrolysis of PIP_2/ M-current inhibition in the absence of agonist-stimulation. Thus, it would be problematic to try to impart the calcium-mobilising properties of bradykinin onto the oxotremorine M response, or to try to remove this property from the bradykinin

response in an attempt to make conditions more similar to those during a muscarinic response. The Ca^{2+}-mobilising properties, or lack of them, are fundamentally integral to the nature of both of these agonist responses; altering them would not really be a practical way of testing whether the difference in Ca^{2+} mobilisation does account for the effect of overexpressing NCS-1 on the bradykinin-induced response and not the muscarinic.

5.4 Possible explanations for the differences seen between bradykinin-induced and oxotremorine M-induced M-current inhibition/ GFP-PLC-δ PH translocation.

The M-current inhibitions induced by bradykinin and oxotremorine M differ in certain ways; the bradykinin-induced inhibition requires that the rise in Ca^{2+} elicited by this agonist remains intact, whereas the oxotremorine M-induced inhibition produces only a very small rise, and the inhibition is not blocked by high concentrations of BAPTA so is therefore mostly Ca^{2+}-independent (see Cruzblanca et al., 1998). The bradykinin-induced I_M inhibition and the GFP-PLC-δ PH translocation induced by this agonist take longer to recover than the responses induced by oxotremorine M. Also, the sensitivities of the I_M inhibitions by both agonists to the PLC inhibitor U73122 differ markedly, and the bradykinin-induced M-current inhibition can be blocked with antisense to PLC-β_4, while, in the same publication, it is reported that the oxotremorine M-induced inhibition is not blocked by the same concentration of this antisense (Haley et al., 2000).

M-current inhibition by both agonists however, is accompanied by translocation of the GFP-PLC-δ PH construct from the membrane to the cytosol, and the recovery of the M-current from inhibition is accompanied by the relocation of the construct to the membrane; this translocation and relocation of the GFP-PLC-δ PH construct occurs with a very similar time course to that of the M-current inhibition and recovery. Both responses (to both agonists) are greatly reduced by overexpression of PI 5-kinase, which suggests that both M-current inhibition and GFP-PLC-δ PH translocation are due to the depletion of PIP_2. It has been shown that higher concentrations of the PLC inhibitor U73122 do indeed block oxotremorine M-induced M-current inhibition (Suh and Hille, 2002) and GFP-PLC-δ PH translocation, and also that the PI 4-kinase inhibitor wortmannin prevents recovery from oxotremorine M-induced inhibition of the M-current (Suh and Hille, 2002; Zhang et al., 2002). Considering all of the above, the question arises "if the inhibition of the M-current by both oxotremorine M and bradykinin is via the same mechanism i.e. PIP_2 depletion, why do they have different sensitivities to calcium chelation and PLC inhibition, and why can the oxotremorine M-induced inhibition not be blocked with antisense to PLC-β isoforms at the same concentration which blocks the bradykinin-induced inhibition ?".

First of all, if both responses are driven by PLC activation, why is bradykinin so much more sensitive to inhibition of this enzyme, and chelation of calcium ?. One theory is that of Gamper and Shapiro (2002), who suggest that the calcium rise, caused by the IP_3 produced from the $G_{q/11}$-coupled initial PLC activation, causes activation of calmodulin, which somehow closes M-channels. Blockade of PLC would prevent the initial IP_3 release and subsequent Ca^{2+} rise,

and therefore the whole response would be blocked. If this were the case though, why is the translocation of the GFP-PLC-δ PH construct in response to bradykinin so complete, and why is it also prolonged, reflecting the time course of the recovery of the M-current from inhibition by this peptide ?. If only the initial "trigger" stage of the bradykinin-induced I_M inhibition involved PLC activity, one would imagine that the translocation of the GFP-PLC-δ PH construct would be incomplete, and more importantly, much briefer than the duration of M-current inhibition. The construct should return to the membrane once PLC has "handed over" the job of inhibiting the M-current to calmodulin.

The theory I favour for the mechanism of M-current inhibition by bradykinin is also a "two-stage" model, but instead of (or possibly as well as) the initial PLC/IP_3-generated Ca^{2+} rise acting as an activator for some other entity like calmodulin, I believe that it could lead to the activation of another, calcium-sensitive isoform of PLC i.e. PLC-δ. As discussed in the Introduction (section *1.3.2*), PLC-δ can be selectively activated by Ca^{2+} alone (Allen et al., 1997), and it has been suggested that sequential activation of PLC-δ isoforms by increased intracellular calcium levels could follow stimulation of PLC-β or –γ isoenzymes, leading to prolonged hydrolysis of inositol lipids (Allen et al., 1997). Indeed it has been shown by Kim et al. (1999) that PLC-δ1 overexpressed in PC12 cells was activated by capacitative calcium entry in response to the PLC-β/ IP_3 Ca^{2+} rise generated by bradykinin. More evidence to suggest that this sequential activation of PLCs occurs is found in the observation by Young et al. who, during dual imaging experiments to measure intracellular Ca^{2+} and translocation of the GFP-PLC-δ PH construct, noticed a secondary, plateau phase of GFP-PLC-δ PH translocation which was particularly sensitive to regulation by

intracellular Ca^{2+} (Young et al., 2003). Their interpretation of the translocation of the GFP-PLC-δ PH construct is that it is measuring IP_3 production, rather than purely PIP_2 degradation, but either way, it shows a secondary, Ca^{2+}-sensitive activation of PLC; Young et al. suggest that this may indicate the recruitment of a Ca^{2+}-sensitive PLC which is not present during initial periods of agonist stimulation (Young et al., 2003).

This theory would explain the longer time course of the bradykinin-induced GFP-PLC-δ PH translocation, which reflects the longer time course of the M-current inhibition by this agonist; prolonged hydrolysis of phospholipids by Ca^{2+}-activated PLC-δ could result in the characteristically slow GFP-PLC-δ PH relocation. It could also explain the ability of antisense to PLC-β_4 to block bradykinin-induced I_M inhibition, as without this initial "trigger" stage, the subsequent activation of PLC-δ would also be blocked. The same explanation can be given for the sensitivity of the bradykinin-induced inhibition to PLC block by U73122; blockade of the relatively small amounts of "trigger stage" PLC-β activity may not require large amounts of the aminosteroid, but would prevent the entire response from taking place. The data in Cruzblanca et al (1998) states that around 25% of the bradykinin-induced M-current inhibition is still intact in the presence of 20mM BAPTA; this could be the proportion of the M-current which is inhibited by PLC-β-mediated PIP_2 hydrolysis.

As oxotremorine M does not have the Ca^{2+}-mobilising ability of bradykinin (see Delmas et al., 2002), this sequential activation of PLC-β and PLC-δ cannot be the mechanism by which this agonist is causing M-current inhibition. From recent publications (see Introduction for references), and from the experiments described in this thesis, there is a strong case for PLC-

mediated hydrolysis of PIP_2 as the mediator of oxotremorine M-induced M-channel closure, but the antisense work of Haley et al. (2002) suggests that this PLC is not of the –β isoform. However, it could be possible that M_1-mACh receptors could couple a lot more strongly to PLC-β isoforms than bradykinin receptors, either due to a greater receptor number, or a more robust coupling to PLC-activating G-proteins. If this were the case, it is possible that the amount of PLC-β antisense used by Haley et al to block the bradykinin-induced M-current inhibition was not enough to counteract this more robust PLC- activation by oxotremorine M. The fact that higher concentrations of the PLC inhibitor U73122 are needed to block the oxotremorine M-induced I_M inhibition suggests that this may be the case.

How to test this theory ?

This theory could be tested by transfecting the cells with a PLC-δ-specific antisense, to see whether this significantly reduced the bradykinin-induced M-current inhibition and not the muscarinic, and also by using the bradykinin-receptor antagonist HOE 140, to see whether the prolonged response to the agonist is due to prolonged receptor occupancy by the peptide, or whether it is due to some other mechanism (i.e. Ca^{2+} rise followed by PLC-δ activation) which is sequential to the initial activation of a PLC-β isoform.

5.5 Closing Remarks

In all, I believe this thesis contributes further to the accumulating evidence that PIP_2 depletion is a mediator for M-current inhibition by both muscarinic agonists and bradykinin. It indicates that hydrolysis of PIP_2 accompanies this inhibition, and that the patterns of onset and offset of the two responses (M-current inhibition and GFP-PLC-δ PH translocation) are remarkably similar. It also demonstrates that if alteration of the activity of a key player in the phosphoinositide cycle (i.e. PLC, PI 4-kinase and PI 5-kinase) can alter the sensitivity of M-current inhibition by either agonist, then the GFP-PLC-δ PH translocation by that agonist will also be altered in a corresponding way.

References

Adams, P.R, Brown, D.A and Constanti, A. (1982). Pharmacological inhibition of the M-current. *J Physiol* **332**: 223-262.

Agard, D.A, Hiraoka, Y, Shaw, P and Sedat, J.W (1989). Fluorescence microscopy in three dimensions. *Methods Cell Biol.* **30**, 353-377.

Beech, D.J, Bernheim, L, Mathie, A and Hille, B (1991). Intracellular buffers disrupt muscarinic suppression of Ca^{2+} current and M-current in rat sympathetic neurons. *Proc Natl Acad Sci USA* **88**, 652-656.

Bender, K, Wellner-Kienitz, M-C and Pott, L (2002). Transfection of a phosphatidyl-4-phosphate 5-kinase gene into rat atria myocytes removes inhibition of GIRK current by endothelin and α-adrenergic agonists. *FEBS Letts* **529**, 356-360.

Bernheim, L, Mathie A and Hille B.,Characterization of muscarinic receptor subtypes inhibiting Ca2+ current and M current in rat sympathetic neurons.(1992) *Proc Natl Acad Sci U S A.* **15;89(20):**9544-8.

Biervert, C, Schroeder, B.C, Kubisch, C, Berkovic, S.F, Propping, P, Jentsch, T and Steinlein, O.K (1998). A potassium channel mutation in neonatal human epilepsy. *Science* **279**: 403-406.

Bofill-Cardona, E, Vartian, N, Nanoff, M, Freissmuth, M and Boehm, S (2000). Two different signalling mechanisms involved in the excitation of rat sympathetic neurons by uridine nucleotides. *Mol. Pharmacol* **57**, 1165-1172.

Brown, DA and Adams, PR (1980). Muscarinic suppression of a novel voltage-sensitive K^+ current in a vertebrate neurone. *Nature* **283**, 673-676.

Brown, DA and Higashida, H (1988). Voltage and calcium-activated potassium currents in mouse neuroblastoma x rat glioma hybrid cells. *J Physiol* **397**: 149-165.

Brown, D.A and Higashida, H (1988). Inositol 1,4,5-trisphosphate and diacylglycerol mimic bradykinin effects on mouse neuroblastoma x rat glioma hybrid cells. *J. Physiol. (Lond.)* **397**, 185-207.

Brown, D.A, Marrion, N.V and Smart, T.G (1989). On the transduction mechanism for muscarine-induced inhibition of M-current in cultured rat sympathetic neurones. *J. Physiol. (Lond.)* **413**, 469-488.

Casteleman, K.R (1996). Digital image processing. Prentice Hall.

Caulfield, M.P, Jones, S, Vallis, Y, Buckley, N.J, Kim, G.D, Milligan, G and Brown, D.A (1994). Muscarinic M-current inhibition via Gαq/11 and α-adrenoceptor inhibition of Ca^{2+} current via Gαo in rat sympathetic neurons. *J. Physiol. (Lond.)* **477**, 415-422.

Charlier, C, Singh, N.A, Ryan, S.G, Lewis, T.B, Reus, B.E, Leach, R.J and Leppert, M (1998). A pore mutation in a novel KQT-like potassium channel gene in an idiopathic epilepsy family. *Nature Genet.* **18**, 53-55.

Chen,X.L.,Zhong,Z.G.,Yokoyama,S.,Bark,C.,Meister,B.,Berggren,P.O.,Roder, J.,Higashida,H.,Jeromin,A. (2001) Overexpression of rat neuronal calcium sensor-1 in rodent NG108-15 cells enhances synapse formation and transmission*J Physiol (Lond)* **532:**649-659

Chen, H, Kurenny, D.E and Smith, P.A (1993). Heparin prevents M-current over-recovery but not M-current suppression in bullfrog sympathetic ganglion neurones. *Brain Res.* **625**, 323-327.

Coburn RF, Jones DH, Morgan CP, Baron CB, Cockroft S.(2002) Spermine increases phosphatidylinositol 4,5-bisphosphate content in permeabilized and nonpermeabilized HL60 cells. *Biochim Biophys Acta.* **1584(1):**20-30.

Constanti, A and Brown, DA (1981). M-currents in voltage-clamped mammalian sympathetic neurones. *Neurosci.Lett.***24**, 289-294.

Constanti, A and Sim, J.A (1987). Muscarinic receptors mediating suppression of the M-current in guinea-pig olfactory cortex neuronsmay be of the M_2-subtype. *Br. J. Pharmacol* **90**, 3-5.

Cox, J.A., Drussel, I., Comte, M., Nef, S., Nef,O.,Lenz,S.E.,and Gundelfinger,E.D. (1994) Cation binding and conformational changes in VILIP and NCS-1, two neuron-specific calcium-binding proteins *J.Biol.Chem* **269,**32807-32814

Cruzblanca, H, Koh, D.S and Hille B (1998). Bradykinin inhibits M-current via phospholipase C and Ca^{2+} release from IP_3-sensitive Ca^{2+} stores in rat sympathetic neurons. *Proc. Natl. Acad. Sci. USA* **95**, 7151-7156.

Czech, M.P (2000). PIP_2 and PIP_3: complex roles at the cell surface. *Cell* **100**, 603-66.

Delmas, P, Wanaverbecq, N, Abogadie, F.C, Mistry, M and Brown, D.A (2002). Signalling microdomains define the specificity of receptor-mediated $InsP_3$ pathways in neurons. Neuron **34**, 209-220.

Delmas, P, Brown, D.A, Dayrell, M, Abogadie, F.C, Caulfield, M.P and Buckley, N.J (1998). On the role of endogenous G-protein beta gamma subunits in N-type Ca^{2+} current inhibition by neurotransmitters in rat sympathetic neurones. *J. Physiol* **506**, 319-29.

Del Rio, E, Bevilacqua, J.A, Marsh, S.J, Halley, P and Caufield, M.P (1999). Muscarinic M_1 receptors activate phosphoinositide turnover and Ca^{2+} mobilisation in rat sympathetic neurones, but this signalling pathway does not mediate M-current inhibition. *J. Physiol* **520**, 101-111.

Dutar, P and Nicoll, R.A (1988). Classification of muscarinic responses in hippocampus in terms of receptor subtypes and second-messenger systems: Electrophysiological studies *in vitro*. *J. Neurosci* **8**, 4214-4224.

Ferguson, K.M, Lemmon, M.A, Schlessinger, J and Sigler, P.B (1995). Structure of a high affinity complex between inositol-1,4,5-trisphosphate and a phospholipase C pleckstrin homology domain. *Cell* **83**, 1037.

Ford, C.P, Stemkowski, P.L, Light, P.E and Smith, P.A (2003). Experiments to test the role of phosphatidylinositol 4,5-bisphosphate in neurotransmitter-induced M-channel closure in bullfrog sympathetic neurons. *J. Neurosci* **23(12)**, 4931-41.

Fukuda, H, Higashida, H, Kubo, T, Maeda, A, Akiba, I et al. (1988). Selective coupling with K^+ currents of muscarinic acetylcholine receptor subtypes in NG108-15 cells. *Nature* **335**, 335-358.

Gafni, J, Munsch, J.A, Lam, T.H, Catlin, M.C, Costa, L.G, Molinsi, T.F and Pessah, I.N (1997). Xestospongins: Potent membrane permeable blockers of the inositol 1,4,5-trisphosphate receptor. *Neuron* **19**, 723-733.

Gamper, N and Shapiro, M.S (2003). Calmodulin involvement in Ca^{2+}-mediated modulation of M-type K^+ channels. *J Gen Physiol.***122(1):**17-31.

Guo, W, Malins, S.A, Johns, D.C, Jeromin, A and Nerbonne, J.M.(2002) Modulation of Kv4-encoded K(+) currents in the mammalian myocardium by neuronal calcium sensor-1. *J Biol Chem* **277(29):**26436-43.

Hadley, J.K, Noda, M, Selyanko, A.A, Wood, I.C, Abogadie, F.C and Brown, D.A (2000). Differential tetraethylammonium sensitivity of KCNQ1-4 potassium channels. *Brit. J. Pharmacol.* **129**, 413-415.

Hadley, JK, Passmore, G.M, Tatulian, L, Al-Qatari, M, Wickenden, A.D and Brown, D.A (2003). Stoichiometry of expressed KCNQ2/KCNQ3 potassium channels and subunit composition of native ganglionic M-channels deduced from block by tetraethylammonium. *J. Neurosci* **23(12)**, 5012-5019.

Haley, J.E, Abogadie, F.C, Delmas, P, Dayrell, M, Vallis, Y, Milligan, G, Caulfield, M.P, Brown, D.A and Buckley, N.J (1998). *J. Neurosci* **18**, 4521-4531.

Haley, J.E, Abogadie, F.C, Delmas, P, Dayrell, M, Vallis, Y, Buckley, N.J and, Brown, D.A (2000). Bradykinin, but not muscarinic, inhibition of M-current in rat sympathetic ganglion neurons involves phospholipase C-β_4. *J. Neurosci.* **20**, RC105.

Haley, J.E, Demas, P, Offermanns, S, Abogadie, F.C, Simon, M.I, Buckley, N.J and Brown, D.A (2000). Muscarinic inhibition of calcium current and M-current in G alpha q-deficient mice. *J. Neurosci* **20**, 3973-3979.

Halliwell, J.V and Adams, P.R (1982). Votage-clamp analysis of muscarinic excitation in hippocampal neurons. *Brain Res.* **250**, 71-92.

Harlan, J.E, Hajduk, P.J, Yoon, H.S and Fesik, S.W (1994). Pleckstrin homology domains bind to phosphatidylinositol-4,5-bisphosphate. *Nature* **371**, 168-170.

Hendricks,K.B.,Wang,B.Q.,Schneiders,E.A,Thorner,J. (1999) Yeast homologue of neuronal frequenin is a regulator of phosphatidylinositol-4-OH kinase.*Nat Cell Biol* **1**:234-241

Higashida, H and Brown, D.A (1986). Two polyphosphatidylinositide metabolites control two K^+ currents in a neuronal cell. *Nature* **323**, 333-335.

Hirose, K, Kadowaki, S, Tanabe, M, Takeshima, H and Iino, M (1999). Spatiotemporal dynamics of inositol 1,4,5 trisphosphate that underlies complex Ca^{2+} mobilisation patterns. *Science* **284**, 1527-1530.

Hoshi, N, Zhang, J.S, Omaki, M, Takeuchi, T, Yokoyama, S, Wanaverbecq, N, Langeberg, L.K, Yoneda, Y, Scott, J.P, Brown, D.A and Higashida, H

(2003). AKAP 150 signalling complex promotes suppression of the M-current by muscarinic agonists. *Nat. Neurosci* **6**, 564-71.

Huang, C.L, Feng, S and Hilgemann, D.W (1998). Direct activation of inward rectifier potassium channels by PIP_2 and its stabilization by Gβγ. *Nature* **391**, 803-806.

Hwang, S.C, Jhon, D.Y, Bae, Y.S, Kim, J.H, Rhee, S.G (1996). Activation of phospholipase C γ by the concerted action of tau proteins and arachidonic acid. *J. Biol. Chem* **271**, 18342-49.

Jin, W, Lo, T.M, Lo, H.H and Thayer, S.A (1994). U73122 inhibits phospholipase C-dependent calcium mobilisation in neuronal cells. *Brain Res* **642**, 237-243.

Jones, G.A and Carpenter, G (1993). The regulation of phospholipase C-gamma 1 by phosphatidic acid. Assessment of kinetic parameters. *J. Biol. Chem* **268**, 20845-50.

Jones, S, Brown, D.A, Milligan, G, Willer, E et al. (1995). Bradykinin excites rat sympathetic neurons by inhibition of M-current through a mechanism involving B2 receptors and Gαq/11. *Neuron* **14**, 399-405.

Kanterman, R.Y, Ma, A.L, Briley, E.M, Axelrod, J and Felder, C.C (1990). Muscarinic receptors mediate release of arachidonic acid from spinal cord and hippocampal neurons in primary culture. *Neurosci Lett.* **118**, 235-237.

Kim, YH, Park, TJ, Lee, YH, Baek, KJ, Suh, PG, Ryu, SH and Kim KT (1999). Phospholipase C delta 1 is activated by capacitative calcium entry that follows phospholipase C beta activation upon bradykinin stimulation. *J. Biol. Chem* **274** 26127-34.

Kirkwood, A, Simmons, M.A, Mather, R.J and Lisman, J.E (1991). Muscarinic suppression of the M-current is mediated by a rise in internal Ca^{2+} concentration. *Neuron* **6**, 1009-1014.

Koizumi,S.,Rosa, P.,Willars, G.B.,Challis, R.A.J.,Taverna,E.,Francolini,M.,Bootman,M.,Lipp,P.,Inoue,K.,Roder,J., and Jeromin,A. (2002) Mechanisms underlying the neuronal calcium sensor-1-evoked enhancement of exocytosis in PC12 cells. *J.Biol.Chem* **277(33):**30315-24

Kobrinsky, E, Mirshahi, T, Zhang, H, Jin, T and Logothetis, D.E (2000). Receptor-mediated hydrolysis of plasma membrane messenger PIP_2 leads to K^+-current desensitization. *Nature Cell Biology* **2**, 507-514.

Lei, Q, Talley, EM, Bayliss, DA. Receptor-mediated inhibition of G protein-coupled inwardly rectifying potassium channels involves G(alpha)q family subunits, phospholipase C, and a readily diffusible messenger (2001). J Biol Chem **1276(20):**16720-30.

Lemmon, M.A and Ferguson, K.M (2000). Signal-dependent membrane targeting by pleckstrin homology (PH) domains. *Biochem J* **350**, 1-18.

Lemmon, M.A and Ferguson, K.M (2000). Pleckstrin homology domains: phosphoinositide-regulated membrane tethers. *Biology of phosphoinositides, edited by S. Cockroft – Oxford University Press* 131-158.

Loijens, J.C., Boronenkov, I.V., Parker,G.J., and Anderson, R.A. (1996) The phosphatidylinositol 4-phosphate 5-kinase family. *Adv.Enzyme Regul.,* **36**,115.

Lopes, C.M.B, Zhang, H, Rohacs, T, Yang, J and Logothetis, D.E (2002). Alterations in conserved interactions between PIP_2 and Kir channels underlie channelopathies. *Neuron* **34**, 933-944.

Lopez, I, Mak, E, Ding, J, Hamm, H and Lomasney, J.W (2001). A novel bifunctional phospholipase c that is regulated by Galpha 12 and stimulates the Ras/mitogen-activated protein kinase pathway. *J Biol Chem* **276(4):**2758-65.

MacKinnon, R and Yellen, G (1990). Mutations affecting TEA blockade and ion permeation in voltage-activated K+ channels. *Science* **250**, 276-9.

Marrion, NV, Smart, TG, Marsh, SJ and Brown D.A. (1989) Muscarinic suppression of the M-current in the rat sympathetic ganglion is mediated by receptors of the M1-subtype. *Br J Pharmacol* **98(2):**557-73

Marrion, N.V (1997). Control of M-current. *Ann Rev Physiol.* **59**, 483-504.

Marrion, N.V (1997). Does r-EAG contribute to the M-current ?. *Trends Neurosci.* **20**, 243.

Marsh, S.J, Trouslard, J, Leaney, J.L and Brown, D.A (1995). Synergistic regulation of a neuronal chloride current by intracellular calcium and muscarinic receptor activation: a role for protein kinase C. *Neuron* **15**, 729-737.

Mathie, A and Watkins, C.S (1997). Is EAG the answer to the M-current ?. *Trends Neurosci.* **20**, 14.

McFerran,B.W.,Graham,M.E., and Burgoyne, R.D. (1998) Neuronal Ca2+ sensor 1, the mammalian homologue of frequenin, is expressed in chromaffin and PC12 cells and regulates neurosecretion from dense-core granules.*J.Biol.Chem.* **273**, 22768-22772

McFerran, B.W., Weiss, J., and Burgoyne, R.D. (1999) Neuronal Ca(2+) sensor 1. Characterization of the myristoylated protein, its cellular effects in permeabilized adrenal chromaffin cells, Ca(2+)-independent membrane

association, and interaction with binding proteins, suggesting a role in rapid Ca(2+) signal transduction. *J.Biol.Chem.* **274**, 30258-30265

McLaughlin, S, Wang, J, Gambhir, A and Murray, D (2002). PIP_2 and Proteins: Interactions, Organisation, and information flow. *Annu. Rev. Biophys. Biomol. Struct* **31**, 151-175.

Meves, H, Schwartz, J.R and Wulfsen, I (1999). Separation of M-like current and ERG current in NG108-15 cells. *Brit. J. Pharmacol.* **127**, 1213-1223.

Moore, S.D, Madamba, S.G, Joels, M and Siggins, G.R (1988). Somatostatin augments the M-current in hippocampal neurons. *Science* **239**, 278-280.

Mora, S, Durham, PL, Smith, JR, Russo, AF, Jeromin, A and Pessin, JE (2002). NCS-1 inhibits insulin-stimulated GLUT4 translocation in 3T3L1 adipocytes through a phosphatidylinositol 4-kinase-dependent pathway. *J Biol Chem* **277(30):**27494-500

Nahorski, S.R, Young, K.W, Challis, R.A.J and Nash, M.S (2003). Visuaising phosphoinositide signalling in single neurons gets a green light. *TINS* **26**, 444.

Nakanishi, S, Catt, K.J and Balla, T (1995). A wortmannin-sensitive phosphatidylinositol 4-kinase that regulates hormone-sensitive pools of inositolphospholipids. *Proc. Natl. Acad. Sci. USA* **92**, 5317.

Nash, M.S, Young, K.W, Willars, G.B, Challis, R.A and Nahorski, S.R (2001). Single-cell imaging of graded $Ins(1,4,5)P_3$ production following G-protein-coupled receptor activation. *Biochem. J.* **356**, 137-142.

Neher, E and Augustine, G.J (1992). Calcium gradients and buffers in bovine chromaffin cells. *J. Physiol. Lond.* **450**, 273-301.

Noh, D.Y, Shin, S.H and Rhee, S.G (1995). Phosphoinositide-specific phospholipase C and mitogenic signaling. *Biochim. Biophys. Acta* **1242**, 99-113.

Oketani, N, Kakei, M, Ichinari, K, Okamura, M, Miyamura, A, Nakazaki, M, Ito, S and Tei, C (2002). Regulation of K(ATP) channels by P(2Y) purinoceptors coupled to PIP_2 metabolism in guinea pig ventricular cells. *Am J Physiol Heart Circ Physiol.* **282**, H757-65.

Olafsson,P.,Wang,T., and Lu,B. (1995) Molecular cloning and functional characterization of the Xenopus Ca(2+)-binding protein frequenin.*Proc. Natl. Acad. Sci. U.S.A.* **92**, 8001-8005

Olafsson, P., Soares, H.D., Herzog, K.H., Wang, T., Morgan, J.I., and Lu, B. (1997) The Ca2+ binding protein, frequenin is a nervous system-specific protein in mouse preferentially localized in neurites. *Mol Brain Res.* **44**, 73-82

Pan,C-Y.,Jeromin, A.,Lundstrom,K.,Yoo,S.H.,Roder,J., and Fox,A.P. (2002) Alterations in exocytosis induced by neuronal Ca2+ sensor-1 in bovine chromaffin cells.*J.Neurosci.* **22(7):**2427-2433

Pfaffinger, P.J. (1988). Muscarine and t-LHRH suppress M-current by activating an IAP-sensitive G-protein. *J. Neurosci.* **8**, 3345-53.

Pfaffinger, P.J, Leibowitz, M.D, Subers, E.M, Nathanson, N.M, Almers, W and Hille, B (1988). Agonists that suppress M-current elicit phosphoinositide turnover and Ca^{2+} transients, but these events do not explain M-current suppression. *Neuron* **1**, 477-484.

Pike, L. (1992) Phosphatidylinositol 4-kinases and the role of polyphosphoinositides in cellular regulation. *Endocrine Rev.*, **13**,692.

Pongs,O., Lindemeier,J., Zhu,X.R.,Theil,T.,Endelkamp,D.,Krah-Jentgens,I.,Lambrecht,H.G.,Koch,K.W.,Schwemer,J.,Rivosecchi,R.,Mallart,A.,

Galceran,J.,Canal,I.,Barbras,J.A.,and Ferrus,A. (1993) Frequenin--a novel calcium-binding protein that modulates synaptic efficacy in the Drosophila nervous system. *Neuron* **11**, 15-28

Rae, J, Cooper, K, Gates, P and Watsky, M (1991). Low access resistance perforated patch recordings using amphotericin B. *J. Neurosci. Methods* **37**, 15-26.

Rajebhosale, M, Greenwood, S, Vidugiriene, J, Jeromin, A and Hiliker, S (2003). Phosphatidylinositol 4-OH kinase is a downstream target of neuronal calcium sensor-1 in enhancing exocytosis in neuroendocrine cells. *J. Biol. Chem* **278**, 6075-6084.

Raucher, D, Stauffer, T, Chen, W, Shen, K, Guo S et al., (2000). Phosphatidylinositol 4,5-bisphosphate functions as a second messenger that regulates cytoskeleton-plasma membrane adhesion. *Cell* **100**, 221-28.

Rhee, S.G (2001) Regulation of phosphoinositide-specific phospholipase C. *Annu. Rev. Biochem* **70**, 281-312.

Rivosecchi, R., Pongs, O.,Theil,T., and Mallart,A. (1994) Implication of frequenin in the facilitation of transmitter release in Drosophila. *J.Physiol.* **474**, 223-232

Robbins, J, Trouslard, J, Marsh, S.J and Brown, D.A (1992). Kinetic and pharmacological properties of the M-current in rodent neuroblastoma x glioma hybrid cells. *J. Physiol (Lond)* **451**, 159-185.

Robbins, J.G, Marsh, S.J and Brown, D.A (1993). On the mechanism of M-current inhibition by muscarinic M_1 receptos in DNA-transfected rodent neuroblastoma x glioma cells. *J. Physiol* **469**, 153-178.

Runnels, L.W, Yue, L and Clapham, D.E (2002). The TRPM7 channel is inactivated by PIP_2 hydrolysis. *Nat. Cell. Biol.* **4**, 329-336.

Saimi, Y and Kung, C (2002). Calmodulin as an ion channel subunit. *Annu. Rev. Physiol* **64**, 289-311.

Sanguinetti, M.C, Curran, M.E, Zou, A, Shen, J, Spector, P.S, Atkinson, D.L and Keating, M.T (1996). Cassembly of KvLQT1 and mink (IsK) proteins to form cardiac I_{Ks} potassium channel. *Nature* **384**, 80-83.

Scalettar, B.A., Rosa, P., Taverna, E., Francolini, M., Tsuboi, T., Terakawa, S., Koizumi, S., Roder, J., and Jeromin, A. (2002) Neuronal calcium sensor-1 binds to regulated secretory organelles and functions in basal and stimulated exocytosis in PC12 cells. *J. Cell Science* **115:**2399-2412

Schaad,N.C.,DeCastro,E.,Nef,S.,Hegi,S.,Hinrichsen,R.,Martone,M.E.,Ellisma n,M.H.,Sikkink,R.,Sygush,J., and Nef,P. (1996) Direct modulation of calmodulin targets by the neuronal calcium sensor NCS-1.*Proc. Natl.Acad.Sci. U.S.A.* **93**, 9253-9258

Schweitzer, P, Madamba, S and Siggins, G.R (1990). Arachidonic acid metabolites as mediators of somatostatin-induced increase of neuronal M-current. *Nature* **346**, 464-467.

Selyanko, A.A and Brown, D.A (1996). Intracellular calcium directly inhibits potassium M-channels in excised membrane patches from rat sympathetic neurons. *Neuron* **16**, 151-162.

Selyanko, A.A, Hadley, J.K, Wood, I.C, Abogadie, F.C, Delmas, P, Buckley, N.J, London, B and Brown, D.A (1999). Two types of K^+ channel subunit, Erg1 and KCNQ2/3, contribute to the M-ie current in a mammalian neuronal cell. *J. Neurosci.* **19**, 7742-7756.

Selyanko A.A, Stansfeld, C.E and Brown, D.A (1992). Closure of potassium M-channels by muscarinic acetylcholine receptor stimulants requires a diffusible messenger (1992). *Proc. Roy. Soc., Lond B* **250**, 119-125.

Selyanko, A.A, Hadley, J.K and Brown, D.A (2001). Properties of single M-type KCNQ2/KCN3 potassium channels expressed in mammalian cells. *J. Physiol* **534.1**, 15-24.

Shah, M.M, Mistry, M, Marsh, S.J, Brown, D.A and Delmas, P (2002). Molecular correlates of the M-current in cultured rat hippocampal neurons. *J. Physiol.* **544.1**, 29-37.

Shyng, S-L, Barbieri, A, Gumusboga, A, Cukras, C, Pike, L, Davis, J.N, Stahl, P.D and Nichols, C.G (2000). Modulation of nucleotide sensitivity of ATP-sensitive potassium channels by phosphatidylinositol-4-phosphate 5-kinase. *Proc. Natl. Acad. Sci. USA* **97**, 937-941.

Simmons, M.A and Schneider, C.R (1998). Regulation of M-type potassium current by intracellular nucleotide phosphates. *J. Neurosci* **18**, 6254-6260.

Singh, N.A, Charlier, C, Stauffer, D, DuPont, B.R, Leach, R.J, Melis, R, Ronen, G.M, Bjerre, I, Quattlebaum, T, Murphy, J.V, McHarg, M.L, Gagnon, D, Rosales, T.O, Peiffer, A, Anderson, V.E and Leppert, M (1998). A novel potassium channel gene, KCNQ2, is mutated in an inherited epilepsy of newborns. *Nature Genet.* **18**, 948-955.

Smrcka, A.V, Hepler, J.R, Brown, K.O, Sternweis, P.C (1991). Regulation of polyphosphoinositide-specific phospholipase C activity by purified Gq. *Science* **251**, 804-807.

Stansfeld, C, Ludwig, J, Roeper, J, Weseloh, R, Brown, D and Pongs, O (1997). A physiological role for *ether-a-go-go* K^+ channels?. *Trends Neurosci.* **20**, 13-14.

Stemkowski, P.L, Tse, F.W, Peuckmann, V, Ford, C.F, Colmers, W.F and Smith, P.A (2002). ATP-inhibition of M-current in frog sympathetic neurons

involves phospholipase C but not Ins P_3, Ca^{2+}, PKC or Ras. *J. Neurohysiol.* **88**, 277-288.

Suh, B-C and Hille, B (2002). Recovery from muscarinic modulation of M-current channels requires phosphatidylinositol 4,5-bisphosphate synthesis. *Neuron* **35**, 507-520.

Taylor, S.J, Chae, H.Z, Rhee, S.G and Exton, J.H (1991). Activation of the beta 1 isozyme of phospholipase C by alpha subunits of the Gq class of G proteins. *Nature* **350**, 516-518.

Tokimasa, T and Akasu, T (1990). Extracellular calcium ions are required for muscarine-sensitive potassium current in bullfrog sympathetic neurons. *J Auton Nerv Syst* **29**, 163-174.

Tokimasa, T, Tsurusaki, M and Akasu, T (1993). Chemosensitivity of C-cells in bullfrog dorsal root ganglia to substance P and adenosine 5'-triphosphate. *Neurosci Lett* **163**, 169-172.

Tolias, K.F and Carpenter, C.L (2000). Enzymes involved in the synthesis of PtdIns(4,5)P_2 and their regulation: PtdIns kinases and PtdInsP kinases. *Biology of Phosphoinositides – edited by S. Cockroft, Oxford University Press*, 109-122.

Urumow, T. and Wieland, O.H. (1986) Stimulation of phosphatidylinositol 4-phosphate phosphorylation in human placenta membranes by GTP gamma S. *FEBS Lett.,* **207**, 253.

Van der Wal, J, Habets, R, Varnai, P, Balla, T and Jalink, K (2001). Monitoring agonist-induced phospholipase C activation in live cells by fluorescence resonance energy transfer. *J Biol Chem* **276(18)**:15337-44.

Vanhaesebroeck, B, Leevers, S.J, Ahmadi, K, Timms, J, Katso R et al. (2001). Synthesis and function of 3-phosphorylated inositol lipids. *Annu. Rev. Biochem.* **70**, 535-602.

Varnai, P and Balla T (1998). Visualisation of phosphoinositides that bind pleckstrin homology domains: calcium- and agonist-induced dynamic changes and relationship to Myo-[^{3}H]inositol-labelled phosphoinositide pools. *J. Cell. Biol* **143**, 501-510.

Varnai, P et al. (2002). Inositol lipid binding and membrane localisation of isolated pleckstrin homology (PH) domains. *J. Biol. Chem* **277**, 27412-27422.

Villarroel, A, Marrion, N.V, Simmons, M.A et al. (1989). Bradykinin inhibits a potassium M-ike current in rat pheochromocytoma PC12 cells. *FEBS Lett* **255**: 42-46.

Wang, H-S, Pan, Z, Shi, W, Brown, B.S, Wymore, R.S, Cohen, I.S, Dixon, J.E and McKinnon, D (1998). KCNQ2 and KCNQ3 potassium channel subunits: molecular correlates of the M-channel. *Science* **282**, 1890-1893.

Wang, Q, Curran, M.E, Splawski, I, Burn, T.C, Millholland, J.M, VanRaay, T.J, Shen, J, Timothy, K.W, Vincent, G.M, de Jager, T, Schwartz, P.J, Towbin, J.A, Moss, A.J, Atkinson, D.L, Landes, G.M, Connors, T.D and Keating, M.T (1996). Positional cloning of a novel potassium channel gene: KVLQT1 mutations cause cardiac arrhythmias. *Nature Genet.* **12**, 17-23.

Wang,C.Y.,Yang,F.,He,X.,Chow,A.,Du,J.,Russel,J.T., and Lu,B. (2001) Ca(2+) binding protein frequenin mediates GDNF-induced potentiation of Ca(2+) channels and transmitter release. *Neuron* **32(1),**99-112

Watkins, C.S and Mathie, A (1996). A non-inactivating K^+ current sensitive to muscarinic receptor activation in rat cultured cerebellar granule neurons. *J. Physiol* **491**, 12.

Weiss,J.L.,Archer,D.A., and Burgoyne,R.D. (2000) Neuronal Ca2+ sensor-1/frequenin functions in an autocrine pathway regulating Ca2+ channels in bovine adrenal chromaffin cells. *J.Biol.Chem* **275**:40082-40087

Willuwett, B and Aktories, K (1988). Heparin uncouples α_2-adrenoceptors from the G-protein in membranes of human platelets. *Biochemical J* **249**, 857-863.

Wu, L et al. (2002). Dual regulation of voltage-gated calcium channels by Ptd Ins (4,5) P_2. *Nature* **419**, 947-952.

Xie, L.H, Horie, M and Takano, M (1999). Phospholipase C-linked receptors regulate the ATP-sensitive potassium channel by means of phosphatidylinositol 4,5-bisphosphate metabolism. *Proc. Natl. Acad. Sci. USA* **96**, 15292-15297.

Yang, W-P, Levesque, P.C, Little, W.A, Conder, M.L, Ramakrishnan, P, Neubauer, M.G and Blanar, M.A (1998). Functional expression of two KvLQT1-related potassium channels responsible for an inherited idiopathic epilepsy. *J. Biol. Chem.* **273**, 19419-19423.

Young, K.W, Nash, M.S, Challis, R.A.J and Nahorski, S.R (2003). Role of Ca^{2+} feedback on single cell inositol 1,4,5-trisphosphate oscillations mediated by G-protein-coupled receptors. *J. Biol. Chem* **278**, 20753-20760.

Yu, S.P (1995). Roles of arachidonic acid, lipoxygenases and phosphatases in calcium-dependent modulation of M-current in bullfrog sympathetic neurons (1995). *J. Physiol* **487**, 797-811.

Zhang, H, Craciun, L, Mirshahi, T, Rohacs, T, Lopes, C.M.B and Logothetis, D.E (2002). PIP_2 activates KCNQ channels and its hydrolysis underlies receptor-mediated inhibition of M-currents. Neuron. 2003 Mar 27;37(6):963-75.

Zhang H, He C, Yan X, Mirshahi T, Logothetis DE (1999) Activation of inwardly rectifying K^+ channels by distinct PtdIns(4,5)P_2 interactions. Nat Cell Biol **1**: 183–188.

Zhao,X.,Varnai,P.,Tuymetova,G.,Balla,A.,Toth,Z.E.,Oker-Blom,C.,Roder,J.,Jeromin,A.,Balla,T. (2001) Interaction of neuronal calcium sensor-1 (NCS-1) with phosphatidylinositol 4-kinase beta stimulates lipid kinase activity and affects membrane trafficking in COS-7 cells. *J Biol Chem* **276**:40183-40189

Zhou, C, Horstman, D, Carpenter, G and Roberts, M.F (1999). Action of phosphatidylinositol-specific phospholipase C gamma 1 on soluble and micellar substrates. Separating effects on catalysis from modulation of the surface. *J. Biol. Chem* **274**, 2786-93.